INFORMATION TO USERS

This manuscript has been reproduced from the microfilm master. UMI films the text directly from the original or copy submitted. Thus, some thesis and dissertation copies are in typewriter face, while others may be from any type of computer printer.

The quality of this reproduction is dependent upon the quality of the copy submitted. Broken or indistinct print, colored or poor quality illustrations and photographs, print bleedthrough, substandard margins, and improper alignment can adversely affect reproduction.

In the unlikely event that the author did not send UMI a complete manuscript and there are missing pages, these will be noted. Also, if unauthorized copyright material had to be removed, a note will indicate the deletion.

Oversize materials (e.g., maps, drawings, charts) are reproduced by sectioning the original, beginning at the upper left-hand corner and continuing from left to right in equal sections with small overlaps.

Photographs included in the original manuscript have been reproduced xerographically in this copy. Higher quality 6" x 9" black and white photographic prints are available for any photographs or illustrations appearing in this copy for an additional charge. Contact UMI directly to order.

ProQuest Information and Learning
300 North Zeeb Road, Ann Arbor, MI 48106-1346 USA
800-521-0600

GENETIC, MOLECULAR AND FUNCTIONAL ANALYSIS OF THE REGION ENCOMPASSING THE *Cmv1* HOST RESISTANCE GENE

By

Chantal Depatie

Department of Biochemistry, McGill University, Montreal, Canada

May 2000

A Thesis submitted to the Faculty of Graduate Studies and Research in partial fulfillment of the requirements for the degree of Doctor of Philosophy

Abstract

Host resistance to murine cytomegalovirus (MCMV) infection is under multigenic control with contributions from both H-2 and non-H-2 genes. *Cmv1* is an autosomal dominant non-H-2 locus mapping to mouse chromosome 6 and controls early viral replication in the spleen of infected host. The *Cmv1* gene has two alleles in inbred mouse strains: the dominant *Cmv1*^{r} allele (low titer; resistant) found in C57BL backgrounds and the recessive *Cmv1*^{s} allele (high titer; susceptible) in BALB/c, A/J and DBA/2J strains. Resistance to MCMV is attributed to the activity of Natural Killer (NK) cells, important players in innate immunity to viral infections. In an effort to clone the *Cmv1* locus, a positional cloning approach was undertaken. The work presented in this thesis applies this approach to the cloning of *Cmv1*. We describe the generation of a high-resolution linkage map of mouse chromosome 6 in the vicinity of the *Cmv1* gene by following the segregation of 45 markers in 2248 backcross mice derived from *Cmv1*^{r} and *Cmv1*^{s} strains. A genetic interval of 0.7 cM was determined to contain *Cmv1*. In addition, tightly linked markers to *Cmv1* were identified. Secondly, we assembled a YAC/BAC contig of the candidate region spanning ~ 3Mb of genomic DNA. An STS content map was generated and anchored 71 markers on a total of 98 genomic clones. Cloning of novel polymorphic markers established a genetic interval of 0.35 cM for *Cmv1*. Restriction analysis of genomic clones was performed to generate a physical map of the region. In addition, a transcript map was established where 14 genes and 14 potential transcripts were identified and mapped on the YAC/BAC contig. Finally, potential candidates *Ly49a*, *Ly49c* and *Ly49g* genes were shown to cosegregate with *Cmv1* and were subjected to

functional analysis by studying their cell surface expression during MCMV infection and performing selective *in vivo* antibody depletion of NK cell subsets expressing the receptors to assess their contribution to resistance. Results of this study suggested that neither of these 3 genes are likely to be responsible for mediating resistance. However, the physical map of the *Cmv1* region will certainly provide a useful substrate from which the true *Cmv1* gene can be cloned.

Résumé

La résistance de l'hôte à l'infection au cytomégalovirus murin est déterminée par la contribution de plusieurs gènes dont une partie seulement provient du complexe majeur d'histocompatibilité. *Cmv1* est un locus autosomal et dominant ne résidant pas dans le complexe d'histocompatibilité. Il contrôle la réplication virale dans la rate de souris infectée. *Cmv1* présente deux allèles: l'allèle résistant $Cmv1^r$ présent chez les souche de la famille de souris C57BL, et l'allèle susceptible $Cmv1^s$ présent chez les souches telles que BALB/c, A/J et DBA/2J. La résistance au MCMV est attribuée à l'activité des cellules "Natural Killer" (NK). Les cellules NK constituent la première ligne de défense contre l'infection virale. Afin d'isoler le gène correspondant à *Cmv1*, nous avons entamé une approche de clônage positionnel. Le travail présenté dans cette thèse décrit les étapes de cette approche en relation avec *Cmv1*. Nous décrivons la génération d'une carte génétique détaillée de la région abritant *Cmv1* en suivant la ségrégation de 45 marqueurs génétiques dans 2248 descendants de rétrocroisements dérivés de parents possèdant les allèles $Cmv1^r$ ou $Cmv1^s$. Cette analyse a permis d'établir un interval génétique de 0.7 cM et d'identifier des marqueurs étroitement liés à *Cmv1*. Par la suite, une collection de groupes de YACs et de BACs contigus a été assemblée, représentant plus de 3 Mb d' ADN génomique et couvrant la région candidate pour *Cmv1*. La collection de 98 clones génomiques obtenus a été criblée avec 71 marqueurs. Le clônage de nouveaux marqueurs génétiques a réduit l'intervalle génétique contenant *Cmv1* à 0.35 cM. L'analyse de fragments de restriction provenant des clones de YACs et BACs, a permis d'établir une carte physique de l'intervalle génétique. Par ailleurs, une carte des unités de transcription de la région a aussi été assemblée, dans laquelle 14 gènes et 3 unités de transcription

potentiels ont été localisés sur le groupe de BACs et de YACs. Finalement, les membres de la famille de gènes *Ly49* ont été souligné comme candidats potentiels étant donné leurs coségrégations avec *Cmv1*, et leurs expressions chez les cellules NK. Une étude fonctionelle utilisant des anticorps monoclonaux a été entamée pour déterminer la candidature de 3 membres de cette famille, *Ly49a*, *Ly49c* et *Ly49g*. Leur cinétique d'expression à la surface des cellules a été étudié au cours d'un infection avec MCMV ainsi que l'effet de déplétions sélectives *in vivo* de population de cellules NK exprimant ces molécules Ly49. D'après ces resultats, il est improbable que ces trois molécules soient directement liées au phenomène de résistance au MCMV. Cependant, la cartographie physique de la region générée servira de substrat pour clôner le véritable gène *Cmv1*.

Acknowledgement

I would like to express my immense gratitude and admiration to my thesis supervisor, Dr. Silvia Vidal. Her patience, guidance and understanding throughout these 5 years have been invaluable and for which I will always be grateful and appreciative. I wish her the best of success in her career and family and hope that she will still be a source of guidance and support in the future. I would also like to express a special thank to my "other" supervisor, Dr. Philippe Gros, looming in the shadows but always there to offer some support, wisdom and a big van. I owe you both very much and look to you as role models.

I am grateful my thesis committee members, Dr. Jerry Pelletier and Dr. Michel Tremblay for their helpful discussion and advice. A special thanks to Dr. Danielle Malo for being a source or guidance, encouragement and laughter. I would also like to mention Dr. Tom Hudson for providing us with helpful reagents along the way.

There are many people with whom I have shared ideas and friendship along the way that I must thank. The hard-working, card-playing, chip-eating and beer-drinking people of 910 and 924, I will remember you fondly (special thanks to Sooz, Normand and Alaka for technical and moral support and Greg for getting me in). To my fellow graduate students in Biochemistry, I enjoyed playing softball and hockey (Go Knockouts!) with all.

To all the people at the MGH, Tom's lab, Joe's lab, Line, Sal, Gary and the other Line, I thank you for your friendship and advice. A very special thanks to Pierre (Mais voyons donc! Qu'est-ce-que tu d'mandes la!) and Giovanna (I miss that coffee in the

morning Gio!) with whom I shared a lot of my ups and downs. To where my journey ended, in Ottawa, I thank Sonia, Denis and Seung Hwan for putting up with me this last year and helping me finish.

Last but not least, I would like to thank my parents, Jean and Dolores, for their undying love and support throughout my first 28 years of life. I would also like to express my thanks to the entire Depatie/Farrah/Burton/Screaton clan. And to my husband Rob, I am forever grateful for your critical reading of this thesis, your patience, and especially your love and support.

Oh! Yeah! Thanks Stinkus.

Table of Contents

List of Figures

List of Tables

List of Abbreviations

ASO Allele Specific Oligonucleotide

BAC Bacterial Artificial Chromosome

cDNA Complementary Deoxyribonucleic Acid

cM CentiMorgans

CMV Cytomegalovirus

DNA Deoxyribonucleic Acid

FCM Flow Cytometry

FISH Fluorescence *in Situ* Hybridization

HCMV Human Cytomegalovirus

IFN Interferon

kb Kilobases

mAb Monoclonal Antibody

Mb Megabases

MCMV Murine Cytomegalovirus

MEF Mouse Embryo Fibroblasts

MHC Major Histocompatibility Complex

NK Natural Killer

NKC Natural Killer Gene Complex

PCR Polymerase Chain Reaction

PFGE Pulse Field Gel Electrophoresis

RFLP Restriction Fragment Length Polymorphism

SSCP Single Stranded Conformational Polymorphism

SSLP Simple Sequence Length Polymorphism

SSR Simple Sequence Repeat

STS Sequence-Tagged Site

TNF Tumor Necrosis Factor

YAC Yeast Artifical Chromosome

Preface

This thesis includes the text of original reports published or submitted for publication and thus, as stipulated in the "Guidelines Concerning Thesis Preparation" from the Faculty of Graduate Studies and Research, the following must be cited:

Manuscripts and Authorship:

"The candidate has the option, subject to the approval of their department, of including as part of the thesis the text, or duplicated published text, of an original paper or papers.

- Manuscript-style theses must still conform to all other requirements explained in the Guidelines Concerning Thesis Preparation.
-Additional material (procedural and design data as well as descriptions of equipment) must be provided in sufficient detail (e.g. in appendices) to allow clear and precise judgment to be made of the importance and originality of the research reported.
- The thesis should be more than a mere collection of manuscripts published or to be published. It must include a general abstract, a full, introduction and literature review and a final overall conclusion. Connecting texts which provide logical bridges between different manuscripts are usually desirable in the interest of cohesion.

It is acceptable for theses to include, in chapters, authentic copies of papers already published, provided these are duplicated clearly and bound as an integral part of the thesis. In such instances, connecting texts are mandatory and supplementary explanatory material is always necessary.
- Photographs or other materials which do not duplicate well must be included in their original form.
- While the inclusion of manuscripts co-authored by the candidate and others is acceptable, the candidate is required to make an explicit statement in the thesis of who contributed to such work and to what extent, and supervisors must attest to the accuracy of the claims at the Ph.D. Oral Defense. Since the task of the Examiners is made more difficult in these cases, it is in the candidate's interest to make the responsibilities of authors perfectly clear.

The work presented in Chapter 2 and 4 of the thesis has been published, and Chapter 3 is to be submitted. The following sections describe the author's contribution to the work in each of Chapters 2 to 4.

Chapter 2

The work in Chapter 2 describes the generation of a high-resolution linkage map of the Cmv1 region. My contribution involved: (1) the genotyping of the Spretus and A/J crosses with a total of 45 markers, (2) identification polymorphisms for 11 known genes that map to the region of chromosome 6, and (3) subsequent mapping of these genes in the Spretus and A/J crosses. The BALB/c backcross also described was characterized by Eric Muise. The phenotypes of recombinant mice for *Cmv1* was determined by Dr. Silvia Vidal. Finally, Dr. Pierre Lepage provided assistance in the cloning of an *Ly49* and *Prp* probe.

Chapter 3

The work described in Chapter 3 describes the physical mapping and transcription map of the *Cmv1* candidate region. My contribution to this work included: (1) generation of a complete sequence-ready BAC contig of the *Cmv1* candidate region, (2) STS content mapping of the YAC/BAC contig , (3) identification and genetic mapping of novel polymorphic markers, (4) identification of novel STSs, (5) screening of RH panels with novel STSs, (6) restriction analysis of the entire BAC contig and selected parts of the YAC contig, and (7) generation of a partial transcription map of the region. Pierre Bérubé was responsible for constructing cosmid libraries from YAC clones and provided

technical assistance for screening BAC and YAC libraries. Dr. Amanda Stafford and Dr. Philippe Avner (Institut Pasteur, Paris) provided YAC clones that map to the region and STS content information pertaining to these clones. Seung Hwan Lee was responsible for cloning YAC end fragments, identifying several polymorphic markers and performed exon amplification described in Chapter 2. In addition, he was involved in the generation of the transcription map.

Chapter 4

The work described in Chapter 4 describes the functional analysis of Ly49 candidates. This work is co-authored with Anick Chalifour (Institut Armand-Frappier, Laval). My contribution to this work includes: (1) identification of polymorphisms for genes in the *Cmv1* region, (2) mapping of these in the informative backcrosses, (3) determining the viral titers in the spleen and livers of all infected animals and (4) involved in the preparation of NK cells from spleen. Anick Chalifour was responsible for preparing NK cell-enriched populations from spleens of mice and performed all the FCM analysis.

Publications

Depatie C., Muise E., Lepage P., Gros P., and Vidal S.M. High resolution linkage map in the proximity of the host resistance locus *Cmv1*. Genomics 39, 154-163 (1997).

Depatie C., Chalifour A,, Paré, C., Vidal S.M., and Lemieux S. Assessment of *Cmv1* candidates by genetic mapping and *in vivo* antibody depletion of NK cell subsets. International Immunology 9, 1541-1551 (1999).

Depatie C., Lee S.H., Stafford A., Avner P., Belouchi, M., Gros P., and S.M. Vidal. Sequence-ready BAC contig, physical and transcription map of a 2-Mb region overlapping the mouse chromosome 6 host resistance locus *Cmv1*. Genomics, in press.

Original Contributions to Knowledge

1. Generation of a high resolution genetic map of the region surrounding the *Cmv1* locus amenable to physical mapping and positional cloning and identification of tightly-linked markers to *Cmv1*
2. Identification of RFLPs for the *Nk1.1, Cd94, Nkg2d, Ly49a, Ly49b, Ly49c, Ly49d, Ly49e, Ly49g, Prp, Kap, A_2m, Cd69, Ret, Gnβ3, Kcna1, Tel* and *Tpi* genes.
3. Genetic exclusion of the *Nk1.1, Cd69* and *Cd94* genes as *Cmv1* candidates
4. Generation of a contigous sequence ready BAC contig overlapping the critical *Cmv1* interval.
5. Generation of 41 new STSs and 20 new polymorphic markers in the *Cmv1* interval
6. STS content map of the YAC and BAC contig overlapping the *Cmv1* interval with coverage of over 3Mb.
7. Physical map of the Cmv1 region based on genomic contigs and FISH analysis
8. Determination of cell surface expression of Ly49A, Ly49C, Ly49I and Ly49G2 during MCMV infection in *Cmv1^r* mice.
9. Determination of importance of Ly49a$^+$, Ly49c$^+$, Ly49I$^+$ and Ly49g2$^+$ NK cell subsets towards resistance to MCMV by performing antibody depletion studies in *Cmv1^R* mice during the course of infection

Chapter 1: Introduction

Chapter 1: Introduction

General Introduction

Human cytomegalovirus (HCMV) is one of the most common viruses that infect the human population. 60% to 80% of the population in developed countries and nearly all individuals in developing countries will become infected with HCMV during their lifetime (Hanshaw, 1995). Cytomegalovirus-associated disease represents a major threat to immunocompromised patients, including graft recipients, AIDS patients and neonates. The overall clinical benefit of the currently available antiviral drugs is reduced by toxicological effects and the continual emergence of drug resistant strains (Erice, 1999). In order for novel therapeutic strategies to be developed, key players in the immune mechanisms that combat cytomegalovirus infection must first be identified.

The last decade has witnessed an exponential growth in genomic research that has provided powerful tools to help uncover genes - and their mutated counterparts - that underlie clinically relevant phenotypes. One such group of genes are those associated with host susceptibility to infectious diseases. While studying genetic susceptibility in humans can be successful, it is also hindered by the greater complexity of the human gene pool, variable penetrance and expressivity of a particular trait. In addition, factors including immune status of a host and prior vaccination, can affect the outcome of the host-pathogen phenotype. As a result, to isolate genes involved in host resistance, much attention has been focused on the mouse as a model organism. Several advantages have established the mouse as an excellent alternative: 1) controlled breeding environment, 2) short gestation periods, 3) large litters, 4) feasibility of gene transfer experiments that can

functionally verify candidate genes, and 5) the possibility of experimental infection. Moreover, the large number of available inbred strains of mice provides a mosaic of different homogeneic backgrounds that facilitate the determination of modes of inheritance, loci identification and subsequent isolation of genes that govern individual phenotypic traits.

Identifying resistance/susceptibility genes constitutes an important step in elucidating the mechanisms of host resistance. Animal models provide a scaffolding system with direct applications to humans, and can assist in the design of therapeutic strategies both to bypass genetic defects in the host's immune response to pathogens and to manipulate the immune system to improve its effectiveness. The mouse model for HCMV, Murine Cytomegalovirus (MCMV), has been well characterized for host susceptibility to infection. Major genetic contributions to the outcome of MCMV infection, are made by H-2 genes located within the major histocompatibility complex (MHC), and the *Cmv1* host resistance locus.

The experiments described in this thesis outline the initial steps in the identification of the host resistance gene *Cmv1* using a positional cloning approach. Positional cloning was selected to clone *Cmv1* as no *in vitro* model has been established to date that can faithfully replicate the *in vivo* viral replication and the host immune response. In brief, positional cloning involves: (1) the generation of a high-resolution linkage map, (2) the generation of a physical map encompassing the critical interval, (3) generation of a transcript map of the *Ly49* gene family and other transcript in the region, and (4) functional testing of *Cmv1* candidate genes. A significant advantage of this approach to cloning is that comparitive mapping with the human genome can be

performed, owing to the extensive structural conservation between human and mouse chromosomes. It is therefore possible to test for susceptibility to cytomegalovirus infection in the human population by looking at the syntenic regions in the human genome.

Topics covered in the literature review that follows this general introduction include: cytomegalovirus infection in humans and mice, the host genetic loci involved in resistance and/or susceptibility to CMV infection, and the experimental approaches associated with positional cloning that form the basis for the work described in this thesis.

1. Cytomegalovirus

1.1. Discovery

Cytomegaloviruses (CMVs) are ubiquitous pathogenic agents that commonly infect higher eukaryotic species (Weller, 1971). CMVs are species-specific viruses that have evolved to give rise to thousands of genetically distinct strains which continually circulate through the world's populations (Alford, 1975). The characteristic effects of CMV infection are the formation of intranuclear inclusions and enlargement of the host cell, hence the term 'cytomegalic' cells.

Goodpasture and Talbot reported similarities between cytomegalic cells found in the parotid glands of infants afflicted with of a variety of diseases and those in dying guinea pigs (Goodpasture and Talbot, 1921). It was later found that filtered inclusion-bearing salivary glands from older guinea pigs were infectious to younger animals, a hallmark of a viral agent (Cole and Kuttner, 1926). This agent became known as

"salivary gland virus". Three decades later, having succeeded in propagating murine CMV in mouse embryo fibroblasts, Smith and Rowe isolated the human virus (Smith, 1954; Smith, 1956; Rowe et al., 1956) which was renamed cytomegalovirus, to reflect the observed cytopathic changes in infected cells (Weller, 1957). Subsequent isolation of other strains of CMV, and the advent of serological methods established that CMV infection is a common, usually subclinical infection that is particularly prevalent in very young, old, debilitated and immunocompromised individuals.

1.2. Classification of CMV

CMV is a large double-stranded DNA virus that shares common architectural features with members of the herpesvirus family. Herpesvirus particles consist of a core containing a linear double-stranded DNA, an icosadeltahedral capsid surrounded by an amorphous material, the tegument, and an envelope containing viral glycoproteins that protrude from the surface. Herpesviruses share four apparent biological properties: first, they encode numerous enzymes involved in nucleic acid metabolism, DNA synthesis and protein processing. Second, viral DNA replication and capsid assembly occurs in the host cell nucleus, the products of which are enveloped upon exiting the nucleus. Third, release of virus particles leads to the destruction of the infected cell, and fourth, herpesviruses are all able to establish latency in their natural hosts.

Herpesviruses can be further categorized into three subfamilies, alpha, beta and gamma. Members of the alpha subfamily display a variable host range, a short reproductive cycle and rapid horizontal spread in culture. Infection leads either to efficient destruction of the host cell or to latency; when it occurs, the virus establishes

latency specifically in primarily sensory ganglia. Alpha subfamily viruses include the genera *Simplexvirus* (Herpes simplex virus 1 and 2: HSV-1 and HSV-2) and *Varicellovirus* (Varicella-zoster virus: VZV). Cytomegaloviruses, together with HHV-6 and HHV-7, are members of the beta subclass of herpesviruses that have a restricted host range and a longer reproductive cycle. HHV-6 and HHV-7 are associated with febrile illnesses and the chilhood disease, exanthem subitum (Levy, JA, 1997). Infection with these cytomegaloviruses frequently causes cytomegaly. Beta herpesviruses preferentially establish latency in secretory glands, lymphoreticular cells, and kidneys. Epstein-Barr virus (EBV) is a member of the gamma subfamily of viruses that specifically infect T and B lymphocytes. The host range of members of this subfamily does not extend beyond the family or order of the natural host.

1.3. The CMV life cycle

The human CMV (HCMV) genome is approximately 245 kb in length and features over 200 open reading frames, predictive of over 100 distinct proteins and glycoproteins (Stinski, 1990). Following adsorption and penetration of the virus into the host cell, the virion is disassembled in the cytoplasm. The double-stranded viral genome enters the nucleus where it is transcribed in sequential order, beginning with the restricted transcription of immediate-early (I-E) genes. The I-E genes reside in the large unique (U_L) segment and encode regulatory proteins. This ordered transcription is required for the subsequent expression of early (EA) genes that direct the synthesis of proteins involved in DNA replication. Transcription of the late (LA) genes, which code for structural proteins and surface glycoproteins, proceeds last, immediately before virion

assembly and eventual lysis of the infected cell. During the lytic cycle, infected host cells express both I-E and LA proteins on their surface, and these are expected to elicit a host immune response. Interestingly, CMV has evolved to express specific gene products upon infection that interfere with host immune response (see Chapter 1; section 3).

1.4. Pathogenesis of HCMV infection

As cytomegaloviruses are ubiquitously expressed and highly species-specific, only humans can act as carriers of HCMV. Epithelial cells in the salivary glands, liver and the kidney, among others, are sites of viral replication. Natural transmission of CMV can occur by direct or indirect person-to-person contact. Such contact must be close or even intimate because of the virus' susceptibility to heat and dessication (Lang, 1975). Most bodily fluids can be a source of virus (Lang, 1975; Reynolds et al., 1973; Stagno et al., 1980). Human CMV infection is endemic and is not subject to seasonal variations, like the influenza virus. The salivary glands are an important target for growth and dissemination of the virus and persistent or recurrent shedding in saliva is one of the principal means of spread in the population.

The prevalence of HCMV infection in the general adult population ranges from 60-90% in developed and developing countries, respectively (Hanshaw et al., 1995). In a normal healthy host, symptoms of infection either remain hidden or resemble that of a mononucleosis syndrome that is indistinguishable clinically from infection with EBV (Horwitz et al., 1979). Primary infections almost always lead to more serious disease than a secondary or superinfection . Moreover, the incidence and severity of HCMV infection is greatly increased in immunosuppressed individuals such as neonates, transplant

recipients and AIDS patients (Bowden, 1995). HCMV infection is the most common congenital viral infection in humans, with an incidence in the United States of approximately 0.2% to 2.2% per live birth or about 40,000 infected infants each year (Demmler et al., 1991). Socioeconomic factors can lead to higher infection rates, both by vertical (intrauterine) and horizontal (extrauterine) transmission (Gold et al., 1982). While the rate of transmission in cases of primary maternal infection ranges from 35% to 50% (Demmler et al., 1991), this drops to 0.2% to 2.0% in mothers previously infected (Medearis, 1982), thus some features of maternal immunity may limit intrauterine transmission. Clinical findings in infected infants can vary from mild (hepatosplenomegaly, thrombocytopenia, microcephaly and hepatitis) to potentially life-threatening organ dysfunction with mortality rates of 10% to 30% (Hanshaw, 1995). CMV-induced damage of the liver and blood-forming organs is self-limiting and resolves without therapy, whereas any neurological damage associated with infection (e.g. hearing loss) is permanent and accounts for long term morbidity (Dahle et al., 1979).

HCMV remains one of the most important opportunistic infections encountered by AIDS patients and up to 40% may develop sight- and/or life-threatening HCMV-induced disease (Gallant et al., 1992). Autopsy studies have shown that 90% of patients with AIDS developed active HCMV infection. Several observations of patients infected with HIV suggest that HCMV is an opportunistic pathogen. These include: 1) the nearly universal HCMV seropositivity in populations at risk for HIV, 2) the significant risk of HCMV reinfection in these populations, and 3) the increased survival of AIDS patients that has resulted from more effective prophylaxis and treatment of bacterial and protozoan infections (Gallant et al., 1992). CMV may facilitate HIV infection by

synthesizing a chemokine receptor homolog that facilitates entry of the virus in the cell (Pleskoff et al., 1997). CMV is a threat posttransplantion to allograft recipients as these patients are routinely subjected to immunosuppressive regimens to prevent rejection of the transplanted organ. The most important factor contributing to the development of severe HCMV disease in the posttransplant period is likely to be the prior serologic status of both the donor and recipient. In general, the degree of drug-induced immunosuppression correlates with the likelihood of clinical risk.

1.5. Treatment of CMV infection

Current approaches to reduce morbidity, mortality and costs of treating patients with CMV infection include pre-emptive therapy, prophylactic therapy, and direct treatment of infection-associated disease (Hibberd et al., 1995). Three antiviral agents, ganciclovir, foscarnet, and cidofir are currently used to treat active infection. Ganciclovir, a nucleotid analog is moderately successful at treating CMV-induced retinitis, pneumonia and gastrointestinal disease. Foscarnet, a pyrophosphate analog that targets DNA polymerase of herpesviruses, has been shown to be effective in treating retinitis in AIDS patients (Oberg, 1989; Reddy et al., 1992). Cidofovir is a nucleotide analog that has a prolonged duration of effect; therefore, it does not have to be administered as often as ganciclovir or foscarnet. While these agents serve to lessen symptoms and lessen damage to vital organs, they are not curative. Moreover, drug-resistant strains of CMV have been reported for most antiviral drugs used to treat CMV infection (Erice, 1999). Most importantly, these drugs exhibit toxicity at therapeutic doses. Ganciclovir induces myelosuppression and exhibits CNS toxicity (Walmsley et al., 1999) whereas both

foscarnet and cidofivir are a renal toxin (Plosker, GL et al., 1999; Fletcher et al., 1994). Finally, herpesviruses present difficult challenges for vaccines development as they have evolved mechanisms that allow them to evade the immune system(see Chapter 1, section 3). Given the state of antiviral therapies available, novel approaches to combat CMV need to be developed. We hope that work described in this thesis will help elucidate host-pathogen interactions and eventually contribute to the design of a safe and effective therapy.

Section 2: Cellular Immune Responses to CMV

Immune mechanisms involved in host response to CMV feature a complex interplay of specific and non-specific responses, both mediated by T cells and Natural Killer (NK) cells. In humans, natural infections indicate that NK cells play a pivotal role in defense against many viral infections, including CMV and other herperviruses. Impaired NK cell-mediated cytotoxicity or an absence of NK cells correlate with increased sensitivity to severe disseminated infections with HCMV (Quinnan et al., 1982), HSV (Ching et al., 1979), EBV (Joncas et al., 1989) and VZV (Biron et al., 1989). These viruses, when taken together, represent all 3 subfamilies of herpesviruses. NK cell defects have also been observed during HIV (Bonavida et al., 1986) and papilloma infections (Ballas et al., 1990). Interestingly, current evidence points to a significant similarity between the immune mechanisms of humans and mice. In mice infected with murine CMV (MCMV) or HSV, induction of NK cell activity correlates with resistance to viral infection (see section 2.1 and 5.2).

NK cells form part of the innate immune system and provide an early host response to viral infections and immune surveillance of tumor cells. These cells have a large granular lymphocyte appearance and their granules contain perforin, a membrane pore-forming molecule, and granzymes, a group of serine proteases (O'Shea and Orthaldo, 1992). NK cells express neither the T cell receptor/CD3 complex nor immunoglobulins on their surface, and they do not rearrange their B cell and T cell antigen receptor genes. They express a variety of receptors involved in antibody-dependent cellular cytotoxicity, NK-cell mediated cytolytic activity and cytokine production.

Given the importance of the NK cell compartment to host control of CMV infection, the following review of immune responses to CMV will focus on the role of NK cells during infection with the relevant mouse model virus, MCMV. As CMVs exhibit strict host specificity, MCMV provides a useful model to help elucidate immune mechanisms involved in CMV infection that can ultimately be applied to studies in humans. The role of T cells, monocytes, macrophages and cytokines will also be discussed.

2.1. The Role of NK cells in MCMV Infection

The importance of NK cells in the regulation of viral infections has been most definitively demonstrated with MCMV. Important observations have been made using the mouse model to implicate NK cells in the response to CMV. Suckling mice, which have low NK cell activity, are sensitive to MCMV, which suggests that NK cells can control MCMV replication. Interestingly, resistance to the virus develops by 3-4 weeks of

age, in concordance with the development of NK cell response (Boos and Wheelock, 1971, Kiessling et al., 1975). Moreover, *beige* mice, which have a NK cell-associated granule deficiency, are more sensitive to MCMV infection than their heterozygous littermates (see section 4.2.1). In addition, when adult C57BL/6 mice are depleted of NK cells, they accumulate higher titers of virus in the spleen, lung and liver (Bukowski et al., 1984, Welsh et al., 1990, 1994, Scalzo et al., 1992).

2.1.1. NK cell activation and blastogenesis during MCMV infection

During MCMV infection, the induction of NK cell response is initiated when virus-infected cells begin to produce cytokines IFNα and IFNβ (Biron, 1997). These cytokines induce NK blastogenesis and activation of its cytolytic function that provide protective immunity during the early phases of MCMV infection (Welsh, 1978; Grundy et al., 1982). Mice depleted of IFNα/β with neutralizing antibodies or by homologous recombination (IFNα/β-/- mice) generate a poor NK cell response to infection (Muller et al., 1994; Orange et al., 1996). IFNα/β have also been demonstrated to induce the migration of NK cells during infection from bone marrow to secondary sites, such as the spleen (Wiltrout et al., 1989; Ishikawa et al., 1993; Salazar-Mather et al., 1996). This migration is predicted to allow NK cells to receive additional activation signals from cytokines in the new environment, and to deliver NK-produced cytokines such as IFNγ (see section 2.1.3).

IL-12 is a pleiotropic cytokine produced by macrophages that can induce production of IFN-γ by NK cells early during infection (Orange et al. 1996). However, neither IFN-γ nor IL-12 affect NK cell cytolytic activity (Orange et al., 1995). Another

strong NK cell activator and chemotactic factor, IL-2, induces activation and blastogenesis *in vitro* (Kuribayashi et al., 1981; Natuk and Welsh, 1987). This cytokine, like IL-12, can also stimulate NK cells to produce IFN-γ (Young and Orthaldo, 1987). TNFα can synergize with IL-12 to induce IFNγ, but negatively influences NK cell blastogenesis and cytolytic activity (Orange and Biron, 1996). Once activated, NK cells mediate control of viral infection through two important mechanisms: their cytolytic function against virally-infected cells and their production of cytokines.

2.1.2. NK cell cytolytic function

The ability of NK cells to preferentially kill mouse tumor cells that lack MHC class I suggested that an immune surveillance mechanism might exist that could eliminate cells with aberrant MHC expression (Ljunggren and Karre, 1985; Karre et al., 1986). Cloning of NK cell receptors that specifically recognize MHC class I molecules provided a molecular basis for this activity (Karlhofer et al., 1992; D'Andrea et al., 1995). MHC class I molecules are recognized by several families of NK cell receptors that possess either inhibitory or activating capabilities (Lanier, 1998, review). In fact, NK cell activity appears to be regulated by a balance between receptors which initiate and inhibitory receptors that suppress cell activation.

NK cell receptors that are involved in MHC class I recognition in mice are clustered on chromosome 6, in a segment called the Natural Killer Cell Complex (NKC) (Yokoyama et al., 1991; see section 5.3.). Although this segment is conserved on human chromosome 12p13, human NK cells also use another gene family located on chromosome 19, the Killer Inhibitory Receptors (KIRs), to recognize MHC class I

proteins (Colonna et al., 1995; Wagtmann et al., 1995). Distinct NK cell receptor gene homologs also on human chromosome 19 and the syntenic region on mouse chromosome 7 have also been recently identified, notably NKp44 and NKp46 (Vitale et al., 1998; Pessino et al., 1998; Biassoni et al., 1999). Both receptors are involved in the activation of NK cell cytotoxicity. Interestingly, MCMV can downregulate the levels of MHC class I proteins on the surface of infected cells (Campbell et al., 1994). This downregulation allows infected cells to evade the MHC-restricted CTL response. However, this same event – loss of MHC - renders infected cells susceptible to lysis by NK cells. Thus the NK cell response provides a failsafe mechanism for the host.

2.1.3. Cytokines produced by NK cells

In addition to having cytolytic activity, NK cells produce cytokines with important antiviral activities such as IFN-γ and TNFα. IFN-γ exerts antiviral effects by stimulating expression of the inducible nitric oxide synthase (iNOS) gene in macrophages and Kupffer cells (Nathan, 1992). In fact, when mice are treated with an iNOS inhibitor, MCMV synthesis in the liver is enhanced (Tay and Welsh, 1997). Mice depleted of IFNγ with neutralizing antibodies or via homologous recombination (*IFNγ-/-* mice) exhibit increased viral replication in the liver and an increase in the incidence of MCMV-induced hepatitis (Orange et al., 1995; Orange and Biron, 1986; Tay and Welsh, 1997). Thus, NK cells are important contributors of IFNγ to the immune response. NK cells also secrete TNFα, a mediator of inflammatory response. However, the role of TNFα in MCMV infection is unclear; mice lacking T or NK cells continue to produce normal levels of TNFα 2-3 days after MCMV infection (Orange and Biron, 1996). Therefore, TNFα

production from NK cells is not pivotal for mounting an effective immune response against MCMV indicative that TNFα production from other cell types such as macrophages, is more important (Beutler et al., 1985).

2.2. Cell-Mediated Immune Responses to MCMV Infection

2.2.1. T Cell-mediated responses

T cell-mediated immunity against MCMV infection involves contributions from $CD8^+$ and $CD4^+$ T cells. $CD8^+$ T cells mediate their antiviral effects through targeted lysis of infected cells. Following prior immune maturation, $CD8^+$ T cells recognize viral epitopes in the context of MHC class I molecules on infected ('self') cells. In contrast, $CD4^+$ T cells produce cytokines that activate the antiviral activities of NK cells and $CD8^+$ T cells. However, host genotype influences the importance of T cell-mediated immunity (Grundy and Melief, 1982; Lathbury et al., 1996) elicited in different strains of mice. Mice of the CBA and C57Bl/6 backgrounds are naturally resistant to MCMV. Viral replication within the visceral organs is primarily controlled by mechanisms of innate immunity, active while a full T cell response develops, including susceptibility of individual cells to infection (Price et al., 1990; Wykes et al., 1990), production of IFNα/β (Allan and Shellam, 1985) and the NK cell mediated response (Shellam et al., 1981; Welsh et al., 1990; Scalzo et al., 1992). In contrast, T cells are essential to the control of MCMV replication and control of lethal infection in strains such as BALB/C, DBA and A/J (Grundy and Melief, 1982; Lathbury et al., 1996). Depletion of both subsets results in severe disease leading to death (Grundy and Melief, 1982). Adoptive transfer of $CD8^+$ T cells into irradiated BALB/c recipients, showed that $CD8^+$ T cells can mediated clearance

of the virus in the absence of $CD4^+$ T cells (Reddehase et al., 1985; Jonjic et al., 1989). However, after long-term depletion of $CD8^+$ T cells (Jonjic et al., 1990) and in $\beta_2 m$ -/- mice that fail to express MHC class I at their cell surface (Polic et al., 1996), $CD4^+$ T cells can partially compensate for the lack of $CD8^+$ T cells in MCMV clearance. In contrast, antiviral response in the salivary glands of both resistant and susceptible strains involves the production of IFNγ, IL-4 and TNF by $CD4^+$ T cells, and is independent of host genotype (Lucin et al., 1992; Lathbury et al., 1996).

2.2.3 Monocytes and macrophages responses

Monocytes and macrophages play a central role in the pathogenesis of MCMV infection, providing functions beneficial to both the virus and the host. Differentiated macrophages are targets for MCMV infection within tissues. They harbor latent MCMV DNA, support viral replication both *in vitro* and *in vivo* and present foreign antigen to $CD4^+$ T cells in the context of MHC class II (Brautigam et al., 1979; Shanley et al., 1983; Hayashi et al., 1985). The beneficial role that macrophages play during MCMV infection stems from IFNγ-induced production of nitric oxide and secretion of other cytokines that mediate inflammatory responses, such as IL-1 and TNFα (He et al., 1995). Depletion of splenic macrophages enhances MCMV replication in the spleen (Hanson et al., 1999). Thus, viral replication in splenic macrophages may protect other highly permissive cell types from infection by mobilizing accessible virus.

In human, HCMV infection of monocyte-derived macrophages results in delayed and non-lytic productive growth suggesting that these cells play a major role in the pathogenesis and latency of HCMV (Fish. et al., 1996). Immunohistochemistry analysis

of tissue sections of various infected organs confirmed the presence of viral proteins representing all stages of permissive HCMV infection in macrophages suggesting that theses cells play a important role in the spread of HCMV in solid organs (Sinzger et al., 1996).

2.2.4. γδ T cells responses

γδ T cells account for a small subset (0.5-6%) of the T cell population (Bluestone et al., 1991), and are most notably implicated in the control of HSV-1 infection (Sciammas et al., 1997). Although involvement of γδ T cells in MCMV infection has not been reported, they have been implicated in response to HCMV infection (Hiromatsu et al.,1992; Monbearts et al., 1993). Renal allograft recipients that develop HCMV infection show selective expansion of a γδ T cell subpopulation (Dechanet et al., 1999). γδ T cells recognize antigen in an MHC-independent manner (Schild et al., 1994), thus increased activity of these cells may compensate for the downregulation of MHC class I in CMV infection (Campbell et al., 1994),

Section 3. Immune evasion by CMV

Herpesviruses in general and in particular CMVs, have developed numerous and sophisticated strategies to evade the immune system. In this section, we will present a review of the mechanisms used to downregulate cellular immunity and to interfere with the cytokine network.

3.1. Downregulation of MHC class I and II molecules

One strategy used by MCMV to compromise antiviral host defense mechanisms is to express a series of viral factors that silence the immune system. Interestingly, these factors are not required for replication *in vitro*. For example, MCMV produces three gene products *m152, m04, and m06* that interfere with MHC class I expression (Del Val et al., 1992, Campbell et al., 1992, Hengel et al., 1995; Ziegler et al., 1997, Kleijnen et al., 1997). Through direct interaction with MHC class I complexes in the host cell, they help the virus avoid MHC class I-restricted $CD8^+$ T cell cytotoxicity. The *m152* gene encodes a 37/40-kDa glycoprotein that causes targeting arrest and subsequent accumulation of MHC class I molecules in the ER-Golgi intermediate compartment (Del Val et al., 1992, Ziegler et al., 1997). The *m04* and *m06* products encode 34 and 48 kDa glycoproteins, respectively, that attach tightly to mature $\beta_2$microglobulin-associated MHC class I molecules in the ER (Kleijnen et al., 1997). The *m06*/gp48-MHC class I complexes are targeted to the late-endosomes and lysosomes where they are rapidly degraded; the *m04*/gp34-MHC class I complex is targeted to the cell surface yet its function is unknown.

MCMV also affects MHC class II expression, not through direct protein-protein interactions, but indirectly by inducing the expression of antiviral cytokines. MCMV-induced expression of INFγ and IL-10 leads to downregulation of MHC class II molecules on the macrophage cell surface, and disrupts antigen presentation to $CD4^+$ T cells (Heise et al., 1998; Redpath et al., 1999).

3.2. Interference with the cytokine network

3.2.1 Viral homologs of host cytokines

MCMV encodes G protein-coupled receptor (GCR) homologs, e.g. *m33*, and chemokine homologs, called virokines (Davies-Poynter, et al., 1997; MacDonald et al., 1997; Fleming et al., 1999). GCRs serve to transduce signals through activating G proteins by binding chemokines, which are known to act as leukocyte chemoattractants. A *m33* gene transcript, arising from alternative splicing, encodes a peptide sequence that is highly conserved among GCRs, suggesting that this *m33* gene product isoform might interact with chemokines. The *m33* gene may stabilize the virus specifically in the salivary gland, as disruption of *m33* restricts viral replication in the salivary gland *in vivo* but not in fibroblasts *in vitro* (Davies-Poynter, et al., 1997). MCMV also produces a hybrid transcript of juxtaposed *m131* and*m129* sequences that encodes a viral homolog of a chemokine. Deletion of the *m131/129* chimeric sequence impairs replication in the salivary glands, and the mutant virus is rapidly cleared from the spleen and liver during acute infection. The accelerated clearance of the mutant was dependent on NK cells, $CD4^+$ and $CD8^+$ T cells (Fleming et al., 1999). These data suggest that *m131/129* may also provide a mechanism for immune evasion by the virus during early infection, possibly through the interference of NK cells and T cells.

3.2.2 Viral homologs of MHC class I molecules

When NK cells encounter the absence of MHC class I expression on target cells, they initiate their cytolytic activity. Thus, whereas the virus can circumvent CTL-mediated lysis of infected cells by downregulating host MHC class I molecules, this same

downregulation increases their susceptibility to lysis by NK cells. According to the missing self hypothesis (Sentman et al., 1995), downregulation of MHC class I would render MCMV-infected cells susceptible to NK cell lysis. However, NK cell-mediated control of infection is normal in *β_2m-/-* animals (Tay et al., 1995). This point can now be explained with the discovery that the virus expresses its own MHC class I homolog to escape surveillance by NK cells. The MCMV *m144* gene encodes a protein homologous to MHC class I proteins (Rawlinson et al., 1988), which forms a heavy chain-$\beta_2$microglobulin complex devoid of endogenous peptide. When mice are infected with a recombinant MCMV carrying a functional deletion of m144, infection is greatly attenuated in the spleen and liver (Farrell et al., 1997). In contrast, transfection of *m144* into fibroblasts can protect these cells from NK cell mediated lysis (Kubota et al., 1999). HCMV also encodes an MHC class I homolog, UL18, where transfection into a human B cell line confers resistance to all NK cells (Rayburn et al., 1998). Whereas no mammalian receptor for m144 has been yet identified to date, UL18, has been shown to bind MHC class I receptors as well as CD94 and a KIR family member, which are both expressed on NK cells (Reyburn et al., 1997; Cosman et al., 1997). Therefore, it is possible that *m144* and *UL18* act as surrogate ligands for these receptors and prevent NK cell-mediated lysis.

Section 4. Host genetic control of MCMV infection

Resistance to MCMV is under multigenic control, with contributions from both H-2 and non-H-2 genes. Whereas H-2 genes modulate the infectivity of individual target cells, non-H-2 genes can influence host resistance to infection by regulating naturally

occurring defense mechanisms. For example, inbred strains with the C57BL background (C57BL/6, H-2b; B10BR, H-2k) support significantly lower levels of MCMV replication in the spleen compared to H-2 syngeneic mouse strains with a BALB/c background (BALB.B, H-2b; BALB.K, H-2k) (Allen et al., 1984). In fact, these data provided some of the first evidence that non-H2 genes could affect host resistance. The following section will discuss the contribution of individual genes from these two classes to the overall response to MCMV infection.

4.1. The effect of H-2 genes

Resistance of adult mice to acute lethal infection with MCMV is controlled in part by genes of the H-2 complex coding for MHC class I molecules. Studies in H-2 congenic mouse strains demonstrated that animals possessing the H-2k haplotype, especially at the K/IA region, are 10 times more resistant than mice of the H-2b or H-2d haplotype. In fact, peritoneal macrophages from H-2d, H-2b, H-2v and H-2r are very permissive to MCMV infection, while H-2k cells remain relatively unaffected (Price et al., 1987, 1995). Moreover, susceptibility is a completely dominant trait (Grundy et al., 1981), and transfection of the H-2Kb or H-2Dd into H-2k macrophage and T cell lines potentiate MCMV infection (Wykes et al., 1993). At first the molecular basis for susceptibility was thought to depend on correct folding of MHC class I molecules, a process that requires β_2-microglobulin (Wykes et al., 1993). However, β_2-microglobulin -/- mice cannot fold MHC class I proteins properly yet exhibit similar organ viral titers and immune clearance as wild-type animals, indicating that proper folding is not required for infection (Polic et al., 1996). In any case, H-2 linked genes affect resistance or susceptibility to MCMV at the level of individual cells.

4.2. The effects of non H-2 genes

So far, non H-2 genes that determine susceptibility to MCMV have been shown to affect NK cell function, ascertaining to the major role of this cell compartment in the control of MCMV infection.

4.2.1. The *beige* mutation

In mice, the *beige* (*bg*) mutation is a recessive trait that causes hypopigmentation, bleeding and generalized dysfunction of immune cells, including NK cells. Mice homozygous for the beige mutation (*bg/bg*) are more susceptible to a lethal viral dose of MCMV than heterozygous *bg/+* C57BL/6 mice, and develop 33- to 43-fold higher virus titers in the liver, spleen, and kidney (Shellam et al., 1980; 1985). The *bg/bg* mouse serves as a model for human Chediak-Higashi syndrome, a disorder that increases generalized susceptibility to a variety of infections (Spritz, 1998).

The sensitization of *bg* mice to MCMV provided the first evidence for the importance of NK cells in early infection. Cloning of the *bg* gene was achieved by positional cloning and confirmed by genetic complementation *in vivo* (Perou et al., 1996; Spritz, 1998, review). *beige* mRNA is found in most mouse tissues, and its product regulates lysosomal fission (Perou et al., 1996, 1997). Interestingly, NK cells use their lysosomal compartment in the cytolytic process to transport reactive serine proteases, known as granzymes, and perforins to the cell surface. Impairment of this delivery process negatively affects NK cell cytolytic function. In support of a role for bg in NK cell function, irradiated recipients of bone marrow from *bg/bg* mice are more susceptible to MCMV and display reduced NK cell response to virus than recipients of *bg/+* marrow.

4.2.2 The *Perforin* gene

Perforin is a monomeric protein found in the cytotoxic granules of cytolytic cells such as CTLs and NK cells, and is a pivotal player in the mechanism of target lysis by NK cells. When NK cell cytolytic activity is initiated, cytotoxic granules are delivered to the plasma membrane. Upon release of perforin into the extracellular milieu, the monomer polymerizes into a pore-forming unit that inserts itself into the external lipid bilayer of the target cell. Unable to exclude ions and water, the target cell is lysed due to osmotic swelling (Abbas et al., 1997). The generation of a perforin-deficient mouse helped to elucidate both the key role of NK cells in clearing MCMV infection and tissue specific mechanims. At three days post-infection with MCMV, perforin$^{-/-}$ and wild-type mice show no differences in liver viral titers, yet splenic titers in perforin$^{-/-}$ mice were higher than those of wild type mice (Tay et al., 1997). When NK cells are depleted from perforin$^{-/-}$ mice, only titers in the liver increased, indicating that NK cells can also suppress infection via a perforin-independent, non-cytolytic mechanism. These results indicated that control of viral replication in the spleen, and not the liver, depends on the cytolytic activity of NK cells. Double mutant animals lacking both perforin and INFγ (perforin$^{-/-}$/INFγ$^{-/-}$) experience increases in both splenic and liver titers, indicating that INFγ production by NK cells is essential to control viral replication in the liver.

4.2.3. The *Cmv1* host resistance locus

Characterization of MCMV viral titers in different inbred mouse strains identified highly resistant (C57BL) and highly susceptible strains (BALB/c, A/J and DBA) that exhibited differences of 10^4-10^5 PFU in the spleen, thymus and bone marrow 3 days post-infection (Scalzo et al., 1990; Gibbons et al., 1997) (Figure 1). Genetic studies using these MCMV resistant and susceptible strains as parental strains to generate segregating F2 and backcross populations identified a single locus, *Cmv1*, which controls viral replication in an autosomal dominant fashion (Scalzo et al., 1990). Several lines of evidence demonstrated that NK cells are the site of phenotypic expression of *Cmv1*. A detailed discussion the process of genetic mapping, the *Cmv1* locus, and an evaluation of possible candidates for *Cmv1* will be discussed in section 5.

Section 5: The *Cmv1* Host Resistance Locus

5.1. Genetic Localization of the *Cmv1* locus

Mendelian analysis of the progeny between MCMV resistant and susceptible strains indicated that genetic control of early viral replication in the spleen segregated as a dominant trait controlled by a single autosomal locus, named *Cmv1* (Scalzo et al., 1990). The locus was assigned two alleles: $Cmv1^r$ (resistance) and $Cmv1^s$ (susceptibility). The chromosomal location of *Cmv1* and identification of nearby loci was determined by assessment of the splenic replication of MCMV in 2 sets of recombinant inbred strains, (RI) CXB/By and BXD (Scalzo et al., 1990, 1992). The distribution patterns of *Cmv1* in the RI strains was identical to that of markers known to reside within a region of

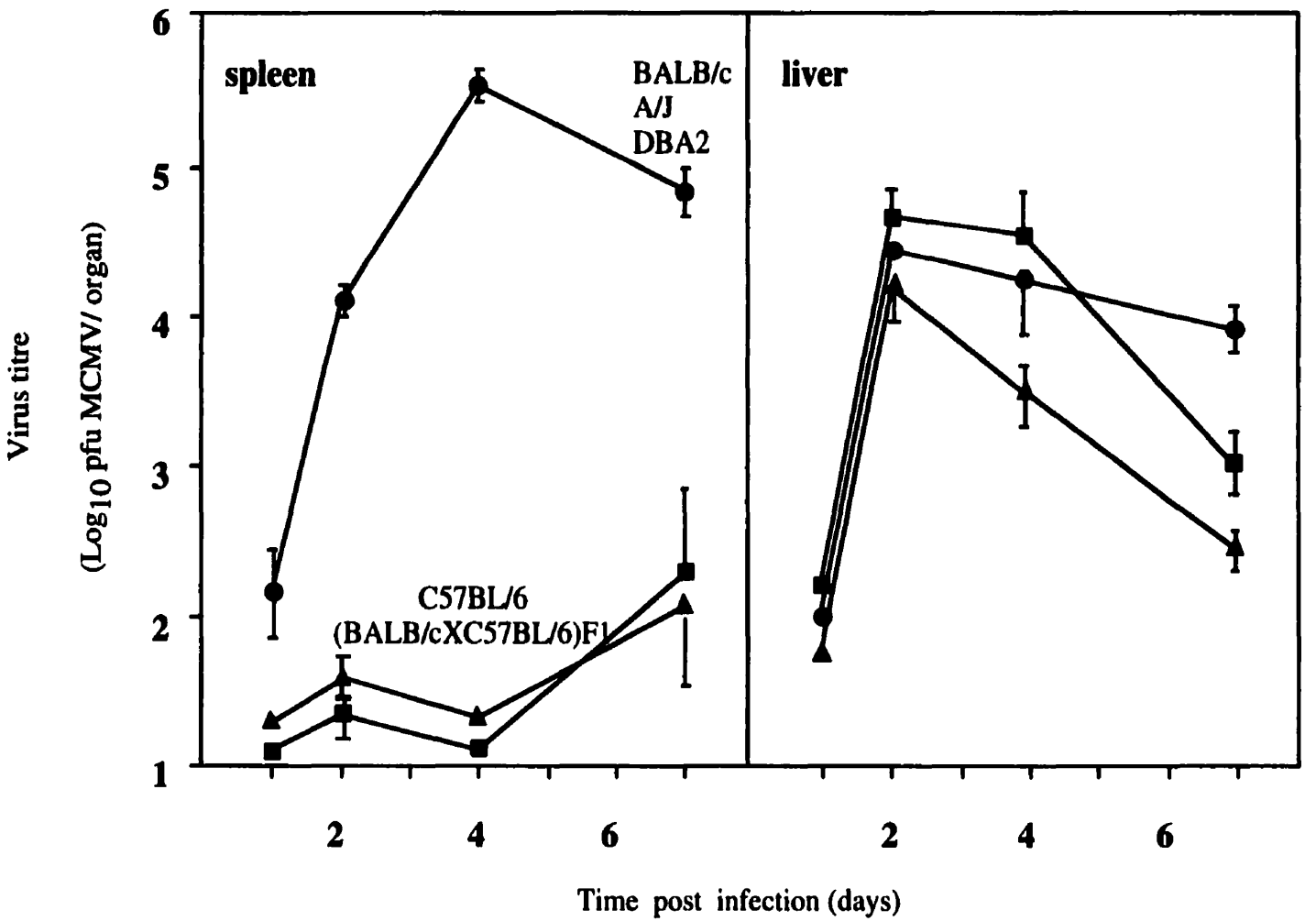

Figure 1: MCMV replication in spleen and liver of *Cmv1*^{r} and *Cmv1*^{s} strains
(From Scalzo et al., 1990)

chromosome 6 coding for genes and gene families preferentially expressed in NK cells, known as the NK complex, or NKC (Yokoyama et al., 1993; Scalzo et al., 1995). Since host NK cell response is responsible for the control of early viral replication, candidates for *Cmv1* may reside within the NKC. The following section will discuss the genes found in this complex and their role in NK cell function. As members of the Ly49 family have proven to the most likely candidates for *Cmv1*, these genes will be discussed in detail.

5.2. Expression of *Cmv1* in NK cells

The early control of splenic MCMV replication by *Cmv1* suggested that this locus should be expressed in a compartment involved in innate immunity that would be active prior to infection or shortly thereafter, such as the NK cell. Several lines of evidence implicate that NK cells are this compartment: (1) the increased susceptibility of *beige* mutant mice that are deficient in lysosomal function (Shellam et al., 1989; see section 4.2.2), (2) transfer of $Cmv1^r$ bone marrow to irradiated syngenic $Cmv1^s$ mice confers resistance (Scalzo et al., 1992), (3) selective *in vivo* antibody depletions of $CD4^+$, $CD8^+$ T cells or NK cells in $Cmv1^r$ mice indicated that NK cells were required for resistance (Welsh et al., 1990; Shanley et al., 1990; Scalzo et al., 1995), and 4) depletion of NK cells in adult C57BL/6 mice with antibodies to the NK cell markers asialo GM_1 or NK1.1 (antibody PK136) enhances viral replication in the spleen (Bukowski et al., 1984, Welsh et al., 1991, 1994, Scalzo et al., 1992). Finally, results stemming from *perforin-/-* mice demonstrated that the NK cells cytolytic activity is necessary for an effective control of viral replication (Kagi et al., 1995). Whereas NK cell-produced INFγ is most important in

controling liver replication (Tay et al., 1997), the *Cmv1* locus appears to be directly involved in the cytolytic activity of the NK cells and not the NK cell-produced cytokines.

5.3. The NK Receptors in the NKC: Candidates for *Cmv1*

In the mouse, many of the genes encoding surface molecules important in the function of NK cells are clustered in a 2 Mb genomic region designated the natural killer gene complex (NKC) (Brown et al., 1997). Genes found in this complex include *Cd69*, *Cd94*, as well as 3 gene families, *Nkrp*, *Nkg2*, and *Ly49* families (Brown et al., 1997; Ho et al., 1998; Vance et al., 1997). Homologous NKC regions can be found in human and rat on the syntenic region of chromosomes 12p13 and 4, respectively (Dissen et al., 1996;Ryan and Seaman, 1997; Suto et al., 1997; Yabe et al., 1993). As yet, all of the structurally defined NKC loci are disulfide-linked type II integral membrane proteins that share C-type lectin homology for Ca^{++}-dependant binding. Despite their structural similarities, these NKC-encoded receptors perform different functions. The following section will briefly describe these genes and their ascribed functions as recognition targets for activation and inhibition of NK cell cytolytic activity.

5.3.1. *Cd69*

The *Cd69* gene product forms disulfide-linked dimers at the cell surface of activated T cells, NK cells and other cell types (Hara et al., 1986; Cebrian et al., 1988; Lanier et al., 1988; Gavioli et al., 1992). Although a specific physiological ligand for the Cd69 receptor has not yet been described, it appears to bind carbohydrates in a calcium-dependent manner (Bezouska et al., 1995). *Cd69* is expressed on the NK cell surface only

upon stimulation with IL-2 or TNFα (Karlhofer et al., 1989). Cross-linking of Cd69 using anti-Cd69 antibodies promotes cellular activation, including calcium ion mobilization and NK cell cytolytic activity (Testi et al., 1989; Karlhofer et al., 1989). A precise role for Cd69 has yet to be determined; however the increased expression of *Cd69* following activation may serve to potentiate NK cell responsiveness (Ziegler et al., 199).

5.3.2. *Cd94* and the *Nkg2d* gene family

In humans, CD94 and NKG2 family members form disulfide-linked CD94/NKG2 heterodimeric cell surface receptors (Lazetic et al., 1996; Carretero et al., 1997; Brooks et al., 1997). Upon binding to polymorphic MHC class I molecules, the heterodimeric complex transduces inhibitory or activating signals to the NK cell (Braud et al., 1998; Borrego et al., 1998). Whereas *Cd94* is a single gene in mice and humans, there are five NKG2 human family members and four murine *Nkg2* family members, *Nkg2a-d* (Ho et al., 1998; Vance et al., 1998; Lohwasser et al., 1999). Interestingly, while *Nkg2a* and *Nkg2b* are the most homologous and *Nkg2d* is the most distantly related member (Lohwasser et al., 1999), only *Nkg2c* is the only member that does not contain an ITIM and thus may serve as an activating receptor. As with the human receptor complexes, mouse Nkg2d and Cd94 heterodimerize and bind to the non-classical MHC class I molecules, Qa-1 (Ho et al., 1998; Vance et al., 1998). It appears that Nkg2d must be disulfide linked to Cd94 for faithful targeting to the cell surface. Thus as Cd94 lacks a cytoplasmic domain and is the common subunit in the heterodimers, it may function primarily as a chaperone to indirectly facilitate Nkg2 receptor diversification.

5.3.3. The Nkrp1 gene family

The first murine NK cell receptor to be cloned, NK1.1, is the target of an activating NK cell-specific monoclonal antibody, PK136 (Ryan et al., 1992). Cross-linking of the NK1.1 antigen with PK136 induces NK cell cytolytic activity. NK1.1 is encoded by the *Nk1* gene, also called *Nkrp1c* (Ryan et al., 1992). Two other highly related family members, *Nkrp1b* and *Nkrp1a*, have also been isolated from mice and rats (Giorda et al., 1992). However, only one human homolog, *NKR-P1*, has been described (Westgaard et al., 1998). Interestingly, NK cells from *Cmv1*^{s} mouse strains do not react with the anti-NK1.1 PK136 antibody, yet almost 85% of*Cmv1*^{r}-derived NK cells do (Scalzo et al., 1995; Depatie et al., 1999), indicating an important phenotypic difference between the two classes of mice. These data elevate members of the Nkrp gene family as possible candidates for *Cmv1*.

Nkrp receptors are expressed on most NK cells and a subset of T cells (Giordia et al., 1990; Ryan et al., 1992; Yokoyama et al., 1993; Lanier et al., 1994), and to date have only been shown to interact with carbohydrates (Bezouska et al., 1994). The addition of monoclonal antibodies to these receptors stimulates phosphoinositide turnover (Ryan et al., 1991) and arachidonic acid production (Cifone et al., 1997) and increases intracellular Ca^{++} levels. Moreover, these reagents activate NK cell-associated cytolytic function and cytokine production (Chambers et al., 1989; Karlhofer et al., 1991; Arase et al., 1996). All rodent Nkrp1 molecules can associate with the phosphorylated form of the src-family kinase $p56^{lck}$ via their CXCP motifs found in their cytoplasmic domains (Turner et al., 1990), but only Nkrp1b has an immunotyrosine inhibitory motif (ITIM) in its cytoplasmic domain. ITIMs have been shown to associate with SH2-containing

molecules, including SHP1, to initiate downstream signaling of NK cell activation (Thomas et al., 1995).

5.3.4. The Ly49 gene family

The Ly49 family is comprised of 14 genes (Smith et al., 1994; McQueen et al., 1998). Of these, cDNAs for 9 members, *Ly49a-i*, have been isolated (Yokoyama et al., 1993; Takei et al., 1997). The presence of 5 additional genes, *Ly49j-n* , was deduced by sequencing of C57BL/6 genomic clones (McQueen et al., 1998). Further analysis of genomic clones and Southern blot analysis with *Ly49*-specific DNA probes have indicated that additional *Ly49* genes remain to be characterized (Lee et al., unpublished). Although it is clear that other *Ly49*-related sequences exist, it is not known if these correspond to bona fide genes, pseudogenes or merely to allelic variations of known *Ly49* genes. *Ly49* genes can be organized in 3 groups based on their degree of sequence homology: the first group includes *Ly49c, h, i, j, k* and *n*, the second includes *Ly49 d, g, l* and *m*, and the third features only *Ly49b*, the most divergent of the *Ly49* gene members.

Ly49 molecules, like Cd69, are also disulfide-linked homodimeric cell surface receptors (Mason et al., 1995; Stoneman et al., 1995; Chan et al., 1989; Yokoyama et al., 1989). Structural and functional diversity in the Ly49 family arise as a result of alternative splicing and allelic polymorphisms that alter sequences in both extracellular and cytoplasmic receptor domains (Brennan et al., 1996; Chan et al., 1989; Yokoyama et al., 1989,1990; Silver et al., 1996; Smith et al., 1994; Sundback et al., 1996). Ly49 cell surface expression is generally restricted to NK cells, although Ly49a is also expressed on a subset of T cells (Chan et al., 1989). Ly49 molecules are expressed in overlapping

subsets of the total NK cell population (Mason et al., 1995, Brennan et al., 1996, Brennan et al., 1994). Interestingly, Ly49 family members appear to be differentially expressed in phenotypically relevant mouse strains, including *Cmv1*^{s} and *Cmv1*^{r} mice; the proportion of the NK cell population that express individual Ly49 members can also vary according to strain (Brennan et al., 1994, 1996; Stoneman et al., 1995; Idris et al., 1999).

All Ly49 receptors bind MHC class I molecules and have a unique specificity for one or more MHC ligands (Karlhofer et al., 1992; Brennan et al., 1994; Mason et al., 1995, 1996; Nakamura et al., 1999). However, Ly49a and Ly49c can also bind carbohydrates through a carbohydrate recognition domain (CRD; Daniels et al., 1994; Brennan et al., 1995). The CRD and stalk regions of Ly49 have been proposed to be binding interfaces for the α1 and α2 domains of MHC class I molecules (Karlhofer et al., 1992, 1994; Brennan et al., 1996). NK cells that express Ly49A at their cell surface are unable to kill target cells expressing H-2^d, an inhibitory effect that could be reversed by addition of anti-Ly49a antibody (Karlhofer et al. 1992). Thus Ly49A on NK cells is an inhibitory receptor to prevent target cell lysis by NK cells.

Recent studies show that while most Ly49 family members possess inhibitory signaling properties, some receptors, including Ly49d and Ly49h, can activate NK cells (figure 2). It appears that such functional divergence arises from amino acid sequence alterations in the cytoplasmic domains of Ly49 receptors. Inhibitory receptors have a long cytoplasmic tail that contains the sequence VxYxxV, an ITIM motif. Recent studies (Olcese et al., 1996; Nakamura et al., 1997) have demonstrated that interaction of Ly49a with its physiological ligand, H-2D^d, overcomes protein tyrosine phosphorylation and phosphoinositide turnover events, hallmarks of early NK cell activation events.

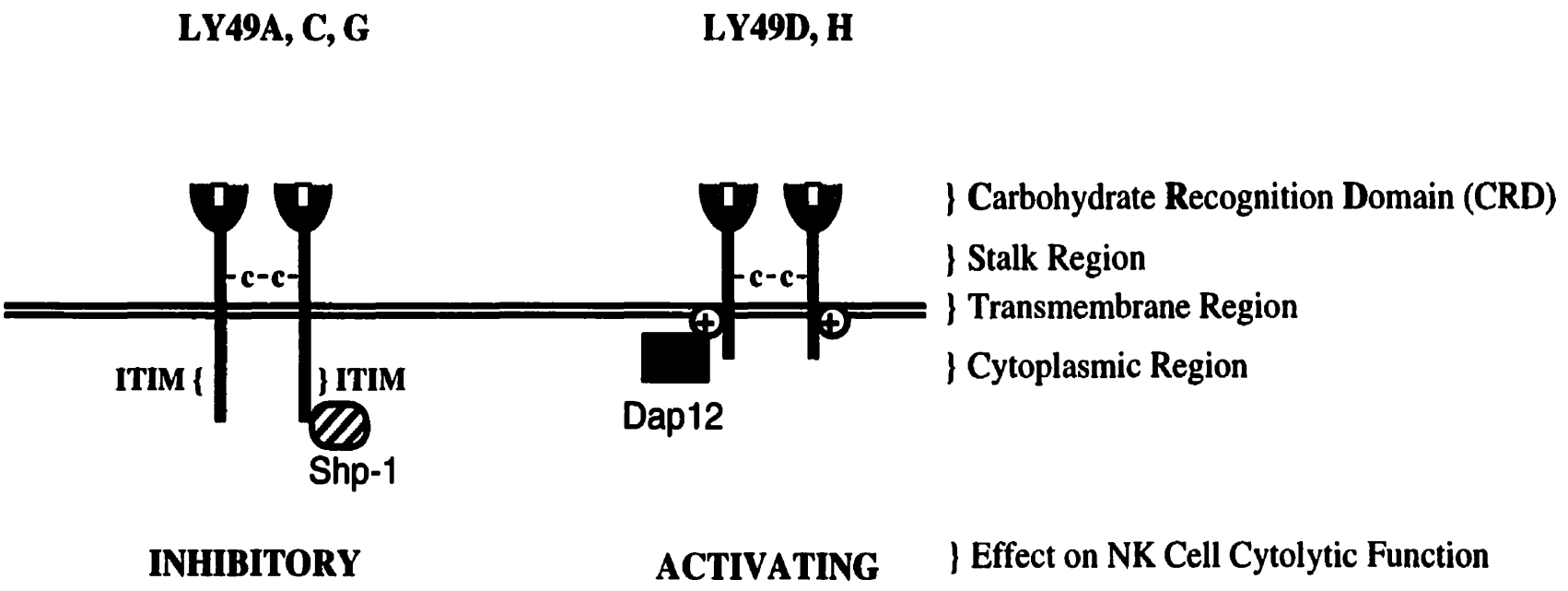

Fig.2: Schematic diagram of Ly49 receptors known to be expressed on the surface of NK cells. Inhibitory receptors have an ITIM (Immunoreceptor Tyrosine-based Inhibitory Motif) in their cytoplasmic tail that gets tyrosine phosphorylated and shown to associate with the phosphotases Shp-1 to attenuate intracellular signaling. Activating receptors have a charged arginine residue in their transmembrane domain that enables binding to neighboring molecules such as DAP12 that can trigger a positive signaling cascade to activate NK cell cytolytic function upon ligand binding.

Inactivation of NK cell cytolytic function by Ly49a involves the direct association of Ly49a with the protein tyrosine phosphatase SHP-1 through its ITIM, an interaction that leads to the subsequent dephosphorylation of phosphotyrosine residues generated upon cell activation (Olcese et al., 1996; Nakamura et al., 1997). Mice which display the 'motheaten' phenotype either display impaired SHP-1 function or lack SHP-1 altogether (Shultz et al., 1993; Koslowski et al., 1993; Tsui et al., 1993). Interestingly, these mice also exhibit impaired Ly49a-associated inhibitory functions in NK cells (Nakamura et al., 1997).

Two Ly49 receptors, Ly49d and Ly49h, have short cytoplasmic tails that lack an ITIM motif and transmit activation signals to NK cells. Ly49d and Ly49h associate with DAP12, a molecule that possesses an immunoreceptor tyrosine-based activation motif (ITAM), through a charged arginine residue in their transmembrane domain (Smith et al., 1998). Cross-linking antibodies induce complex formation between Ly49d/Ly49h and DAP12 and subsequent phosphorylation of both DAP12 and the tyrosine kinase Syk (Smith et al., 1998), events that result in NK cell activation. The decision of killing or sparing a target cell results from a balance between positive and negative signals received by the NK cell.

5.4 Other NKC host resistance loci

In addition to *Cmv1*, other phenotypically defined loci related to innate immunity have been assigned to the NKC. Other such loci include the *Chok* and *Rmp1* loci in mice (Idris et al., 1998; Delano et al., 1995) and the *Nka* locus in rats (Dissen et al., 1996). The

genetic and molecular dissection of the NKC will help clarify if these loci are allelic or correspond to different genes.

5.4.1 The *Chok* locus

The *Chok* locus underlies the differing capacity of BALB/c and C57BL/6-derived NK cells to lyse target CHO cells (Idris et al., 1998). Whereas IL-2-activated NK cells from BALB/c and C57BL/6 mice have an equivalent reactivity to most target cells, such as the prototypical NK cell targets, YAC-1 cells, BALB/c-derived NK cells are not able to lyse CHO cells as efficiently as their C57BL/6 counterparts. The *Chok* locus was recently identified as the *Ly49d* gene (Idris et al., 1999). In fact, the use of a recombinant vaccinia virus expression system to transfer expression of $Ly49d^{C57BL/6}$ into BALB/c ($Cmv1^{s}$) derived NK cells restored the capacity of NK cells to lyse xenogeneic CHO cells (Idris et al., 1999). As expression analysis of BALB/c mice demonstrated that this strain fails to express Ly49d at their cell surface, this could perhaps explain the deficiency.

5.4.2. The *Rmp1* locus

The *Rmp1* locus is one of four loci involved in susceptibility to ectromelia virus (mouse pox) and maps to the NKC (Brownstein et al., 1991, 1992, 1995; Delano and Brownstein, 1995). Ectromelia is an orthopox virus that infects most inbred strains of mice (Brownstein et al., 1989). DBA/2 mice, among others, are highly susceptible to this virus, yet C57BL/6 mice can control viral replication in major target organs such as the spleen and liver (Brownstein et al., 1989). Segregation analysis of crosses between DBA/2 and C57BL/6 strains has identified four noncontiguous *Rmp* loci on chromosome

6 (*Rmp1*), chromosome 2 (*Rmp2*), chromosome 17 (*Rmp3*) and chromosome 1 (*Rmp4*) (Brownstein et al., 1991, 1992, 1995; Delano and Brownstein, 1995). Infection of congenic strains containing the subchromosomal regions of all 4 C57BL/6-specific loci in a DBA/2 background has demonstrated that *Rmp1* is involved in mediating resistance in both the liver and spleen and *Rmp2* and *Rmp4* specifically affect splenic replication (Brownstein and Gras, 1997). Phenotypic similarity between the *Rmp1* and *Cmv1* loci indicate that these two loci may be allelic - antibody depletion of NK cells with the PK136 antibody in C57BL/6 mice renders these otherwise resistant mice susceptible to ectromelia infection (Brownstein and Gras, 1997).

5.4.3. The *Nka* locus

The *Nka* locus is located on rat chromosome 4, a region syntenic to mouse distal chromosome 6, and is associated with control of NK cell-mediated lysis of allogeneic lymphocytes (Dissen et al., 1996). Lysis of allogeneic cells, or alloreactivity, is the process underlying graft rejection in which MHC-incompatible cells are selectively recognized by NK cells and destroyed. PVG rats display alloreactive competence, unlike DA rats (Vaage et al., 1994; Rolstad et al., 1987; Fossum et al., 1987). This phenotypic difference is determined by *Nka*, an autosomal dominant gene located in the NKC (Dissen et al., 1996). *Nka* segregates from the *Cd94* and *Nkrp1*, but is tightly linked to the *Ly49* genes.

Section 6: Towards positional cloning: genetic and physical mapping

6.1 Linkage analysis

6.1.1 Generation of a high resolution genetic map

There are three steps in the process of positional cloning. First, formal linkage analysis is used to identify tightly linked markers that are closely linked to a locus of interest. Second, these markers are used to identify genomic clones that overlap the region which are used to construct a physical map. Finally, to identify sequences corresponding to genes, these genomic clones are screened for the presence of transcription units.

Linkage analysis can be performed at different degrees of precision, ranging from a broad chromosomal assignment to a high-resolution map, from which the order and interlocus distances between loci can be precisely determined. A stratified approach is used to position a locus with the highest resolution possible. First, to construct a low-resolution map, linkage data from a small number of animals (50-100 animals) that segregate a particular phenotype is obtained. This step confirms the chromosomal assignment of a locus and reduces the genetic interval of a particular locus. Moreover, the small number of animals involved allows for manageable testing of each animal for phenotype and genetic type using markers spanning the region of interest (see section 5.1.2). As crossover sites will be distributed at an average distance of 2 cM, a linkage analysis using 50 animals can specify a genetic interval with a minimum of 4 cM, whereas such intervals can average 20 cM prior to low-resolution mapping. The decrease

from 20 cM to 4 cM, and the identification of close flanking markers are essential for optimizing the construction of a high-resolution map.

As the resolution of a linkage map increases as the number of recombinant animals being analyzed increases, it is generally desirable to breed up to 1000 animals that segregate the mutant allele and then prepare a high-resolution map. Markers that were identified with the low-resolution map which flank the locus are used to screen for animals that have undergone a recombination event between the most closely linked markers. To limit the number of animals that require a complete determination of phenotype and genotype without decreasing the resolution of the linkage analysis, only these of recombinant animals are characterized further.

The breeding scheme used for a large panel of animals is the backcross. The breeding panel for linkage analysis of a resistance/susceptibility locus that segregates as a dominant trait would be as follows: (R x S) F1 x S, in which the dominant resistant allele is represented by R and the recessive susceptible allele by S. Progeny resulting from such a cross will display either the homozygous (SS) or the heterozygous (RS) genotype. Genetic markers are used to identify the location of crossovers; the order of these markers is also determined. Because the frequency of recombination between two loci is proportional to the length of DNA that separates them, markers that are closely linked will have fewer recombination events between them. Thus genetic distances can be determined by calculating the frequency of recombination between two markers.

Recombinant breakpoints can be located by following the segregation of the R allele, and the markers can be ordered with respect to the locus of interest to each other by minimizing the number of crossovers. The locus can then be positioned by inferring a

genotype from the phenotypic status of the recombinant animal. As novel markers are mapped within the interval defined by the limiting markers, the position of the locus can be further resolved by decreasing the original interval, and identifying new closely-linked genetic markers. The ultimate goal when generating a high-resolution map is to identify markers that exhibit one crossover on each side of the locus and as a consequence establish the minimal genetic interval in the cross.

6.1.2. Genetic markers

Linkage analysis involves monitoring the segregation of specific parental alleles in a mapping panel using polymorphic markers to genotype recombinant animals. Although cDNAs markers are often used, they are limited in number and their use requires labor-intensive detection methods. An important advance in genetic analysis was the discovery and use of PCR-based DNA markers, or microsatellites. Microsatellites, also known as simple sequence repeats (SSRs), consist of mono-, di-, tri- or tetranucleotide units that are repeated multiple times in a tandem array. They are found on average once every 18 to 30 kb of mouse genomic DNA, and there are an estimated 10^5 in the entire genome. Interestingly, SSRs are not conserved amongst distant species and have no apparent function. A distinct advantage of using SSRs is that they are highly polymorphic and can be rapidly typed in large mapping panels.

The class of SSRs most frequently found in the mouse feature repeats of $(CA)_n$, known as CA repeats. Allelic variation in these repeats arises from differences in the value of n. As the likelihood of detecting a polymorphism is proportional to the number of repeated units, polymorphisms are most often observed in CA-repeats with a value of

$n \geq 15$ (Weber, 1990; Dietrich et al., 1992). Sequence-specific primers that flank the SSR can be used to amplify the region surrounding the CA-repeat by PCR. The length of the resulting products will expand and contract with the number of repeat units, giving rise to a detectable size difference using gel electrophoretic techniques.

6.2 Physical mapping

6.2.1 Overview of physical mapping

Once a high-resolution genetic linkage map has been established for a particular locus, and closely linked markers have been identified, construction of a physical map of the region can begin. The purpose of generating a physical map is to: (1) clone fragments of the region to allow for molecular manipulation, (2) generate novel polymorphic markers that can be used to reduce the genetic interval, and (3) to determine physical distances between linked markers to convert genetic distances (cM) into physical ones (kb). The development of genomic libraries using different cloning vectors (e.g. YACs, BACs, and cosmids) has greatly facilitated cloning of large fragments of genomic DNA.

Assembling genomic clones that overlap the interval into a contig facilitates the generation of new markers called sequence tagged-sites (STS) (see section 6.3.3). Subsequent mapping of these new STS markers can establish overlap between genomic clones. In addition to using genomic clones to estimate physical distances, long-range restriction mapping of the inserts can be performed. Restriction mapping uses pulse field gel electrophoresis (PFGE) to characterize large genomic fragments (see section 6.3.4). Physical distances between markers can also be estimated by fluorescence *in situ* hybridization (FISH; see section 6.3.6).

6.2.2 Genomic Contig Assembly

6.2.2.1 Yeast artificial chromosome (YACs)

YAC cloning vectors contain the minimal sequences needed for propagation as a yeast chromosome, and can thus be used to clone large DNA fragments ranging from 200 kb to over 1 Mb. All YAC libraries have the following fundamental elements: (1) a cloning site within the SUP4 gene, (2) an autonomous replication sequence (ARS1) that provides the origin of replication necessary for propagation, (3) a centromere (CEN4), (4) two telomeric sequences (TEL) and (5) selectable markers on both sides of the centromere, TRP1 (tryptophane) and URA3 (uracil). The SUP4 gene encodes a tyrosine aminoacyl transferase ochre suppressor. Upon integration of a DNA insert, its sequence becomes disrupted and the recombinant yeast host undergoes a diagnostic color change (white to red). TEL and CEN4 provide telomere and centromere functions, respectively.

Although cloning large DNA fragments through YACs is very useful, the high frequency of chimerism, rearrangement and deletion within the YAC libraries complicates faithful recovery of the chromosomal region within the genetic interval. Chimerism can result from coligation of multiple genomic fragments or homologous recombination between repetitive regions. Although the use of recombinant deficient mutant yeast strain *rad52* (Chartier et al., 1992) has decreased the rate of chimerism, this problem still persists. Care must also be taken to manipulate YACs as they contain large DNA fragments that are susceptible to shearing, therefore, isolation protocols often involve embedding the clones in agarose to minimize shearing. Alternatively, YAC DNA

is often subcloned into more manageable vectors such as cosmids (see section 6.2.2.3) or commonly used bacterial vectors.

6.2.2.2 Bacterial Artificial Chromosome (BACs)

The BAC cloning vector is based on the *E. coli* fertility F factor plasmid and has an insert capacity of 300 kb (Shizuya et al., 1992). The vector contains all of the regulatory F factor genes that are essential for its replication: *oriS, repE, parA* and *parB*. The *oriS* and *repE* genes mediate the unidirectional replication of the F factor, while *parA* and *parB* maintain plasmid copy number at one or two per cell. Importantly, parA and parB activity also reduces recombination in the DNA inserts. The vector contains two cloning sites (HindIII and BamHI) flanked by T7 and Sp6 promoters thereby allowing direct sequencing of BAC ends for chromosomal walking. As BACs propagate large genomic fragments with a very low frequency of chimerism, their use in physical mapping projects is now widespread. Moreover, BAC manipulation and purification is more efficient than larger insert clones such as YACs. In practice, most BAC libraries contain inserts ranging from 30 to 300 kb and the insert size distribution, e.g. the proportion of large versus small inserts, can vary from library to library.

6.2.2.3 Cosmids

Cosmids, like other cloning vectors have cloning sites, an origin of replication and a selectable marker, and can accommodate inserts of foreign DNA up to 50 kb. What distinguishes the cosmid cloning vector is the presence of a lambda bacteriophage-derived *cos* site, a DNA segment from the phage genome that can be cleaved by the

lambda ter protein to generate a 12-bp cohesive (cos) overhang. When foreign genomic DNA is ligated to the linear cosmid vector, producing a concatamer, two *cos* sites that are separated by 40-50 kb are cleaved by ter to produce two cohesive ends. During incubation with bacteriophage head, tail and packaging proteins, these linear lambda-genomic DNA hybrids are packaged into mature phage particles. Upon injection into the bacterial cell, the recombinant cosmid DNA circularizes via the complementary cos ends, which are ligated by the host cell's ligase. The resulting circular molecule can replicate independently of host DNA. This type of system is most often used as a tool to clone YAC DNA into a more manageable form for manipulation.

6.2.3 Sequence tagged site content mapping

Positional cloning projects often require generation of novel markers within the region using genomic clones as substrates for cloning. Sequence tagged site (STS) content mapping is an important physical mapping method that meets this end. Briefly, STSs are unique genomic sequences that can be amplified by a defined set of PCR primers. Such sequences can be categorized as microsatellites, randomly derived genomic fragments, sequences from cDNAs or expressed sequence tags (ESTs). Although STS markers are densely packed in the genome, still greater resolution is required for physical mapping associated with positional cloning project.

STS content mapping involves screening of genomic clones for the presence of a particular set of STSs, in order to identify clones that contain an identical subset of STSs. As STSs are generally single copy probes, it can be inferred that clones with similar hybridization signals must overlap. Using this approach sets of contiguous overlapping

clones can be established. The Genome Mapping projects have placed great emphasis on the construction of STS content maps for YAC and BAC clones of both human and mouse DNA (see: http://www-genome.wi.mit.edu/) .

6.2.4 Pulse field gel electrophoresis (PFGE)

To characterize a candidate region and assign physical distance to genetic distances, long-range restriction maps are required. One of the most important techniques used in physical mapping, pulse field gel electrophoresis (PFGE), was introduced by Schwartz and Cantor (1984), and can resolve chromosomal fragments up to 9 megabases in length (Barlow and Leharch, 1987). Genomic DNA must be fractionated prior to electrophoresis. To restrict genomic clones into large, yet manageable sizes, rare cutting restriction enzymes that have recognition sites of 8 nucleotides and/or a site that has a CpG dinucleotide are used. CpGs dinucleotides are often associated with the 5' ends of genes and serve as excellent markers for the presence of transcribed genes (Bird et al., 1996).

High molecular weight genomic DNA, YAC and BAC clones are all digested with rare-cutting enzymes and the resulting restriction fragments are separated by PFGE. By monitoring Southern hybridization patterns using repeat-free probes derived from sequences in the region of interest, a detailed physical map of the region can be constructed. This mapping technique can unambiguously establish physical distances between probes and help establish colinearity between genomic clones (in YACs and BACs) used for contig construction and genomic DNA.

6.2.5 Radiation hybrid (RH) mapping

The generation of radiation hybrids involves the fusion of an irradiated cell line from one species to a second non-irradiated cell line from a second species (Cox et al., 1990). For example, commercially available mouse RH panels arise from the fusion of irradiated mouse cells to donor hamster cells (Research Genetics). The genetic heterogeneity between these two organisms provides sufficient sequence divergence to allow specific PCR-based detection of mouse and not hamster sequences.

In RH mapping, the order and distance of loci can be determined by assuming that the locations of X-ray-induced DNA fragmentation are randomly distributed throughout the genome. The calculated distance between two markers therefore is proportional to the length of DNA between them as the closer two markers are from each other, the more likely they will be retained on the same fragment. Using a PCR-based approach, hybrid clones that containing a given locus can be identified. Moreover, closely linked loci generally display similar retainment patterns that allow proximity of a set of loci to be inferred. RH panels are also useful in testing for chimerism in genomic clones from YACs and BACs. By determining similarities in retainment patterns between new markers and genetically anchored loci, it is possible to infer that a particular marker is linked or not using statistical analysis.

6.2.6 Fluorescence *in situ* hybridization (FISH)

The FISH technique uses fluorescent nucleic acid probes to localize genes or DNA sequences on intact chromosomes. Briefly, DNA (cDNAs, cosmids, BACs) or RNA probes are labeled with reporter molecules, such as biotin, and are then hybridized

to denatured metaphase chromosomes or interphase nuclei. Following addition of fluorescein-avidin, a probe-dependent fluorescent signal is visible by microscopy. When fluors with different fluorescent emission wavelengths are used simultaneously, distances between two or more target sequences can be estimated.

The choice of cell stage is dictated by the extent of resolution required. Staining metaphase chromosomes allows for the ordering of probes with a resolution of 2-3 Mb (Lawrence et al., 1990). Using interphase nuclei or extending chromatid fibers with mechanical stress can increase resolution to 50 to 1000 kb distances (Lawrence et al., 1988; Trask et al., 1991). When genomic clones that contain repetitive sequences are used (e.g. cosmids or BACs), unlabeled DNA enriched for repetitive sequences is added to prevent non-specific binding of the probe. Chromosome identification by G-band patterning can be achieved by staining with DAPI.

CHAPTER 2

HIGH RESOLUTION LINKAGE MAP IN THE PROXIMITY OF THE HOST RESISTANCE LOCUS *Cmv1*

We present, in this chapter, a high-resolution linkage map of the *Cmv1* host resistance gene on the distal part of mouse chromosome 6. The basis of this work was to initiate a positional cloning approach to clone *Cmv1*. Results described in this chapter have precisely mapped *Cmv1* and have identified closely markers to begin the process of establishing a physical map of the region.

The manuscript that follows has been published and is reproduced with the permission from the editor. Depatie C., Muise E., Lepage P., Gros P., and Vidal S.M. High resolution linkage map in the proximity of the host resistance locus *Cmv1*. Genomics 39, 154-163 (1997).

Abstract

The mouse chromosome 6 locus *Cmv1* controls replication of mouse Cytomegalovirus (MCMV) in the spleen of the infected host. In our effort to clone *Cmv1*, we have constructed a high resolution genetic linkage map in the proximity of the gene. For this, a total of 45 DNA markers corresponding to either cloned genes or microsatellites were mapped within a 7 cM interval overlapping the *Cmv1* region. We have followed the cosegregation of these markers with respect to *Cmv1* in a total of 2248 backcross mice from a preexisting interspecific backcross panel of 281 (Mus spretus X C57BL/6J)F1 X C57BL/6J and two novel panels of 989 (A/J X C57BL6)F1 X A/J and 978 (BALB/c X C57BL/6J)F1 X BALB/c segregating *Cmv1*. Combined pedigree analysis allowed us to determine the following gene order and intergene distances (in cM) on the distal region of mouse chromosome 6: *D6Mit216* - (1.9) - *D6Mit336* - (2.2) - *D6Mit218* - (1.0)- *D6Mit52* - (0.5) - *D6Mit194* - (0.2) - *Nkrp1/ D6Mit61/135/ 257/ 289/ 338* - (0.4) - *Cmv1/ Ly49A/ D6Mit370* - (0.3) - *Prp/ Kap/ D6Mit13/ 111/ 219* - (0.3) - *Tel/ D6Mit374/ 290/ 220/196/ 195/ 110* - (1.1) - *D6Mit25*. Therefore, the minimal genetic interval for *Cmv1* of 0.7 cM is defined by 13 tightly linked markers including two markers *Ly49A* and *D6Mit370* that did not show recombination with *Cmv1* in 1967 meiosis analyzed; the proximal limit of the *Cmv1* domain was defined by 8 cross-overs between *Nkrp1/ D6Mit61/ 135/ 257/ 289/ 338* and *Cmv1/ Ly49A/ D6Mit370* , and the distal limit by 5 cross-overs between *Cmv1/ Ly49A/ D6Mit370* and *Prp/ Kap/ D6Mit13/ 111/ 219*. This work demonstrates tight linkage between *Cmv1* and genes from the Natural Killer Complex (NKC), such as *Nkrp1* and *Ly49A*, suggesting that *Cmv1* may represent an NK cell recognition structure encoded in the NKC region.

Introduction

During their lifetime, 60-80% of individuals in developed countries and virtually 100% of those in developing countries will become infected with human Cytomegalovirus (HCMV) (Hanshaw, 1995). In most individuals HCMV infection will remain asymptomatic. In contrast, primary infection or reactivation of endogenous virus in immunosuppressed people, such as organ transplant recipients, newborn infants and AIDS patients may be severe and sometimes fatal (Alford and Britt, 1990; Gehrz, 1991). The infection of mice with murine Cytomegalovirus (MCMV) has served as a useful model of HCMV infection, since both viruses have similar biological properties and produce similar pathophysiology in their respective host (Staczek J., 1990).

Through the use of mouse models it is possible to dissect complex phenotypes of MCMV disease into distinct phases of host responses such as innate resistance/susceptibility or immune clearance of MCMV. The molecular genetic analysis can then identify single genes controlling those phenotypes. Genetic control of resistance to MCMV is indeed under multigenic control, with contribution of both H-2 and non-H-2 genes (Grundy et al., 1981). Whereas H-2 genes have been shown to modulate the infectivity of individual target cells (Price et al., 1990; Wykes et al., 1993), non-H-2 genes regulate naturally occurring defense mechanisms, such as those mediated by IFN and Natural Killer (NK) cells (Quinnan and Manischewitz, 1987; Shellam et al., 1985).

Cmv1 is an autosomal dominant non-H-2 locus that controls MCMV replication in the spleen, bone marrow, and thymus and also plays a role in determining the outcome of lethal infection (Scalzo et al., 1990; Price et al., 1993). The *Cmv1* gene has two alleles in inbred mouse strains: the dominant *Cmv1*^{r} (low titer, resistant) allele, present in

mouse strains with the C57BL background, and the recessive *Cmv1*^{s} (high titer, susceptible) allele, present in strains such as BALB/c, DBA/2J, and A/J. The course of infection following intraperitoneal inoculation of sublethal doses is characterized either by a rapid proliferation of MCMV in the spleens of *Cmv1*^{s} strains or a restriction of MCMV replication in *Cmv1*^{r} strains (Scalzo et al., 1990). Studies in radiation chimeras and bone marrow transplantation together with *in vivo* depletion of lymphocytic lineages with specific monoclonal antibodies have shown that the phenotypic expression of *Cmv1* is at the level of the NK (Scalzo et al., 1992). Thus, the differential capacity of inbred strains of mice to control viral replication would reflect the level of NK cell activity against virally infected targets by an as yet unknown mechanism (Scalzo et al., 1992).

Using recombinant inbred strains and a backcross panel of 99 animals (Scalzo et al., 1992; 1995), earlier studies placed the *Cmv1* on the distal part of chromosome 6 linked to the NK-cell complex (NKC). To precisely define the genetic interval delineating *Cmv1* we have generated a high-resolution linkage map of the *Cmv1* region by extensive segregation analysis. We have followed the segregation of 45 polymorphic DNA markers in two novel panels of 989 (A/J x C57BL/6J)F1 x A/J and 978 (BALB/C x C57BL/6J)F1 x BALB/C backcross progeny that are informative for *Cmv1*, and in a pre-existing interspecific backcross (C57BL/6J x Mus spretus)F1 x C57BL/6J composed of 281 mice. This analysis allowed to developed a detailed linkage map that spans 7.9 cM and established at 0.7 cM the minimal genetic interval of *Cmv1*.

Materials and Methods

Mice

Inbred mouse strains A/J, BALB/cJ, C57BL/6J were purchased from the Jackson Laboratory (Bar Harbor, ME). Resistant (*Cmv1*^{r}) C57BL/6J and susceptible (*Cmv1*^{s}) A/J and BALB/cJ inbred strains were used to produce 989 (C57BL/6J X A/J)F1 X A/J and 978 (C57BL/6J X BALB/cJ)F1 X BALB/cJ segregating backcross mice. We have previously described the breeding and maintenance of 281 (*M. spretus* X C57BL/6J)F1 X C57BL/6J interspecific backcross animals (Schurr et al., 1990).

Virus stock

The Smith strain of murine Cytomegalovirus (MCMV) was obtained from the American type Culture Collection (ATCC, Rockville, MD) and passaged twice in mouse submaxillary glands to restore virulence. Briefly, 3 week old BALB/cJ female mice were infected by intraperitoneal injection with 10^4 plaque forming units (PFU) of virus. Three weeks later, the mice were sacrificed and the salivary glands removed and pooled. The tissue was homogenized in a polytron in 5 volumes of Dulbeco minimal essential medium (D-MEM; Gibco/BRL) containing 10 % of eat inactivated Fetal Calf Serum (Gibco/BRL), before being clarified by low speed centrifugation, aliquoted and stored at -70^{o}C.

Typing of mice for resistance to MCMV infection

Backcross animals recombinant between anchor loci *D6Mit52* and *D6Mit25* were crossed to the respective susceptible parental strain (either A/J or BALB/c) to generate progeny retaining the recombinant chromosome and allow progeny typing. Mice were infected intraperitoneally with 0.1 ml of physiological saline containing 2 X 10^3 plaque

forming units (PFU) of MCMV. Three days after infection, mice were sacrificed, their spleens and livers removed and homogenized as described above. Whereas the *Cmv1* locus determines viral replication in the spleen, it does not affect viral load in the liver. Therefore, to ensure that mice were properly infected we have routinely determined the level of MCMV replication in the liver. The degree of infection was assessed by determining the number MCMV PFU per organ by plaque assay. Briefly, NIH 3T3 cells were seeded in 24-well tissue culture trays at 2 X 10^5 cells/ml/well in D-MEM medium supplemented with 2mM L-glutamine, 50 U/ml penicillin, 50 _g/ml streptomycin and 10 % heat inactivated FCS. After incubation for 24 h at 37 ^oC in a 95 % air 5 % CO2 atmosphere, the monolayers were washed once with absorption medium (D-MEM medium supplemented as before but containing 2 % FBS) and were infected with 0.2 ml of serial tenfold dilutions of organ homogenates in absorption medium. Virus was allowed to absorb for 90 min. at 37 ^oC in a 90 % air 10 % CO2 atmosphere before overlaying the plates with 2 ml of absorption medium containing 0.5 % SeaPlaque Agarose (FMC Corp., Rockland, ME). Four days later, infected cells were fixed for 20 min. with 10% formalin and MCMV plaques were revealed by staining with 1% methylene blue in 70% ethanol.

Molecular probes

A total of 34 simple sequence repeats (SSR) type markers defined by oligonucleotide primer pairs *D6Mit13, 12, 24, 25, 44, 52, 61, 109, 110, 111, 135, 151, 193, 194,195, 196, 197, 216, 217, 218, 219, 220, 256, 257, 289, 290, 300, 301, 333, 334, 336, 338, 370, 374* initially described by Dietrich et al. (1994) and known genes (*Ret, Gnb3, Nkrp1, Kcna1, Kap, Ly49A, Tpi , Prp, Cd69 , TEL* and *A2M* mapped to mouse

chromosome 6 and /or to the syntenic region of human chromosome 12p, were used to generate the linkage map. The primers used to amplify the microsatellite probes were purchased from Research Genetics (Huntsville, AL). Probes *Nkrp1*,*Tpi* and *A2M* were obtained from ATCC (Rockville, MD). *Ret* was kindly provided by Dr. Franklin Costantini (Columbia University, Department of Genetics and Development, New York), *Gnb3* by Dr. Michael Levine (Johns Hopkins University, Department of Endocrinology and Metabolism, Baltimore) and *Kcna1* was a generous gift of Dr. Bruce L. Tempel (VA Medical Center, Geriatric Research Education and Clinical Center, Seattle). *Kap*, *Ly49A* and *TEL* probes were amplified by reverse transcription of mouse polyA RNA from kidney and lung and from human lung RNA respectively followed by PCR, as described in Vidal et al. (1993). After a 2 min. denaturing step at 94 °C the PCR conditions were 1 min at 94 °C, 1 min at 55 °C, and 1 min at 72 °C for 30 cycles followed by a final extension of 7 min at 72 °C. Probes *Prp* and *Cd69* were amplified from genomic C57BL/6J DNA using the same conditions for PCR described above. The characteristics, sources, and nomenclature of clones corresponding to known genes used in restriction fragment length polymorphism (RFLP) analysis are summarized in Table 1.

Detection of polymorphisms and genetic typing

Genomic DNA was prepared from tail tip of individual backcross mice by incubation (12-16 h, 55 °C) in 700 µl of a buffer (100 mM Tris-HCl, pH8.0.5 mM EDTA, 200 mM NaCl, 0.2% SDS) containing 0.5 mg/ml Proteinase K, followed by RNase treatment (0.3 mg/ml; 2 h at 37°C). DNA was purified by serial phenol-chloroform extractions and ethanol precipitation. For simple sequence repeat polymorphisms (SSLPs), a 20 ng aliquot of genomic DNA was used for PCR

amplification in a 10 µl volume reaction. One of the two primers was end labeled with [γ-^{32}P]ATP using T4 polynucleotide kinase. The thermocycling program was as previously described (Dietrich et al., 1994). ^{32}P-labeled products were diluted two-fold in 100% formamide, denatured 5 min at 90 °C and electrophoresed in denaturing 8 % polyacrylamide gels containing 7 M urea and 1 X TBE buffer (0.09 M Tris-borate, 0.002 M EDTA, pH 8). For restriction fragment length polymorphism (RFLP), 5-10 µg of genomic DNA from different parental mouse strains was digested with a variety of restriction endonucleases (under conditions recommended by the supplier: Pharmacia, Montreal, Canada), electrophoresed in 1.0 % Agarose gels containing 1 X TAE buffer (40 mM Tris-acetate, pH 7.6, 20 mM sodium acetate, 20mM EDTA) and transferred by capillary blotting onto nylon membranes (Hybond-N, Amersham) in 20 X SSC (1 X SSC is 0.15 M sodium chloride, 0.15 M sodium citrate). Southern blots were hybridized with cDNA or genomic probes labeled to high specific activity with [α-^{32}P]ATP under conditions previously described (Vidal et al., 1992). Any RFLPs observed were further used to genotype backcross DNA samples. The polymorphisms of probes used for RFLP analysis in this study are listed in Table 1.

Linkage analysis

Genetic linkage was determined by segregation analysis. Gene order was deduced by minimizing the number of crossovers between different loci within the linkage group (Green, 1981). The combined recombination frequencies, estimated distances, and standard errors on these values were derived from Map Manager Program analysis version v2.6.5 (Manly et al., 1993) distributed by The Jackson Laboratory (Bar Harbor, ME) and available on the Web at http://mcbio.med.buffalo. edu/mapmgr.htlm.

Results

Genetic mapping strategy

Earlier studies have localized *Cmv1* on a 6.6 cM interval on distal mouse chromosome 6 flanked by the centromeric marker *D6Mit217* and the telomeric marker *D6Mit25* (Scalzo et al., 1995). We pursued two parallel experiments with the goal of identifying new genetic markers and generating more informative crossovers within the *D6Mit217/D6Mit25* genetic interval. First, to saturate efficiently the *Cmv1* candidate region with polymorphic markers, *D6Mit217* and *D6Mit25* were used as anchor loci to type an interspecific backcross panel of 281 (*M. spretus* X C57BL/6J) F1 x C57BL/6J backcross mice (referred to as the SBB cross). Recombinant animals identified between the anchor loci were further typed with a large number of polymorphic markers previously assigned to the distal portion of mouse chromosome 6. Although this panel was not phenotyped for *Cmv1* and hence does not provide direct information on the linkage to *Cmv1*, the approach is useful for rapid detection of markers localized within the *Cmv1* interval and their position with respect to one another. Secondly, to generate more informative cross-overs in the vicinity of *Cmv1*, two large intraspecific backcrosses segregating at the *Cmv1* locus were bred: an (A/J x C57BL/6J)F1 X A/J cross (referred to as the A/J cross, 989 mice) and a (BALB/cJ X C57BL/6J)F1 x BALB/cJ cross (referred to as the BALB/c cross, 978 mice). These 1967 animals were first typed with anchor loci *D6Mit216* (co-segregating with *D6Mit217* in the interspecific backcross panel) and *D6Mit25* to identify recombinant animals used for further analysis.

Virus stock and Cmv1 phenotype

In this study, we used the Smith strain of murine Cytomegalovirus (MCMV) propagated *in vivo* to restore virulence. This commercially available viral strain (ATCC) is different from the K181 laboratory strain originally used to phenotypically define the *Cmv1* locus (Scalzo et al., 1990). *In vivo*, the K181 strain of MCMV is more virulent than the Smith strain, whereas *in vitro* the K181 virus gives rise to foci of infection (or plaques) smaller than the typical Smith foci and in addition, the two strains of virus show small but significant differences in their DNA restriction endonuclease profiles (Misra and Hudson, 1980; Hudson et al., 1988), although differences in their major immediate early, early or late proteins have not yet been demonstrated (Hudson et al., 1988). We set out to reproduce the *Cmv1* phenotype with the Smith ATCC viral stock (see Material and Methods). Three fold dilutions of the viral stock were used to infect groups of 6 mice from the parental strains C57BL/6J, A/J and BALB/c to define the optimal inoculum. Three days after intraperitoneal infection with $2X10^3$ PFU, virus titers in the spleens of C57BL6/J (*Cmv1*^{r}) mice were 10^1-10^2 PFU/spleen (Log_{10} PFU/spleen = 1.4 +/- 0.67) whereas virus titers measured 10^3-10^4 PFU/spleen in animals from both *Cmv1*^{s} strains A/J (Log_{10} PFU/spleen = 4.43 +/- 0.55) and BALB/c (Log_{10} PFU/spleen = 3.88 +/- 0.50). In contrast to the spleen, the levels of MCMV replication in the livers were all similar for C57BL/6J, A/J and BALB/c (Log_{10} PFU/liver of 3.08 +/-0.27, 3.95 +/- 0.22 and 3.63 +/-0.34 respectively), consistent with the previous observation that the *Cmv1* locus is not manifested in this organ (Scalzo et al., 1990).

A total of 25 crossover animals were identified in the A/J cross and a total of 29 recombinants in the BALB/c cross yielding respectively estimated recombinational

distances of 2.5 cM and a 2.9 cM for the genetic interval flanked by loci *D6Mit52* and *D6Mit25*. These mice were typed for resistance to infection with MCMV. The *Cmv1* phenotype of the recombinant animals is shown in Figure 1. In 24 A/J recombinants tested over 25 (one recombinant mouse died before being tested), 15 had spleen titers greater than 3 X 10^3 PFU/spleen (Log_{10}= 4.1 +/- 0.32) and were typed as $Cmv1^s$. The remaining 9 mice had titers less than 2 X 10^2 (Log_{10}= 1.4 +/- 0.55) and were classified as $Cmv1^r$. By contrast, all mice showed similar liver titers of the virus, an organ where *Cmv1* is not phenotypically expressed. Out of the 29 recombinants from the BALB/c cross, 15 were typed as $Cmv1^s$ (Log_{10}= 3.66 +/- 0.43) and 14 as $Cmv1^r$ (Log_{10}= 0.82 +/- 0.19). The ratio of $Cmv1^s$ to $Cmv1^r$ backcross progeny (30:23) observed in our analysis is compatible with the predicted Mendelian ratio of 1:1 for a dominant trait under monogenic control.

Linkage analysis

The 11 cDNA markers tested were polymorphic in the interspecific backcross (*Mus spretus* x C57BL/6J)F1 x C57BL/6J. *CD69* and *A2M* were non-polymorphic in the A/J and BALB/C crosses and thus could not be mapped in both our informative crosses. Among the 34 SSLP-type markers, *D6Mit 111* was noninformative for the A/J cross while *D6Mit12*, *24*, *109*, *193*, *195* , *256*, *300*, *334* and *338* were not informative for both the A/J and BALB/C crosses. *D6Mit13* and *D6Mit52* were the only SSLP- type markers that could not be typed in the Spretus cross. The two markers *D6Mit217* and *D6Mit25*

Figure 1: Replication of MCMV in the spleens (◆) and livers (◘) of backcross progeny of the A/J cross (A) and the BALB/c cross (B) for recombinants between *D6Mit52* and *D6Mit25*. Three days after challenge with an intraperitoneal injection of 2X103 PFU of MCMV mice were sacrificed, their spleens and livers removed and homogenized before determining virus titers by plaque assay on NIH3T3 cell monolayers.

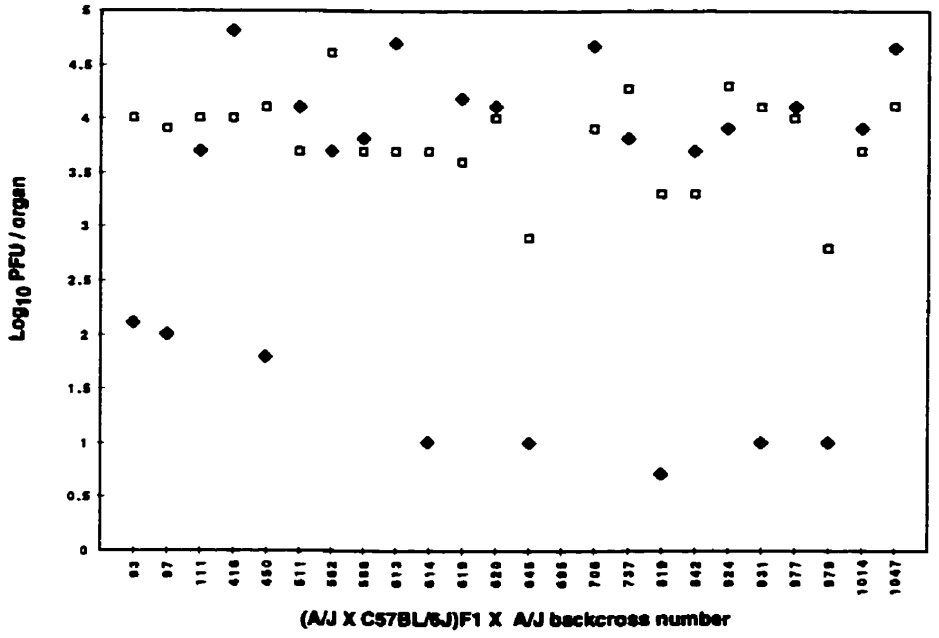
Log10 PFU / organ
(A/J X C57BL/6J)F1 X A/J backcross number

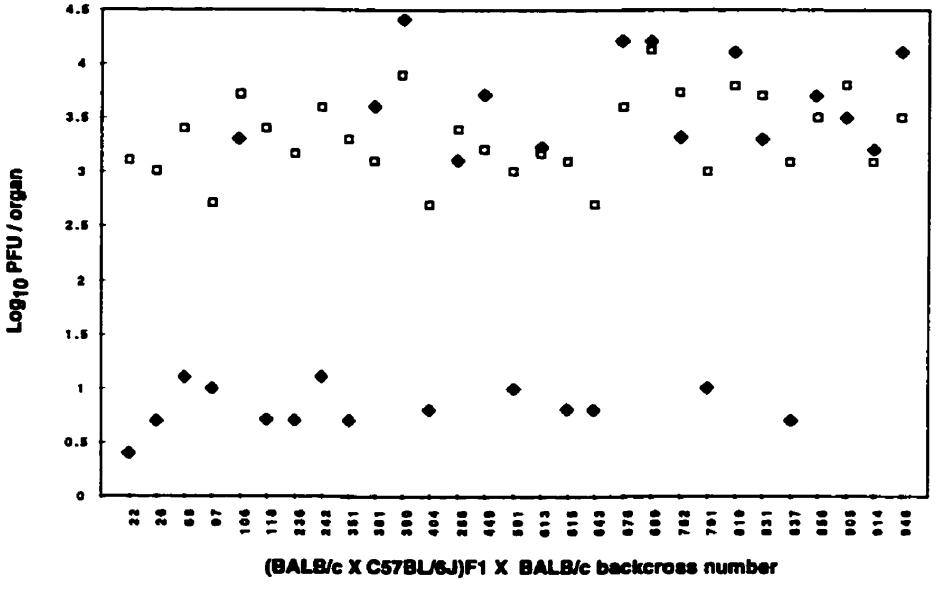
Log10 PFU / organ
(BALB/c X C57BL/6J)F1 X BALB/c backcross number

Figure 2: Haplotype analysis of backcross progeny. Each column represents a chromosomal haplotype identified in the backcross progeny (C57BL/6J X A/J)F1 X A/J (A) and (C57BL/6J X BALB/cJ)F1 X BALB/cJ (B). Open boxes: C57BL/6J (A)and (B). Closed boxes: A/J (A) and BALB/c (B). Hatched boxes: unknown. Only recombinant mice were tested for markers between *D6Mit216 and D6Mit25* , therefore the haplotype for non-recombinant mice is inferred. The number of animals possessing a specific haplotype is indicated at the bottom of each column.

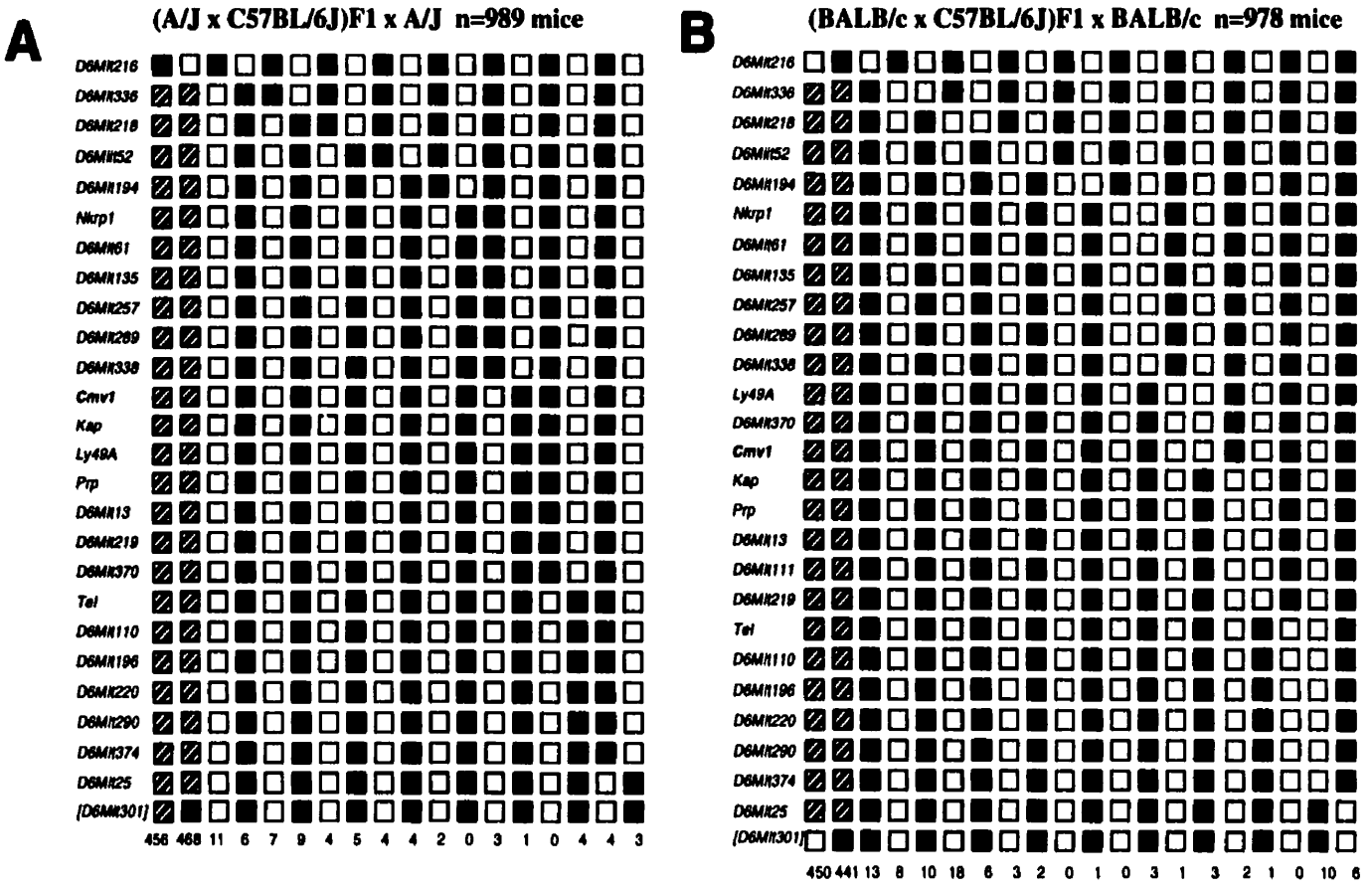
A
(A/J x C57BL/6J)F1 x A/J n=989 mice
D6Mit216
D6Mit336
D6Mit218
D6Mit52
D6Mit194
Nkrp1
D6Mit61
D6Mit135
D6Mit257
D6Mit289
D6Mit338
Cmv1
Kap
Ly49A
Prp
D6Mit13
D6Mit219
D6Mit370
Tel
D6Mit110
D6Mit196
D6Mit220
D6Mit290
D6Mit374
D6Mit25
[D6Mit301]
456 468 11 6 7 9 4 5 4 4 2 0 3 1 0 4 4 3
B
(BALB/c x C57BL/6J)F1 x BALB/c n=978 mice
D6Mit216
D6Mit336
D6Mit218
D6Mit52
D6Mit194
Nkrp1
D6Mit61
D6Mit135
D6Mit257
D6Mit289
D6Mit338
Ly49A
D6Mit370
Cmv1
Kap
Prp
D6Mit13
D6Mit111
D6Mit219
Tel
D6Mit110
D6Mit196
D6Mit220
D6Mit290
D6Mit374
D6Mit25
[D6Mit301]
450 441 13 8 10 18 6 3 2 0 1 0 3 1 3 2 1 0 10 6

flanking the *Cmv1* locus (Scalzo et al., 1995) were used as anchor loci to type the 281 animals of the interspecific SBB cross. We identified 14 crossover events, corresponding to a calculated interval of 5.1 cM (Fig. 3A) and used these mice for further genotyping of all other markers mapping within the two anchor loci. The ordering of markers within the most proximal (*D6Mit12, 24, 151, 193, 216, 217, 300, 334, 336, Ret, Gnb3*)and distal (*D6Mit25, 197, 301*) boundary clusters could not be accurately determined and probably reflects the fact that DNA markers mapping outside this interval will appear to cosegregate with the anchor loci used to detect crossovers since only recombinant mice were tested for all of the markers. Three other large clusters of DNA markers have been identified including 5 (*Kcna1, Tpi, D6Mit218, 256* and *333*), 7 (*A2m, Cd69, Nkrp1, 61, 135, 194* and *257*) and 6 (*D6Mit110, 111, 195, 196, 290* and *370*) loci and are respectively located at 1.8 cM, 2.9 cM and 3.3 cM from the proximal *D6Mit217* marker. Genetic mapping in the segregating (A/J x C57BL/6J)F1 x A/J backcross panel involved DNA typing from 989 individual backcross progeny with microsatellites *D6Mit216* and *D6Mit25*. We identified 67 recombinational events between *D6Mit216* and *D6Mit25*, producing a map distance of 6.8 cM between these two flanking markers (Fig 2A and 3B). Haplotype analysis for intervening polymorphic DNA markers identified in the interspecific cross and DNA markers previously reported to map on distal mouse chromosome 6 or human 12p. In this cross, *Cmv1* cosegregated with *Ly49A, Prp, Kap, D6Mit13, 219* and *370*. The proximal boundary of the *Cmv1* interval is defined by 4 crossovers between *Cmv1* and a cluster consisting of 5 SSLPs (*D6Mit 61, 135, 257, 289, 338*) and the *Nkrp1* gene. The distal marker to *Cmv1* is defined by 4 recombinational events between *Cmv1* and the cluster of 6 loci *Tel, D6Mit110, 196, 220,*

Figure 3: Genetic linkage map of mouse chromosome 6 surrounding the *Cmv1* locus. (*M. spretus* X C57BL/6J)F1 X C57BL/6J (A), (C57BL/6J X A/J)F1 X A/J (B) and (C57BL/6J X BALB/cJ)F1 X BALB/cJ (C). The gene order and the mapped loci were determined by pedigree analysis, and the intergene distances are given as estimates of recombination frequencies within backcross animals. The centromere of each chromosome is represented by a black circle. Recombination frequencies are shown to the right of the chromosome.

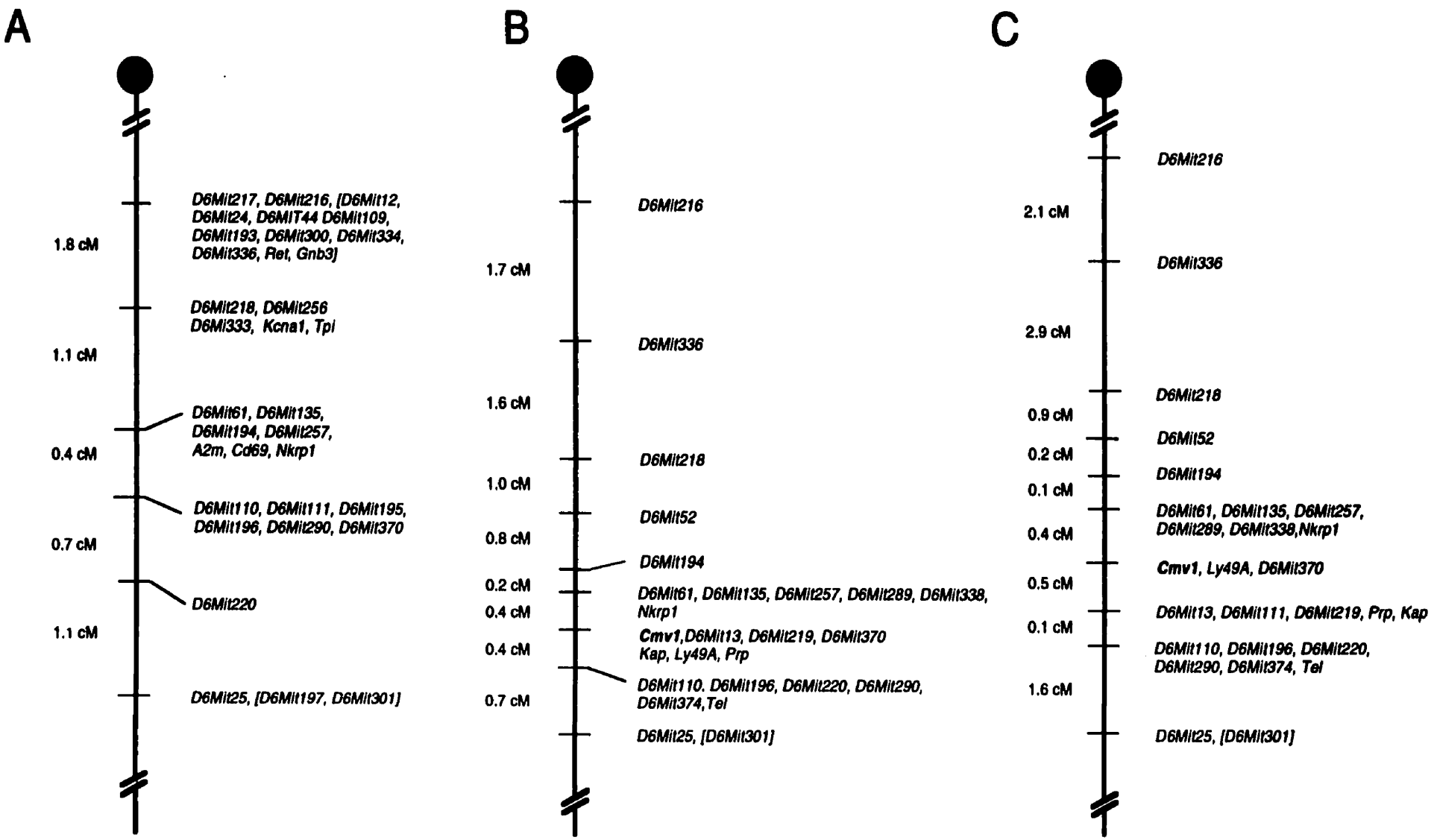
A
D6Mit217, D6Mit216, [D6Mit12, D6Mit24, D6MIT44 D6Mit109, D6Mit193, D6Mit300, D6Mit334, D6Mit336, Ret, Gnb3]
1.8 cM
D6Mit218, D6Mit256 D6Mi333, Kcna1, Tpi
1.1 cM
D6Mit61, D6Mit135, D6Mit194, D6Mit257, A2m, Cd69, Nkrp1
0.4 cM
D6Mit110, D6Mit111, D6Mit195, D6Mit196, D6Mit290, D6Mit370
0.7 cM
D6Mit220
1.1 cM
D6Mit25, [D6Mit197, D6Mit301]
B
D6Mit216
1.7 cM
D6Mit336
1.6 cM
D6Mit218
1.0 cM
D6Mit52
0.8 cM
D6Mit194
0.2 cM
D6Mit61, D6Mit135, D6Mit257, D6Mit289, D6Mit338, Nkrp1
0.4 cM
Cmv1,D6Mit13, D6Mit219, D6Mit370 Kap, Ly49A, Prp
0.4 cM
D6Mit110. D6Mit196, D6Mit220, D6Mit290, D6Mit374,Tel
0.7 cM
D6Mit25, [D6Mit301]
C
D6Mit216
2.1 cM
D6Mit336
2.9 cM
D6Mit218
0.9 cM
D6Mit52
0.2 cM
D6Mit194
0.1 cM
D6Mit61, D6Mit135, D6Mit257, D6Mit289, D6Mit338,Nkrp1
0.4 cM
Cmv1, Ly49A, D6Mit370
0.5 cM
D6Mit13, D6Mit111, D6Mit219, Prp, Kap
0.1 cM
D6Mit110, D6Mit196, D6Mit220, D6Mit290, D6Mit374, Tel
1.6 cM
D6Mit25, [D6Mit301]

290 and *374*. These results produced a recombinational distance of 0.8 cM for the minimal genetic interval of the *Cmv1* locus in which *Cmv1* was equidistantly localized at 0.4 cM from the distal and proximal limits.

In the other intraspecific (BALB/c x C57BL/6J)F1 x BALB/c cross, 87 recombinational events were identified between the two anchor loci used above giving a map distance of 8.9 cM. These recombinants were typed for all polymorphic DNA markers positioned with respect to *Cmv1* (Fig 2B and 3C). In a total of over 978 meioses analyzed, no recombinational events were detected between the *Cmv1* locus and *Ly49A* and *D6Mit370* in this cross. The proximal limit of the *Cmv1* genetic interval was defined by 4 crossovers (0.4 cM) between *Cmv1/Ly49A/D6Mit370* and the cluster *Nkrp1*, *D6Mit61*, *135*, *257*, *289*, *338* and the distal limit by 5 crossovers between *Cmv1/Ly49A/D6Mit370* and *Prp*, *Kap*, *D6Mit13*, *219* and *111* (0.5 cM), resulting in an estimated genetic distance of 0.9 cM for the *Cmv1* minimal genetic interval.

Table 2 summarizes the combined analysis of recombinational frequencies and intergene distances obtained from the 2 intraspecific crosses. The proximal boundary of the *Cmv1* interval was identical in both informative crosses and defined by the cluster *Nkrp1/ D6Mit61/ D6Mit135/ D6Mit257/ D6Mit289/ D6Mit338* 0.4 cM from *Cmv1* . The order of these six markers could not be determined because no crossovers were detected in a total of 1967 meioses. In contrast, genetic analysis of the BALB/c cross allowed us to identify informative crossovers and to order markers cosegregating with *Cmv1* in the A/J cross and to define the distal boundary with a higher resolution. Combined pedigree analysis for the 7.9 cM segment encompassing *Cmv1* on mouse chromosome 6 (Fig. 4) produced the following locus order and interlocus distance(cM): *D6Mit216* - (1.9) -

D6Mit336 - (2.2) - *D6Mit218* - (1.0)- *D6Mit52* - (0.5) - *D6Mit194* - (0.2) - *Nkrp1/ D6Mit61/135/ 257/ 289/ 338* - (0.4) - *Cmv1/ Ly49A/ D6Mit370* - (0.3) - *Prp/ Kap/ D6Mit13/ 111/ 219* - (0.3) - *Tel/ D6Mit374/ 290/ 220/196/ 195/ 110* - (1.1) - *D6Mit25.* In conclusion, these results delineate a minimal genetic interval for *Cmv1* of 0.7 cM defined by 13 tightly linked markers.

Figure 4: Composite genetic linkage map of mouse Chromosome 6 in the vicinity of the *Cmv1* locus. The order of the mapped loci was determined by pedigree analysis. Calculated recombination frequencies are shown to the left of the chromosome. the centromer is represented by a black circle. Human gene map location of mapped cDNAs (according to Unigene at **http://www.ncbi.nlm.nih.gov/UniGene/index.html**) are shown to the left of the chromosome.

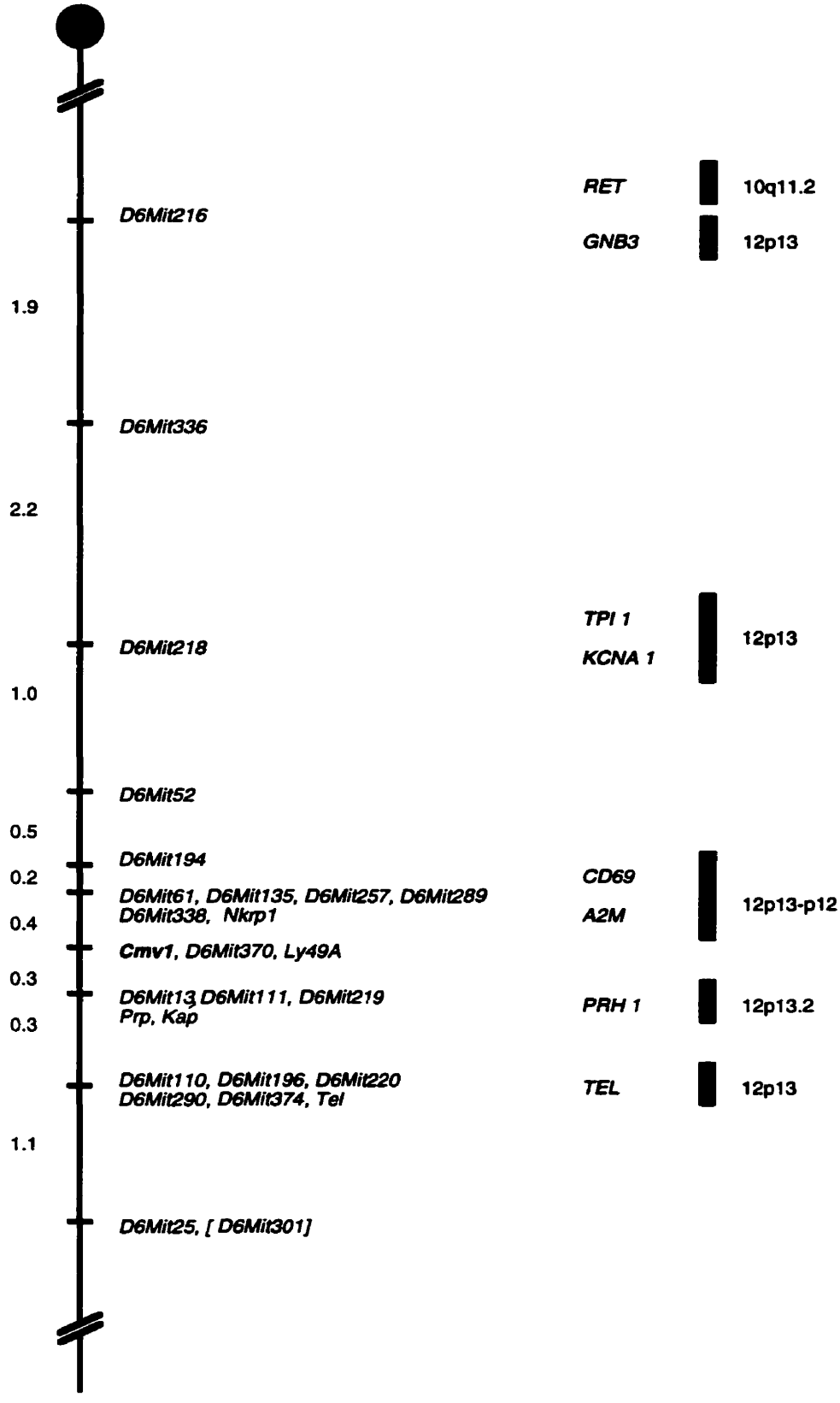
D6Mit216
1.9
D6Mit336
2.2
D6Mit218
1.0
D6Mit52
0.5
D6Mit194
0.2
D6Mit61, D6Mit135, D6Mit257, D6Mit289
D6Mit338, Nkrp1
0.4
Cmv1, D6Mit370, Ly49A
0.3
D6Mit13, D6Mit111, D6Mit219
Prp, Kap
0.3
D6Mit110, D6Mit196, D6Mit220
D6Mit290, D6Mit374, Tel
1.1
D6Mit25, [D6Mit301]
RET
10q11.2
GNB3
12p13
TPI 1
KCNA 1
12p13
CD69
A2M
12p13-p12
PRH 1
12p13.2
TEL
12p13

Discussion

The role of NK cells in defense against MCMV has been established through a variety of independent approaches: first, endogenous NK cell cytotoxic activity correlates with resistance to MCMV infection (Bancroft et al., 1981; Bukowski et al., 1984); second, *beige* mutant mice with defective NK cells are more susceptible to lethal MCMV infection (Shellam et al., 1981); third, in vivo depletion of NK cells by antibody treatment results in increased sensitivity to MCMV infection (Welsh et al., 1990). Whereas the evidence supporting the role of NK cells in defense against MCMV infection is persuasive, the mechanism for NK cell-mediated defense is still debated. The natural resistance *Cmv1* locus plays a key role in initial host defenses against virus infection by controlling NK cell function (Scalzo et al., 1990; 1992). The mechanisms by which NK cells bearing the $Cmv1^r$ allele are able to control early replication of MCMV are unknown but appear to be unlinked to either $IFN\gamma$ production or NK cell cytolytic activity against the T-cell lymphoma derived YAC-1 cell line (Scalzo et al., 1992). Characterizing the *Cmv1* gene and corresponding protein implicated in the natural resistance phenomena against MCMV should identify key host defense mechanisms regulated by the NK cells.

In the absence of an *in vitro* system or a known protein product, we have initiated a positional cloning approach to identify the chromosome 6 *Cmv1* locus. A pre-requisite for the success of this approach is the construction of a dense genetic map of the chromosomal gene region. Identification of closely linked markers can be used to construct a physical map of the region and serve as entry probes for chromosome walking towards the gene. As part of our effort to identify the *Cmv1* gene, we generated three

genetic maps using one interspecific and two intraspecific mouse backcrosses, involving a total of 2248 meioses. A preexisting Spretus backcross non-informative for *Cmv1* but highly polymorphic for mapping cDNAs was first typed to select anchor loci and intervening markers to be mapped in our A/J and BALB/c crosses, both informative for *Cmv1*. In both intraspecific crosses, the *Cmv1* locus maps to distal chromosome 6, as expected from previously reported backcross and recombinant inbred strain data (Scalzo et al., 1990; Scalzo et al., 1995). The combined analysis of our backcross data positions *Cmv1* with respect to 45 other chromosome 6 DNA markers. Our study delimits a 0.7 cM region overlapping the *Cmv1* locus where its proximal boundary is defined by 1 cDNA probe mapped by RFLP (*Nkrp1*) along with five microsatellites (*D6Mit61/ 135/ 257/ 289/ 338*), while the distal limit is formed by 2 cDNAs (*Prp/ Kap*) and three microsatellites (*D6Mit13/ 111/ 219*). Furthermore, we identified a microsatellite marker, *D6Mit370*, and a cDNA, *Ly49A*, that showed no recombination with *Cmv1* over 1967 meiosis analyzed and are thus considered to lie within 0.1 cM of the *Cmv1* locus, at the 95% confidence interval. If recombination frequencies were uniformly distributed along the chromosome, 0.1 cM of genetic distance should correspond to a physical interval of 214 kb (3000 Mb / 1400 cM = physical size of the mouse genome / genetic size of the mouse genome), an interval amenable to cloning in YACs.

Our results resolve the local order for 34 SSLP markers and 11 known genes on the distal region of mouse chromosome 6 keeping in agreement with a low resolution genetic map previously developed for these region (Scalzo et al., 1995).Two discrepancies have been identified with the Whitehead Institute SSLP Genetic Map for mouse chromosome 6 (Dietrich et al., 1994; last update June 11, 1996:

http://www.genome.wi.mit.edu/). First, in our Spretus cross *D6Mit109* localizes proximal of loci *D6Mit218, 256* and *333* whereas in the Whitehead map *D6Mit109* is positioned distal to them. Second, *D6Mitt290* maps distally of *D6Mit13* in our two intraspecific crosses whereas their order is inverse in the Whitehead map. The fine mapping of markers we have determined will hopefully serve to narrow down the localization of other major disease and modifier loci assigned to this region, including the genes responsible for *Bordetella pertussis*-induced histamine sensitization (*Bphs*, Sudweeks et al., 1993), an insulin-dependent diabetes susceptibility modifier gene (*Idd6*, Ghosh et al., 1993), a gene with major effect on susceptibility to induced lung tumors (*Pas1*, Malkinson et al., 1985) and a locus contributing to thymocyte-resistance to dexamethazone-induced apoptosis (Penha-Goncalves et al., 1996).

Comparative mapping of the mouse and human genomes have revealed a large region of homology between the distal region of mouse chromosome 6 and the short arm of human chromosome 12 including more than 30 human loci covering a genetic distance of more than 22 cM (Elliot and Moore, 1994; Seldin/Debry Human/Mouse Homology Map: http://www3.ncbi. nlm.nih.gov/Homology/). Many of these genes have been physically ordered on a second generation human chromosome 12 YAC contig (Krauter et al., 1995) thereby serving as a comparison map and a novel source of probes not yet mapped in the mouse. In doing so, we were able to assign the homologue of *TEL* (Translocation-ets-leukemia; Golub et al., 1994) to mouse chromosome 6, providing additional evidence for the human-mouse synteny in this region. Moreover, we observed a conservation of gene order between mouse and human loci *TPI -A2M/CD69-PRB3-TEL* mapping to YACs overlapping a 2.5 Mb interval (Krauter et al., 1995).

Our results show that *Cmv1* is tightly linked to loci of the NK gene complex (NKC) on the distal portion of mouse chromosome 6. The NKC is a cluster of gene families preferentially expressed in NK cells and encoding for receptors of the C-type lectin superfamily (reviewed in Yokoyama, 1995). Members of the *Nkrp* family encode for activation receptors, such as *Nkrp1* which encodes the NK1.1 mouse antigen (Giorda and Trucco, 1991; Ryan et al., 1992) and triggers NK cell activation pathways through target lysis. (Yokoyama et al., 1991; Bezouska et al., 1994). The *Ly49* gene family encodes for receptors which inhibit the NK cell's ability to kill upon binding to MHC class I molecules (Daniels et al., 1994; Karlhofer et al., 1992). Recent studies demonstrated that the T cell activation antigen *Cd69* , also a member of the C-type lectin superfamily, maps to the same region (Ziegler et al., 1994). Cd69 is expressed in B cells, NK cells and neutrophils where it might serve as a signaling receptor (Ziegler et al., 1994).

We were most interested in mapping *Nkrp1* since the presence of its gene product, NK1.1, seemed to correlate with MCMV resistance in inbred and recombinant inbred strains of mice (Scalzo et al., 1992; 1995). Our mapping effort was able to exclude *Nkrp1* as a candidate for *Cmv1* since these two loci segregate in both our informative crosses with distances of 0.4 cM and 0.5 cM. In contrast, *Ly49A* did not segregate from *Cmv1* in a total of 1967 meiosis. Because of its reported inhibitory function in NK cell activity, *Ly49A* does not appear as a likely candidate for *Cmv1*. In addition, *Ly49A* belongs to a family of at least 8 highly polymorphic genes (Smith et al., 1994) encoding each several alternatively spliced messengers. In all probability, sequencing of *Ly49* cDNAs among different inbred strains will not suffice to validate their candidacy on the

basis of molecular differences and it will be necessary to turn to "knock-out" experiments. The *Cd69* locus appears as another putative candidate for *Cmv1* although we were not able to determine its map position in respect to *Cmv1* in our intraspecific crosses as yet.

Although it seems likely that *Cmv1* may represent one of the encoded NKC genes, the possibility that *Cmv1* is a yet uncharacterized gene involved in the activation pathway or the cytolytic machinery of the NK cells is still valid. Interestingly, a recent report has localized an innate resistance locus to lethal ectromelia virus infection, named *Rmp1*, close to the NKC (Delano and Brownstein, 1995). Ectromelia are poxviruses which replicate in the cytoplasm and, unlike other DNA viruses, do not enter latency or persistence. As for cytomegalovirus, poxvirus infection results in down-regulation of MHC class I molecules surface expression. NK cells and interferon are involved in clearance of the viral infection and have been associated with genetic resistance to lethal infection with ectromelia virus (Jacoby et al., 1989). Identity between *Cmv1* and *Rmp1* could suggest that the gene encodes an effector molecule rather than a recognition molecule. The identification of tightly linked markers to *Cmv1*, we present here should help to elucidate whether *Rmp1* and *Cmv1* are allelic.

Although no evidence for genetic influence on pre-disposition to HCMV infection has been reported, studies with kidney transplantation recipients indicate that host factors influence the outcome of HCMV infection where the incidence of primary infection may vary from 34% to 64% as opposed to an 8% incidence of symptomatic infection (Ho, 1994). Although little is known about the role of NK cells in HCMV infection, *in vitro* experiments (Borysiewicz et al., 1985) and case-control studies (Biron et al., 1988;

Venema et al., 1994) suggest that NK responses may be equally relevant in both murine and human infections. Based on comparative genetic maps a *Cmv1* human homologue is predicted to exist, the high-resolution linkage map reported herein should help test the hypothesis that such a locus may be involved in HCMV susceptibility in high risk populations having a depressed immune response.

Acknowledgement

We wish to thank Dr. Ellen Bushman for critical reading of the manucript. We would like to acknowledge Susan Gauthier for technical assistance with animal breeding. This work was supported by a research grant to S.M.V. from the Medical Research Council (MRC) of Canada. S.M.V. is a recipient of a career award from the Fonds de Recherche en Santé du Québec.

TABLE 2

Combined Analysis of Recombination Fractions in (A/J X C57BL/6 J)F1 X A/J and (BALB/c X C57BL/6J)F1 X BALB/c Backcross Offspring for Chromosome 6 Loci in the Vicinity of *Cmv1*

	(A/J X C57Bl/6J) F1 X A/J	(BALB/c X C57Bl/6J) F1 X BALB/c	Genetic distance (cM ± SE)
D6Mit216-D6Mit336	17/ 989[a]	21/ 978	1.9 + 0.3
D6Mit336-D6Mit218	16/ 989	28/ 978	2.2 + 0.2
D6Mit218-D6Mit52	10/ 989	9/ 978	1.0 + 0.2
D6Mit52-D6Mit194	8/ 989	2/ 978	0.5 + 0.2
D6Mit194-D6Mit61	2/ 989	1/ 978	0.2 + 0.2
D6Mit61-D6Mit135	0/ 989	0/ 978	
D6Mit135-D6Mit257	0/ 989	0/ 978	
D6Mit257-D6Mit289	0/ 989	0/ 978	
D6Mit289-D6Mit338	0/ 989	0/ 978	
D6Mit338-mNKR-P1	0/ 989	0/ 978	
mNKR-P1-Cmv1	4/ 989	4/ 978	0.4 + 0.1
Cmv-1-Ly-49A	0/ 989	0/ 978	
Ly-49A-D6Mit370	0/ 989	0/ 978	
D6Mit370D6Mit13	0/ 989	5/ 978	0.3 + 0.1
D6Mit13-D6Mit111	0/ 989	0/ 978	
D6Mit111-D6Mit219		0/ 978	
D6Mit219-Prp	0/ 989	0/ 978	
Prp-Kap	0/ 989	0/ 978	
Kap-Tel	4/ 989	1/ 978	0.3 + 0.1
Tel-D6Mit110	0/ 989	0/ 978	
D6Mit110-D6Mit196	0/ 989	0/ 978	
D6Mit196-D6Mit290	0/ 989	0/ 978	
D6Mit290-D6Mit374	0/ 989	0/ 978	
D6Mit374-D6Mit220	0/ 989	0/ 978	
D6Mit220-D6Mit25	7/ 989	16/ 978	1.1 + 0.2
D6Mit25-[D6Mit301][b]	0/ 989	0/ 978	

[a]Recombination fractions are expressed as the number of recombinants divided by the number of backcross animals tested. Boxes indicate that only the proximal and distal markers at the boundaries of the boxed segments were tested.

[b]Position of locus in bracket is tentative as only recombinant mice were tested.

CHAPTER 3

Sequence-ready BAC contig, physical and transcriptional map of a 2 -Mb region overlapping the mouse chromosome 6 host resistance locus *Cmv1*

We present, in this chapter, an integrated YAC and BAC contig overlapping the *Cmv1* region. Tightly linked markers identified in Chapter 2 were used as anchor loci to screen for genomic clones. Analysis of these genomic clones have enabled the characterization of the physical region containing *Cmv1*, the identification of novel markers, the assembly of a transcription map and sequence-ready substrates in the form of a contiguous BAC contig spanning the *Cmv1* interval.

The manuscript that follows has been accepted for publication. Depatie C., Lee, S.H., Stafford, A., Avner, P., Belouchi, M., Gros P., and Vidal S.M. Sequence-ready BAC contig, physical and transcription map of a 2 Mb region overlapping the mouse chromosome 6 host resistance locus *Cmv1*. Genomics, in press.

Abstract

The host resistance locus *Cmv1* controls viral replication of murine cytomegalovirus (MCMV) in the spleen of infected mice. *Cmv1* maps on distal chromosome 6, very tightly linked to the *Ly49* gene family within a 0.35-cM interval defined proximally by *Cd94/Nkg2d* and distally by *D6Mit13/D6Mit111/D6Mit219/Prp/Kap* . To facilitate the cloning of the gene, we have created a high-resolution physical map of the *Cmv1* genetic interval that is based on long-range restriction mapping by PFGE, fluorescence in situ hybridization analysis of interphase nuclei, and the assembly of a cloned contig. Contig assembly was performed essentially by PCR screening of YAC libraries and hybridization of genomic BAC libraries, prior to clone validation by (1) restriction digest fingerprinting, (2) STS analysis, (3) Southern hybridization's, and (4) mapping of clone ends. This contig contains 25 YACs anchored by 71 STSs and 73 BACs anchored by 49 STS. We also report the cloning of 31 new STSs and 18 new polymorphic markers. A minimum tiling path (MTP) was defined that consists of either 4 YACs or 13 BACs covering 1.82 Mb between the closest proximal marker *D6Ott8* and *D6Ott115*, the closest distal marker. Gene distribution in the region includes 14 *Ly49* genes as well as 3 new additional transcripts. This high-resolution, sequence-ready BAC contig provides a backbone for the identification of *Cmv1* and its relationship with genes involved in innate immunity.

Introduction

Despite advances in the use of antiviral agents, disseminated cytomegalovirus (CMV) infection is a life threatening consequence of immunosuppression in neonates, graft recipients and AIDS patients (van der Meer, 1996). Host defense mechanisms against this infection and mechanisms underlying long term persistence and replication of CMV remain unclear and need to be better understood. To this end, experimental infection of mice with mouse cytomegalovirus (MCMV) is an excellent model of CMV disease that allows the dissection of different stages of infection facilitating the identification of possible genetic determinants (Stazcek, 1990).

In laboratory mice, the early response to murine cytomegalovirus (MCMV) infection is determined by an autosomal dominant non-H-2 locus, designated *Cmv1* (Scalzo *et al.*, 1990). *Cmv1* controls MCMV replication in the spleen, bone marrow, and thymus but not the liver (Scalzo *et al.* 1990, Price *et al.*, 1993, Tay *et al.*, 1997). The *Cmv1* host resistance gene presents two alleles: the susceptibility allele $Cmv1^s$, expressed in BALB/c, A/J and DBA strains, and the resistance allele $Cmv1^r$, expressed in C57BL-related strains. Phenotypically, resistant mice display splenic viral titers 10^3 to 10^4 times lower than those found in susceptible mice from day 2 post-infection following injection with a sublethal dose of virus (Scalzo *et al.*, 1990). *In vivo* antibody depletion of specific cell populations has indicated that the Natural Killer (NK) cell is the site of phenotypic expression of the genetic difference at *Cmv1* (Welsh *et al.*, 1990; Scalzo *et al.*, 1992). NK cells constitute a component of the natural immune system that provides the first line of defense against a variety of viral and bacterial infections and tumor surveillance (Biron, 1997; Scott and Tinchieri, 1995; Whiteside and Herberman, 1995). However, the exact mechanism by which NK cells bearing the $Cmv1^r$ allele control MCMV replication remains unknown. Studies in mice bearing targeted disruptions at specific genes together with

antibody depletion experiments indicate that the action of *Cmv1* is comprised of a perforin-dependent and IFN-γ independent function (Kagi et al., 1995; Tay et al., 1997).

Cmv1 has been mapped initially to the distal portion of mouse chromosome 6 (Scalzo *et al.*, 1990) within a well-defined cluster of NK cell receptor genes termed the Natural Killer gene complex (NKC) (Yokoyama *et al.*, 1991; Brown et al., 1997). These receptors belong to the C-type lectin superfamily and form either homodimers, such as the NK1.1 and Ly49 families, or heterodimers, such as Cd94/Nkg2d, that modulate NK cell cytolitic activity (reviewed in Lanier, 1998). In addition to *Cmv1*, three phenotypically defined loci controlling NK-cell-mediated innate immunity have been recently associated to the NKC: *Rmp1*, one of the 4 loci controlling resistance to ectromelia virus in mice (Delano and Brownstein, 1995); *Chok*, a mouse locus controlling tumor killing by NK cells (Idris et al., 1998) and *Nka*, a rat autosomal dominant locus that controls NK cell lysis of allogeneic lymphocytes (Dissen et al., 1996). These results indicate that either a single master locus or very tightly linked loci determine NK-cell function and establish genes of the NKC as strong candidates.

To understand the mechanism of action of *Cmv1* and its relationship with innate immunity loci, we have initiated a positional cloning approach to isolate the gene. Using segregation analysis in populations of informative backcross mice we localized *Cmv1* to a 0.35-cM interval (Depatie et al., 1997; 1999). Gene order and intergene distances (in cM) in the vicinity of *Cmv1* were: *Nk1.1/D6Mit61/D6Mit135/D6Mit257/D6Mit289/D6Mit338* - 0.3 - *Cd94/Nkg2d-* (0.05)-*Ly49a/Ly49c/Ly49g/D6Mit370/Cmv1-* (0.3)-*Prp/Kap/D6Mit13 /111/219* (Depatie *et al.*, 1997; 1999). These results exclude *Nk1.1*, *Cd94* and *Nkg2d*, while retaining *Ly49a, -c* and *-g* as candidates for *Cmv1*. A similar cloning effort by Forbes *et al.* (1997) excluded *Ly49* genes as potential candidates by placing *Cmv1* distal to *Ly49a* gene. However, several critical recombinant mice had intermediate phenotypes that may reflect aberrant titers or involvement of other NKC genes in the *Cmv1* phenotype. As

well, the development of 18 intra-NKC recombinant and congenic strains showed no recombination between *Cmv1* and the *Ly49* gene cluster (Scalzo *et al.*, 1999).

The full complexity of the *Ly49* family remains to be understood: up to date 14 *Ly49* genes (designated *Ly49a-n)* clustered on mouse chromosome 6 have been cloned and other as yet uncharacterized *Ly49* genes may be localized within the *Cmv1* interval (Takei *et al.*, 1997; McQueen *et al.*, 1998). One human, *Ly49L*, and several rat homologues have been localized to the respective syntenic regions to mouse chromosome 6 on human 12p12-13 and rat chromosome 4 (Westgaard *et al.*, 1998; Dissen *et al.*, 1996). *Ly49* receptors are specifically expressed in subsets of NK cells and T cells (reviewed in Takei et al., 1997). They encode MHC class I receptors that elicit intracellular signals that turn on/off the lytic machinery of NK cells and they present allelic variants specific to $Cmv1^r$ and $Cmv1^s$ mouse that preclude assessment of their candidacy based on mutation analysis (Brennan et al., 1996; Sundback et al., 1996, Yokoyama et al., 1990; Smith et al., 1994). Using *in vivo* antibody depletion experiments targeted against Ly49A, Ly49C, Ly49G2 and Ly49I expressing cell subsets, we (Depatie *et al.*, 1999) and others (Tay *et al.*, 1999) have shown that these cell populations are unlikely to be involved in MCMV resistance during early infection. However, other family members are likely to localize to the *Cmv1* interval and *Ly49d* has been identified recently as the gene product of the cytotoxicity locus *Chok*. (Idris *et al.*, 1999). Therefore, the candidacy of this gene family for *Cmv1* cannot be disregarded at this point.

As the next step for the positional cloning of *Cmv1*, we have established a detailed physical map of the region of chromosome 6 carrying the *Cmv1* interval based on fluorescence *in situ* hybridization (FISH) and a high-resolution YAC/BAC contig. Whereas YAC clones allow a rapid walk on the chromosome, this benefit is undermined by a high rate of chimerism and re-arrangements (Chartier, 1992). Therefore, to complement YAC mapping we generated a physical map based on BACs. The fidelity of BACs (i.e.

absence of chimeras, deletions, rearrangements) together with the ease of purification make this an excellent source of intact genomic DNA for gene identification and gene transfer experiments. We report here on the construction of a contiguous 2 Mb BAC array overlapping the *Cmv1* critical genetic interval. Forty-one new STSs, 18 new genetic markers and 17 transcription units were mapped to the contig. The availability of a high-density BAC contig overlapping the *Cmv1* region should greatly facilitate further transcriptional mapping, positional cloning and sequencing of this important region.

Materials and Methods

Genomic Library Screening and Contig Assembly

Oligonucleotide primer pairs corresponding to 13 anchor loci located in the vicinity of *Cmv1* were used to isolate YAC clones by PCR based screening of the ICRF (Larin *et al.*, 1991), WI/1, MIT II (Kusumi *et al.*, 1993) and WI/MIT820 (Haldi *et al.*, 1996) YAC libraries. PCR conditions were as described for genetic mapping (Depatie *et al.*, 1997). YACs were propagated in AHC medium (1L contains 1.7 g yeast nitrogen base without amino acids, 5.0 g $(NH_4)SO_4$, 10 g acid hydrolyzed casein, 20 mg adenine hemisulfate, pH 5.8). Genomic DNA was isolated from yeast cultures as previously described (Philippsen *et al.*, 1991). YAC end fragments were isolated with the bubble PCR amplification method (Riley *et al.*, 1990) or the YAC-end rescue method (Hermanson et al., 1991).

Initial BAC clones were obtained by screening two C57BL/6-derived BAC libraries spotted on high-density filters (Genome Systems Inc. and Research Genetics) with several anchor probes including *Ly49a* cDNA. BAC DNA was prepared using a Qiagen midi-prep kit (Qiagen) according to the manufacturer's instructions for BAC isolation. At least 1 μg of BAC DNA was used for BAC-end direct sequencing (with Sp6 or T7 oligonucleotides) using the BigDye™ terminator cycle sequencing chemistry (Perkin Elmer) or ThermoSequenase™ radiolabelled terminator cycle sequencing kit (Amersham Life Sciences) following conditions specified by the manufacturer. Sequences derived from BAC and YAC ends (Table 1 and 2) were compared to sequences in public databases through the BLAST server at the National Center for Biotechnology Information (Altschul *et al.*, 1983). Identified single-copy sequences were used to derive primer pairs for STS-content mapping by PCR using conditions described for genetic mapping (Depatie *et al.*, 1997) in addition to serving as radiolabeled probes (Feinberg and Vogeslstein, 1983) for

bi-directional chromosomal walking on the gridded BAC libraries.

Restriction analysis was performed on YAC clones embedded in agarose blocks prepared as described previously (Philippsen et al., 1991). Prior to pre-equilibration with 1x restriction buffer, agarose blocks were digested with restriction enzyme *BssH* II, *Mlu* I, *Not* I and *Nru* I (New England Biolabs). Blocks (1/4 block per lane) were loaded on a 1% agarose gel with 0.5 X TBE and resolved by contour-clamped homogeneous electric field (CHEF, Bio-Rad) using these PFGE conditions (6 V/cm, 120° angle, linearly ramped switching times from 70-120 sec for 24h or 40-70 for 20 h). Gel transfer and hybridization were performed as previously described (Malo et al., 1993). BAC DNA digestions with the above enzymes were loaded on a 1% agarose gel with 0.5X TBE (14°C) and resolved as these PFGE condition (6 V/cm, 120° angle, fixed pulse time of 8 s for 15 h). Results were visualized by ethidium bromide staining.

Genetic mapping

Mice backcross panels and high resolution genetic mapping protocols for the *Cmv1* locus, have been described previously (Depatie *et al.*, 1997). New polymorphic markers derived from genomic clones were typed on animals recombinant between *D6Mit52* and *D6Mit25* (n=37), two anchor loci encompassing the *Cmv1* locus. Genotyping by SSLP was performed as previously described (Depatie et al., 1997) and SSCP conditions for *Ly49b* were performed with the following electrophoretic conditions: 6% polyacrylamide (99:1) gels containing 5% glycerol and run at 15W for 4-8h at room temperature. Gels were dried and exposed to film with intensifying screens at –80 °C for 12 hrs. Some nucleotide variations were confirmed by automated sequencing of selected PCR products.

Identification of Novel Simple Sequence Length Repeats (SSLP)

SSLPs were cloned from either YAC-derived cosmids or from BACs. Characteristics of the SSLPs used in this study are listed in Table 2. Selected cosmid clones derived from an *Mbo* I digestion of YAC 109B5 and YAC 87M6F7 (see Table 3 for source) were subcloned into the *BamH* I site of plasmid pBluescript II KS^+ (Stratagene) and transformed into *E.coli* DHα5 strain to create small insert libraries. BAC DNA digested with *Hae* III was also subcloned as described above. The nylon filter replicates (Hybond N: Amersham Life Science) of the small insert libraries were screened for dinucleotide repeats using poly dAdC:dTdG (Pharmacia Biotech) labeled to high specific activity with [α-^{32}P]dATP by the random-primer method (Malo et al., 1993) and hybridized at 42°C as described. Filters were washed as described and exposed 12-16 hrs at -80 °C using Kodak XAR film with intensifying screen. Plasmid DNA inserts for positive clones were sequenced as described. Other SSLP were derived from sequences of BAC ends (Table 2).

Subcloning of DNA Inserts from YAC Clones

Agarose-embedded high molecular weight genomic DNA from individual yeast clones carrying YAC 109B5 or 87M6F7 was prepared (Phillipsen et al., 1991) and subjected to partial digested with *Mbo I* to produce an average fragment size of 35-50 kb and ligated into the *BamH* I cloning site of the cosmid vector, SuperCosI (Stratagene). The ligation was packaged *in vitro* (Gigapack II Gold; Stratagene) and used to infect *E. coli* XL1-MRF', which was subsequently plated on LB agar containing 100 µg/ml ampicillin. Replicate filters were made for each plate and hybridized with [α-^{32}P]dATP-radiolabeled total mouse genomic DNA to identify cosmid clones containing mouse DNA. Positive colonies were grown and cosmid DNA was purified using a standard protocol (Sambrook et al., 1989).

FISH Analysis

BAC DNA was purified using the Qiagen Midi Prep kit (Qiagen) according to the manufacturer's instructions for BAC isolation. Purified DNAs were labeled with either biotin dATP or digoxigenin dUTP by nick translation. Labeled probes were combined with sheared mouse DNA and hybridized as differentially labeled pairs to interphase nuclei derived from mouse embryo fibroblasts in a solution containing 50% formamide, 10% dextran sulfate, and 2X SSC. Specific hybridization signals were detected by incubating the hybridized slides in fluorescein conjugated antidigoxigenin antibodies as well as Texas red avidin. The slides were then mounted in an antifade medium and analyzed. The mean distance between the two clones was calculated from the measurements made from photographs of interphase cells exhibiting paired red and green signals. The photographs have been standardized using a micrometer and represent an enlargement of 1435 times. The square of the mean interphase distance in microns was multiplied by 450.8 and 11.4 was then added to this product to provide an estimate of the actual distance in kilobase (kb) pairs (performed by Genome Systems Inc.).

Exon Amplification

Exon Trapping System Kit (GibcoBRL) was used on BAC clones overlapping the *Cmv1* candidate region to identify splicing competent sequences. In brief, purified BAC DNA was completely digested with *BamH I/Bgl* II and fragments were introduced into *BamH* I-digested and dephosphorylated pSLP3 cloning vector, followed by transformation into E. Coli strain XL-Blue (Stratagene). Miniprep plasmid DNA from the shut-gun library was transfected into COS-7 cells by electroporation, followed by incubation for 48 hrs at 37 °C. Total RNA was isolated using TRIzol® reagent (Gibco BRL). RT-PCR of 3 μg of total RNA was performed according to manufacturer's instructions (Gibco BRL). PCR-amplified exons were fractionated by gel electrophoresis on low-melting agarose gels and

cloned directly into a dT-tailed (Marchuk et al., 1991) *EcoR* V-digested pBluescipt II KS (+) plasmid vector (Stratagene). Inserts were sequenced as described above.

Results

We present the assembly of an integrated YAC/BAC clone contig spanning approximately 3 Mb of genomic DNA overlapping the *Cmv1* domain. To further study this region, we assembled a sequence-ready BAC contig overlapping the *Cmv1* critical interval delineated by novel markers *D6Ott8* and *D6Ott115*. Based on a BAC-based physical map and FISH analysis, the candidate region is estimated to span 1.82 Mb of genomic DNA and include at least 17 genes.

Construction of an integrated YAC/BAC contig

The construction of the YAC contig was initiated by screening the IRCF (Larin et al., 1991) and MIT (Kusumi et al., 1993; Haldi et al., 1996) YAC libraries with markers across a 1 cM genetic interval overlapping *Cmv1* (Depatie et al., 1997). The identified YAC clones were then organized in 4 independent contigs: contig [1] contained markers *Nk1.1/D6Mit61/135/257/289*, proximal to *Cmv1*; contig [2] contained *Ly49a*, co-segregating with *Cmv1*; [3] contained markers *Prp/D6Mit13 / D6Mit219* defining the distal boundary; and [4] representing the*Kap/D6Mit220* cluster also distal to *Cmv1*. Expansion and closure of these contigs was completed by STS mapping and subsequent rounds of chromosomal walking with novel markers derived from either end sequences of YAC clones or YAC sub-libraries (Tables 1 and 2). Confirmation of proper chromosomal assignment of newly generated STS was verified by screening a panel of hamster/mouse radiation hybrids prior to further analysis. A summary of all the YAC clones, their source, size, and STS content is presented in Table 3. The resulting contig spanning markers *Cd27* to *D6Mit220* contains 25 YAC clones and anchors 71 STS markers. The ordering of markers across the contig established by STS content mapping, is in agreement with existing genetic maps Depatie et al., 1997; Forbes et al., 1997). Moreover, it was possible to physically segregate the marker *D6Mitt111* from the distal cluster *D6Mit13/111/219*,

thereby positioning *D6Mit111* as telomeric to this cluster. Therefore, the contig is contiguous across the critical domain: clones 87M7E6/87M6F7 provide physical coverage between *Cd94* and the *Ly49* cluster that define the 0.05 cM proximal side of the *Cmv1* by one crossover. YAC clones 52A6/109B5 are linked proximally to 87M7E6 and distally to the contig 452H5/242D11/392D6 linking physically the 0.3 cM interval defined by 5 crossovers between the *Ly49* cluster and distal markers *D6Mit13/219*. The size of the contig can be estimated at 2.5 to 3 Mb based on long-range restriction mapping.

To facilitate further characterization of the *Cmv1* region, we assembled a BAC contig over the critical domain delineated by novel YAC derived markers *D6Ott8* and *392D6L*. The construction of the BAC contig was initiated by screening high-density gridded libraries (Genome Systems and RPCI-23) with a *Ly49a* cDNA probe. As most *Ly49* genes are highly-related and clustered within a genomic fragment of ~ 500 kb (Brown et al., 1997), clones identified by cross-hybridization are likely to cover this region. Additional entry probes included a marker representing the 3'end of *Ly49b*; the most distantly related *Ly49* member (Smith et al., 1994) and YAC end derived markers *392D6L* and *242D11L*. In parallel, the CITB BAC library (Research Genetics; Shizuya et al., 1992) was screened by PCR with markers *Ly49a*, *D6Mit370* and *D6Mit13*. Positive clones were isolated and organized into several independent contigs by STS content with entry probes and by DNA fingerprinting using *EcoR I* and *Hind III* digestion profiles (data not shown). Direct sequencing of BAC ends or clones from small insert BAC sub-libraries provided nucleotide information used to derive novel STSs (Tables 1 and 2) for finer STS mapping and consecutive rounds of library screening. Several STSs, such as *116m19T7*, *116m19Sp6*, *204d20Sp6* and *52A6L*, presented closely related variants across the region. To preclude misalignment of the contig, SSCP analysis or direct sequencing (data not shown) was performed to establish the presence of a specific variant in a clone. This strategy enabled the building of a contiguous BAC contig for the *Cmv1* target interval comprised of 73 BAC clones anchored by 40 STS markers and 14 *Ly49* genes (Table 3). A

minimum tiling path (MTP) consisting of the following 13 BACs covers this interval: 461n11 - 402g10 - 177i23 – 116m19 – 224i3 – 17e4 – 204d20 – 109n22 – 240c11 – 13a21 – 293m2 – 76n21 – 13j11 (Figure 1).

Genetic mapping

During the assembly of the YAC/BAC contig, 43 novel markers were generated of which 18 are polymorphic between *Cmv1*^{r} and *Cmv1*^{s} mouse strains. To better delineate the minimal interval for *Cmv1*, polymorphic markers together with *Ly49b*, *Ly49d* and *Ly49e*, were used for linkage studies in our reported intraspecific panels (Depatie et al., 1997). Locus nomenclature and characteristics together with the polymorphisms used for genetic analysis are listed in Table 2. The segregation of polymorphic markers was followed on a subset of animals (n=37) exhibiting a recombination event between the anchor loci *D6Mit52* and *D6Mit25* from our backcross panels. As these panels have been phenotyped for *Cmv1*, this approach provided direct information regarding *Cmv1* linkage. To determine gene order, the individual haplotypes of the 37 informative meioses were established, and the location of the new markers and genes was integrated with the established 50 markers (Depatie et al., 1997, 1999). Assuming that there were no double crossover events, a single crossover was detected between *D6Ott8* and *Cmv1*, and no recombination was observed between *D6Ott8* and *Cd94 / Nkg2d*. This result positions *Cd94/Nkg2d/D6Ott8* proximal to *Cmv1* at an estimated recombinational distance of 0.05 cM. Five crossovers were observed between *Cmv1* and *D6Ott115/392D6L/242D11L/170n17T7*, whereas no recombination was observed between this cluster and anchor loci *D6Mit13/111/219*. These results indicate an estimated genetic distance of 0.3 cM for the distal domain of *Cmv1*. Finally, no recombination events were detected between *Cmv1* and the remaining 14 novel loci. Combined pedigree analysis for the 0.35 cM segment encompassing *Cmv1* produced the following locus order and interlocus distance (cM): *Nkg2d/Cd94/D6Ott8* -(0.05)-*Cmv1/Ly49a (D6Ott11)/*

Ly49c/Ly49g(D6Ott22)/D6Mit370/Ly49e/Ly49d/43f9Sp6/D6Ott112/D6Ott32/52A6L/204d20Sp6/Ly49b/200H7L/D6Ott113(0.3)-*D6Ott115/392D6L/242D11L/170n17T7/D6Mit13/111/219*. These results delineate a minimal genetic interval for *Cmv1* of 0.35 cM that is defined by 24 tightly linked markers.

Long-range restriction map and FISH Analysis

Restriction mapping of YAC and BAC clones enabled us to assemble a long-range physical map and identify several CpG islands indicative of transcription units (Bird, 1986). YAC clones overlapping the *Cmv1* region were first digested with rare cutting restriction enzymes *NruI*, *NotI*, *MluI*, and *BssHII*, then resolved by PFGE and finally subjected to Southern hybridization with YAC arm probes, total genomic DNA and STSs to determine the presence and size of genomic fragments in the *Cmv1* region (data not shown). Probing with YAC ends provided a means to orient these clones within the contig whereas hybridization with genomic DNA identified internal restriction fragments. Subsequent restriction mapping analysis of BACs confirmed the presence of the rare cutting restriction enzyme sites in addition to identifying several CpG islands not detected by YAC analysis. The set of YAC and BAC clones studied together with the probes used to derive a 2.2 Mb long-range physical map are presented in Figure 1B.

The physical map of the YAC/BAC contig presents a single *Nru* I recognition site at position 0.19 Mb detected by *D6Ott8* on the YAC 87M6F7 and the BAC 461n11; and a single *NotI* site at 1.18 Mb found in YAC 109F12, 452H25 and all BAC clones anchored by *D6Ott95*. The sizes of internal *Mlu* I fragments were essentially consistent between YAC and BAC with the exception of two positions that are represented by diagonal slashes (*//*) on Figure 1B. This limitation of the map resulted from the tentative localization of a *MluI* site to position 0.815 Mb based on an alignment of the YAC and BAC maps assuming minimal overlap. *BssH* II sites are clustered on the distal end of the interval at around position 1.6 and 1.8 Mb, where high-resolution analysis on BACs revealed the presence of 2 and 4 recognition sequences respectively. Clustering of rare-cutter

Figure 1: Schematic representation of the *Cmv1* candidate region. (A) STS content mapping of markers along the chromosome. The order of markers was established based on the YAC and BAC contig. Markers in bold have also been mapped genetically. The chromosomal orientation is indicated as centromeric (CEN) and telomeric (TEL). (B) Restriction map of the *Cmv1* region. Solid bar, genomic DNA. Restriction sites for 4 enzymes, *Mlu I*, *Not I*, *Nru I* and *BssH II*, are indicated and represented by different symbols (see legend). Solid boxes below the physical map represent the region recognized by the indicated probes corresponding to *Ly49a* cDNA, *D6Ott8*, the left (L) and right (R) arms of the pYAC4 vector, and a repeat-enriched probe from genomic DNA (G). The fragment sizes from PFGE for two segments (*//*) containing *Ly49a* and the *Zfp-like* (*287g15T7*) probe, respectively, is based on tentative alignment of the YAC and BAC map. (C) The physical and STS content map of the YAC contig. Orientation of YAC inserts in the contig is indicated when possible. Black and gray circles represent markers anchored to the genomic clones. Position of some markers with respect to the restriction sites may not be accurate. The shaded line for clone 109B5 indicated rearrangement. (D) The physical and STS content map of the BAC contig as described above. Boxed clones represent BACs used for FISH analysis (figure 2). (E) Transcription map of the *Cmv1* candidate region. Position and order of the genes is based sequencing analysis and STS mapping. The direction of transcription for *Ly49a*, *Ly49d* and *Ly49e* is indicated. Gray circles in (C and D) represent the anchoring of the transcripts to the BAC and YAC contig.

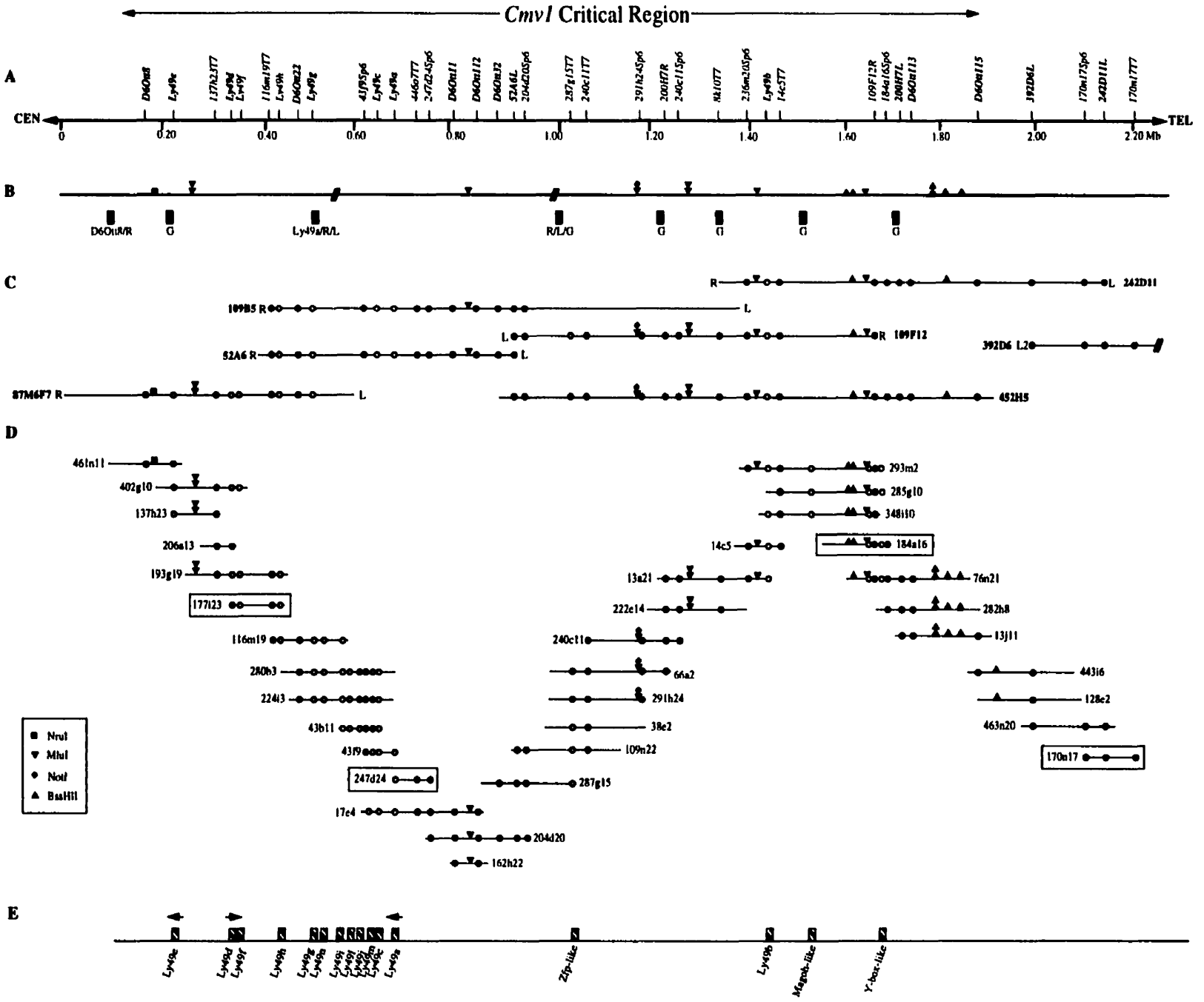
Cmv1 Critical Region
A
CEN
TEL
0
0.20
0.40
0.60
0.80
1.00
1.20
1.40
1.60
1.80
2.00
2.20 Mb
B
C
D
E
Nrul
MluI
NotI
BssHII
Ly49e
Ly49d
Ly49f
Ly49h
Ly49z
Ly49b
Ly49i
Ly49j
Ly49m
Ly49c
Ly49a
Zfp-like
Ly49b
Magnb-like
Y-box-like

recognition sites is characteristic of CpG islands often found associated with the 5' end of transcriptionally active genes (Bird, 1986). Three other CpG islands were identified in the interval at positions 0.18, 1.18 and 1.27 Mb. Integration of the physical and genetic maps indicate that the closest proximal and distal markers to *Cmv1* are *D6Ott8* and *D6Ott115* respectively. Therefore, the size of the *Cmv1* physical interval can be estimated at 1.82 Mb of genomic DNA. The proximal boundary of *Cmv1*, defined by a single crossover, is localized within a maximum distance of 200 kb within the interval *D6Ott8* - *Ly49e* contained in the BAC clone 461n11. Interestingly, neighboring YAC clones 52A6 and 109F12 that both carry only non-recombinant markers, cover 1.3 Mb of genomic DNA. The distal boundary defined by 5 crossovers, lies between *D6Ott113* and *D6Ott115*, both included in the 220 kb clone 13j11. We note that the rate of recombination across this area is much higher that the average recombination rate of 1 cM/Mb of mouse DNA (Silver, 1995).

To provide an independent estimate of distances derived from the YAC/BAC-based physical map, two-color fluorescence *in situ* hybridization (FISH) was performed on interphase nuclei (Trask et al., 1990). BAC pairs defining three intervals across the candidate region were used as probes (Figure 2), yielding the following estimated distances (in kb): centromere - 177i23 - 188 kb +/- 126 - 247d24 - 430kb ± 170 - 184a16 - 370kb ± 149 - 170n17 (Figure 2). Inter-BAC distances for the proximal and distal intervals are in close agreement with the distances of ~300 kb and ~500 kb calculated by physical mapping. In contrast, there is a two-fold difference in the estimation of the size of the 247d24-184a16 interval valued at 900 kb on the YAC/BAC contig. Several possibilities may account for this discrepancy including the overestimation of physical distances and based on clone alignment. Alternatively, the limits of resolution for FISH applied to interphase nuclei (Trask et al., 1989), may underestimate the actual distance between these clones.

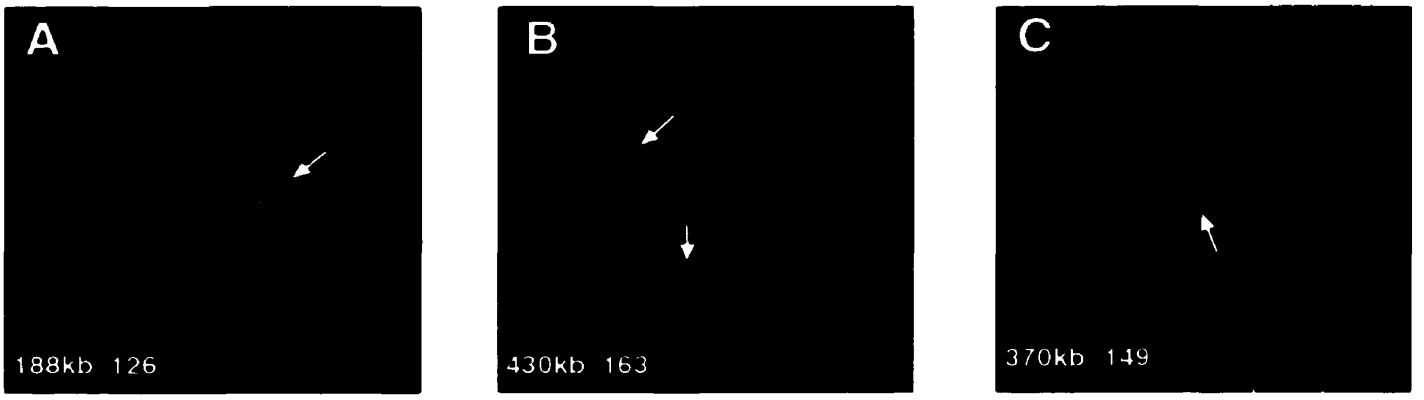
A
188kb 126
B
430kb 163
C
370kb 149

Figure 2: Two-color fluorescence *in situ* hybridization (FISH) on interphase nuclei with pairs of BAC clones derived from a BAC contig overlapping the *Cmv1* candidate region. (A) Hybridization of BAC clone 177i23 with 247d24. FISH analysis predicts a physical distance of 188 kb ± 126 compared to an estimated value of 300 kb based on physical mapping data. (B) Hybridization of clones 247d24 with 184a16. A distance of 430 kb ± 163 was obtained versus a value of ~900 kb from the physical map. (C) Hybridization of clone 184a16 with 170n17. The FISH distance of 370 kb ± 149 is similar to the value derived from the physical map. Location of these BACs within the contig are shown in Figure 1D (boxed clones). Integration of the values derived from the FISH analysis, predicts an estimated distance of 988 kb between BAC clone 177i23 and 170n17.

Transcription map of the Cmv1 Interval

To initiate the construction of a comprehensive transcription map of the *Cmv1* domain, we employed three parallel approaches: (1) systematic BLAST searches of newly cloned sequences, (2) BAC sequencing and STS content mapping with *Ly49* gene specific oligonucleotides and (3) exon amplification. Using BLAST searches, it was determined that the sequences derived from 137h23Sp6 corresponded to exon 4 of *Ly49e*, that of 247d24T7 contained exon 6 of *Ly49a* and 43f9T7 presented the 3' UTR of *Ly49a*. This information enabled the accurate placement of these transcription units within the BAC contig and assigned a transcription orientation telomeric to centromeric for the two genes. Moreover, the end sequence of 287g15T7, represented by STS *287g15T7*, was found to be homologous to a zinc finger motif characteristic of the C2H2-type proteins (Pieler and Bellefroid, 1994) suggesting the presence of a transcription unit. Highest homology (54/70 amino acids) is obtained with mouse Zfp35 protein (Cunliffe et al., 1990a). Out of the 14 *Ly49* family members identified up to date, 10 genes were analyzed by direct BAC sequencing with a panel of gene specific oligonucleotides (Table 4), whereas *Ly49a*, *-b*, *-g* and *-e* were by STS content mapping (Table 3). By analyzing the retention pattern of specific sequences across the contig (Fig. 1D) we determined that all 14 members were localized to the BAC contig with the following transcript order: centromere - *Ly49e- Ly49d - Ly49f/Ly49k - Ly49h - Ly49g/Ly49n - Ly49i - Ly49l/Ly49j - Ly49m/Ly49c - Ly49a - Ly49b*. All genes are clustered within a 420 kb of genomic DNA anchored to *D6Ott8* with the exception of *Ly49b* that lies ~750 kb telomeric to the cluster. Interestingly, sequence analysis of *Ly49d* fails to detect the 3' end of this gene in the BAC 206a13, indicating that the transcription orientation of *Ly49d* is centromeric to telomeric, contrary to all other known transcription orientation for *Ly49* genes as determined by us and others (McQueen *et al.*, 1998).

Finally, the cloned domain was systematically analyzed for the presence of transcription units using the technique of exon amplification (Buckley et al., 1991). This method is devised to screen large genomic DNA fragments for the presence of splicing competent exons. Except the region covered by BACs 224i3 and 17e4, that together contain 8 Ly49 genes, 17 BACs over the *Cmv1* domain were analyzed. A total of 31 putative exons ranging from 58 to 250 bp were recovered (Lee, S.H. et al., unpublished) and their nucleotide sequence was determined and compared to publicly available databases for homology searches. Using this approach, 11 homologous sequences were identified, 8 of which correspond to known *Ly49* exons (*Ly49e* from BAC 402g10; *Ly49d*, *Ly49k* and *Ly49f* from BAC 177i23; *ly49m* from 43f9 and *Ly49b* from 14c5) and one, a 148 bp exon from BAC 177i23, was found to be highly homologous to *Ly49d* exon 3, possibly defining a new member of the family. In addition, unrelated sequences to *Ly49* were identified indicating the presence of three supplementary transcription units. A 58-bp exon from 184a16 exhibited 90% homology to the serum-inducible protein gene *Magoh* (Zhao et al., 1998). An exon of 185 bp, recovered from BAC 285g10 exhibited 100% homology to both mouse Y-box binding protein gene (Duh et al., 1995) while also displaying significant homology to other DNA binding proteins. This would suggest that this exon might by part of a gene encoding a DNA binding protein. Exons were precisely anchored to the BAC contig using specific oligonucleotides (Table 4) for direct BAC sequencing. A schematic representation of the transcript map for the 17 potential genes localized in this study is presented in Figure 1E.

Discussion

As part of an effort to identify the host resistance locus *Cmv1*, a high-resolution linkage map was established and localized *Cmv1* to a minimal genetic interval of 0.35 cM studying 1967 informative meiosis (Depatie et al., 1997; 1999). To advance the cloning of the gene, the objective of this study was to generate a clone-based physical map of the *Cmv1* interval. This resource was used to generate new probes for linkage analysis and physical mapping allowing us to further delineate the *Cmv1* candidate region and initiate the construction of a detailed transcriptional map. Previously, physical maps in this region of mouse chromosome 6, including the Natural Killer gene complex, have been constructed based primarily on YAC contig assembly (Brown et al., 1997; 1999). However, considering the possibility of clone rearrangements, the calculated order and distances between loci can be affected when based solely on YAC contigs. As an alternative to YAC mapping, we present here an integrated YAC/BAC contig extending from *Cd27* to *D6Mit220*. This map, anchored by 61 markers over 3 Mb of genomic DNA, has enabled a more precise measurement of the physical distance and marker order in the region. The BAC contig has an STS content density of ~ 1 markers/30 kb of genomic DNA where each STSs is represented in 3 to 10 BAC clones, with an average of 5, providing the depth of coverage required for large-scale sequencing projects.

During the construction of the contig, it became apparent that several end clone-derived sequences, including *52A6*, *204d20Sp6*, *116m19T7* and *116m19Sp6*, indicated the presence of highly homologous repeats dispersed within the region containing the *Ly49* gene cluster. Although this was a drawback for contig assembly, the presence of these repeats sheds some light on the mechanisms governing the unfolding of the region. Unequal crossover and gene conversion have both been evoked as possible events playing a major role in the evolution of the *Ly49* gene family (Takei, et al., 1997). In contrast to gene conversion where homologous genes in a cluster are separated by non-conserved

sequences, unequal crossover results in tandem arrays of genes that are spaced by conserved sequences (Lewin, 1997). The homogeneity of local repeats in intergenic regions strongly supports the latter mechanism. Similar observations have been documented for other domains of the mouse chromosome bearing gene families such as the *Naip* cluster on chromosome 13 (Scharf et al., 1996; Diez et al., 1997). Recently, this locus has been completely sequenced and annotation of the repeats to the 5' end of the genes raised the hypothesis that repeats could function as functional promoter regions determining tissue specificity (Endrizzi et al., 1999).

During the course of this study, 44 new markers were generated including 18 polymorphic markers that were genetically mapped with respect to *Cmv1*. Although the genetic interval for *Cmv1* remains at 0.35 cM, information from the physical map determined that the closest proximal and distal markers to *Cmv1* are the novel loci *D6Ott8* and *D6Ott115* spanning a 1.8 Mb genomic region. A similar linkage study (Forbes et al., 1997), reported analogous genetic distances based on 2 crossovers proximal between *D6Wum9* and *Cmv1* and 3 distal crossovers between *Cmv1* and *D6Wum16*. However, the observed physical distribution of crossovers with respect to *Cmv1* is strikingly different and demonstrates a physical interval of 390 kb (Brown et al., 1999). Observations of equivocal phenotypes in animals presenting key recombination events or the use of different viral strains (Smith versus K181 strains) may account for some of these differences. Interestingly, integration of both maps based on the presence of common YAC clones would identify a minimal physical interval for *Cmv1* of less than 200 kb contained within the single BAC clone 13j11.

YAC and PAC maps have been established for the *Ly49* cluster accounting for 14 known genes up to date (Brown et al., 1997; McQueen et al., 1998). The complete organization of this large family has not been possible as reported studies do not demonstrate mapping of same family members. Our BAC contig provides a scaffold able to organize the *Ly49* transcriptional units by enabling the localization of all family members

to the same physical map. Using exon amplification and direct BAC sequencing *Ly49k* has been anchored to the map in close proximity to *Ly49d* and *Ly49f* whereas previous studies were not able to link this member to the gene cluster (McQueen et al., 1998). Furthermore, the ordering of some genes could not be defined in the previous maps. Results from this study show that *Ly49d* is located upstream of *Ly49f*, and that *Ly49i* is positioned between *Ly49n* and *Ly49g* in contrast to the previously assigned telomeric position of *Ly49i* to both of these (McQueen et al., 1998). Finally, sequences derived from exon amplification studies suggest the presence of other *Ly49* related sequences (Lee, S.H. et al., unpublished) as predicted by McQueen et al. (1998). The *Ly49* cluster spans ~1.2 Mb of genomic DNA and does not segregate from *Cmv1*, indicating that *Ly49* genes stand as attractive candidates. A consensus map of the family can be proposed as follows: cen-*Ly49e – Ly49d – Ly49f/Ly49k/Ly49new - Ly49h - Ly49g- Ly49n - Ly49i - Ly49l - Ly49j - Ly49m - Ly49c - Ly49a - Ly49b*.

In addition to *Ly49* genes, 3 potential transcription units were localized to the *Cmv1* interval, each exhibiting a high degree of homology to either the Zfp35 gene (Cunliffe et al., 1990a) and other zinc-finger protein genes, the *Magoh* gene (Zhao et al., 1998), or the Y-box protein gene (Duh, et al., 1995). The predicted amino acid sequence from *287g15T7* identifies two zinc-finger motifs of type C2H2 (Cys-X_2-Cys-X_3-Phe-Sx-Leu-X_2-His-X_3-His), a motif reportedly involved in DNA-binding (Pieler and Bellefroid, 1994). Human and mouse genome contain hundreds of genes coding for finger proteins of this type, therefore common functional features between a putative protein partly encoded by *287g15T7*and Zfp35 remains to be determined. *Zfp 35* is a mouse chromosome 18 locus (Cunnlife et al., 1990b) expressed in adult testis where it may play a role in spermatogenesis (Cunliffe et al., 1990a). Translation of exon 285g10 predicts an 18 amino acid strech highly conserved in mouse, human and rice *Magoh* sequences. *Magoh* has been assigned to mouse chromosome 4 (Zhao et al., 1998), indicating that the exon sequences identified probably correspond to a related gene. *Magoh* is the mammalian homolog of the

Drosophila *mago nashi* gene (Newmark and Boswell, 1994) involved in posterior pole determination of the fly oocyte. Although the function of *Magoh* in mice has not been elucidated yet, mRNA expression is ubiquitous in adult tissues and can be induced by stimulation of quiescent fibroblasts (Zhao et al., 1998). Y-box proteins comprise a family of DNA and RNA-binding proteins conserved through evolution from *E. coli* to humans (Wolffe, 1992). Their recognition element is the Y-box, an inverted CCAAT motif contained within the promoter sequence of many genes including all MHC class II genes, histone H2B, the cystic fibrosis CFTR gene (Wolffe et al., 1992). Their DNA binding domain spans an 80-amino acid region near the NH_2 terminus overlapping the homology region identified by the 184a16 exon.

At this time, it is not known whether *Cmv1* encodes for a recognition molecule or it is involved in the activation pathway of NK cells. Therefore, parsimonious characterization of these positional candidates is warranted to assess their candidacy for *Cmv1*. Finally, exon amplification identified 12 exons corresponding to unique sequences with no homology to known genes. Interestingly, most of these exons were isolated from CpG-island-associated BAC clones 240c11, 13a21 and 293m2, suggesting the presence of at least 3 more transcription units to the region. Studies are now underway to isolate full-length transcripts, determine expression patterns for these novel transcripts and exons, and identify polymorphisms between $Cmv1^r$ and $Cmv1^s$ strains. In summary, construction of this preliminary transcription map precisely localizes 17 transcription units to the *Cmv1* interval. This resource, together with the BAC contig presented here should provide the means to determine the precise localization of *Cmv1* by *in vivo* complementation using BAC transgenesis. Used systematically, this approach will determine allelism between *Cmv1* and the ectromelia resistance locus, *Rmp1* and other phenotypically defined loci including the *Nka* locus affecting reactivity of NK cells against allogeneic lymphocytes predicted to map to this region of mouse chromosome 6 (Delano and Brownstein, 1995; Dissen et al., 1996).

Acknowledgements

The authors thank Sonia Gerard and Pierre Bérubé for assistance with YAC and BAC screening, isolation and propagation. This work was supported by research grants to SM. Vidal from the Medical Research Council (MRC) of Canada and to P. Gros. from the Network of Centers of Excellence (Canadian Genetic Diseases Network). S.H. Lee is supported by a scholarship of OGS, P. Gros is supported by a Senior Scientist Award from the MRC and is an International Research Scholar of the Howard Hughes Medical Institute, and S.M. Vidal is recipient of an MRC scholarship.

Table 1

Summary of Non Polymorphic Probes

Locus name[1]	Accession No.	Primer Sequence 5' to 3'	Product size (bp)	Comments[2]
8k10T7	G54748	CAGGCCATAGTTCCAGTGG CCACCTCCCACACAATACAC	391	C
14c5Sp6	G54730	CATTTATTTGCTTTCTGTGC CTATGAATGCAATGAATCATGG	475	C
14c5T7	G54731	GGACTTAAACCACAGTCCAC CTATGATGTTACTCGAAGAGTC	127	T
33g14Sp6	NA[3]	GAGTGGGTGAAGAGAGGAATG CATATCAAGTTGTGGTAGTCATTGG	~380	T
65M5F9R	NA	GGAAGACCTGCTTGAAGACC AGGAACCCAGATGGGATAGAG	158	T
66M4E12R	NA	GCAGAAAGTTCTATTCTGGCA TTTCAGGTCTCCACAAGTTGA	237	C
87M6F7R	NA	GGCAGAGCTTCAGAAGTCTTG GCCCAGGTTACTTGACTGTAGG	100	C
102g4T7	G54728	GGAGCACATAGATCTATGCA CATTATTTAAATTCTGCCAATAA	111	T
109F12R	G54762	AAACATAAGTAAAAGGCAAT GTTCAGCTGTTCTATCTCTT	151	T
116m19Sp6	G54772	GGGAAGCCTTGTGATATATTGG GAGGGAGACAGGTGTTGGTG	122	T
116m19T7	G54756	AAAAACAAGTGTTGGTTCTTTTAG GCCAAACAGGAGACCTGAAG	216	C
137h23T7	G54729	ACTCCCATCCATAAATAGAGG CTGTCCTGACACATGTTCTG	316	T
156l3T7	G54732	TTCCTACCCAAGAGACACC AATGATTTTCCACAGTTACTAA	135	T
170n17Sp6	G54733	GCACTGTTGGCTTTCACTGG TGCCTTCTAGCCCTCATAGC	204	C
174g24Sp6	G54770	GAGTCACAGTAGAGTAAATAACAAC CCGTCCAGCCAGTGAA	368	
177i23Sp6	G54735	GCTCACAGACTTTGCATGATG TCCTTATCTCTGCTAAGAGG	124	C
170n17T7	G54734	TTCCTCACTACCAAGAAATAT CCCCTTGGCACATCC	168	T
184a16Sp6	G54736	TTTAATGAGCTCTGGTGAGTGC TGTTGTCTGGGACTTTGTAG	149	T
200H7R	G54761	CCTGACTTGGGCAGGTGAAT TGGCCATTTGTCCTTCGAAT	204	C
204d20Sp6	G54757	GTACAGGGACATTTAGGGCATTTG TGTGTGCAGAATTAGCAAAAAGTA	205	T

Continued

Locus name[1]	Accession No.	Primer Sequence 5' to 3'	Product size (bp)	Comments[2]
236m20Sp6	G54737	GAAGAAAATACCTAATTAAAATAAAG ACTGAGCTTAATGCTGGATGC	155	C
236m20T7	G54738	ATGGTAGCTTCTAATGAACC GTATAAGCCAGGGAGAAGTAG	356	T
240c11Sp6	G54739	TTCCAAATCACAGGAGGTCA ATCCCTGTACAGACTACTTG	134	T
240c11T7	G54740	GTGTCATATGCCACTATGTC AACACGTATTCCCTGCCTC	434	C
247d24Sp6	G54741	AATGGAATCAAATCAAAGCCAC AGCATAGTTGAATCTTGTAGTAG	389	T
287g15T7	G54743	ATTCACCCAGGAGAGAAACC GGCTTCTCTCCAGTATGG	210	T
291h24Sp6	G54744	GGGTTAGTGGCGTTGG CAATTATGGGTTAGAGATGGG	307	T
301l2Sp6	G54771	GCCATTGGGCATTCTAGTCT AAAAATGTGCAGCCTCAGTG	142	C
446o7T7	G54746	GAAGACCCTTTAGCTATGAG AACAGATATTTGTACTCACAG	160	T
463o20Sp6	G54747	TATTCACTGTCACTCTACATG ATTGCAAGAAGATTCACTGC	377	T
A2m	U06977	Depatie et al., 1997		
Cd27	L24495	TGAAGACCGGCAGGCAGTG AAGGGTAGAAAGCAGGCTCG	120	from cDNA
Cd69	S68405	Depatie et al., 1997		
D6Ott37	NA	CATGCATTAATCATATCCATTCAC TGCCAATATTCCGACAGGTATAC	174	from 139o7
Ly49a	L13874	GATTTCCCATCACCGTGAC GTGTCGCTAGCAAGAAGTGG	553	5' UTR
Ly49c	U56404	Brown et al., 1997		
Ly49f	U10092	Brown et al., 1997		
Ly49g	U10093	Brown et al., 1997		
Ly49h	L78253	Brown et al., 1997		
Nk1.1	53390	TCACGACGCCAGTGTCAAG GAGATGGAGGTGAATCATGCT	112	Exon 1
Tel	Y07915	Depatie et al., 1997		

[1]Name derived from clone number when possible

[2]Orientation indicated when possible (C=centromeric, T=telomeric) and source of STS when not derived from clone end

[3]NA= Not Available

Table 2
Summary of Polymorphic Probes

Locus name[1]	Accession No.	Primer sequence 5' to 3'	Product size (bp)	Polymorphism	Comments[2]
43f9Sp6	G54760	GACCTTCACAGAAACATGGC GTCAGATTTCTCTATTAGGG	343	C57BL/6 allele amplified only	C
52A6L	G54763	CACAACTAGGGTCACCCTAATTGAC GGAGAGTCTGTCAGTTAGGGAAGGT	200	SSLP	T
200H7L	G54764	GAATTCAAAAGGGTTCTCAA CCCTCTTTCCTTCCCTGTC	150	RFLP-PCR with Alu I	T
282h8Sp6	G54742	GCAGTTAGTAGCTGGCAGG TCACAGTCATTCCAAGAGGC	265	RFLP-PCR with Nla III	C
330B9L2	G54765	AAGTGTAACAGTGGGCCAAT GAATTCCCTCACCTAATA	370	C57BL/6 allele amplified only	C
392D6L	G54766	CTTCATGAACCCTATATCTG GTTTAACTCTATACCCCACT	120	SSLP	C
Cd94	AF039025	Depatie et al., 1999			
*D6Mit**		www-genome.wi.mit.edu		SSLP	
D6Ott8	G54759	TGACTTTGTTCTTTTGCAGGG GGTACTTGTGAGGCAAAGGC	229	SSLP	from 87M6F7
D6Ott11	G54856	Depatie et al., 1999			
D6Ott22	G54774	Depatie et al., 1999			
D6Ott32	G54767	CCTGGATTTATCTTTGTGGCTGG CTGAGATCAAACTGACAATCCTCC	400	SSLP	from 204d20
D6Ott112	G54773	CTCTCTGCTTGCCACTTTGG TCTGCCATGCTAATCACTGC	150	SSLP	from 109B5
D6Ott113	G54769	CTGGTGAGCAGATGGGTG CCAGATATTTCTTATATGTTTCA	201	SSLP	from 13j11
D6Ott115	G54768	ACCAATTGTATTGTGCCAGC CCCCAAAGACCATGTGGATA	110	SSLP	from 13j11
242D11L	AF106671	GTTTAAAGAGTTTTAGGAAG GTTCCAGGAACTCAGACCC	288	SSLP	
Ly49b	U10304	AGCAGAAGCCATCTTCCTTC TTTTCAGGTTAATTCTCCTACCTC	281	SSCP	from 3' UTR
Ly49d	L78247	Brown et al., 1997		C57BL/6 allele amplified only	
Ly49e	U10091	Brown et al., 1997	1100	RFLP-PCR with Hinc II	
Nkg2d	AF030313	Depatie et al., 1999			

[1]Name derived from clone number when possible

[2]Orientation indicated when possible (C=centromeric, T=telomeric) and source of STS when not derived from clone end

Table 3

STS content map of a YAC/BAC contig overlapping the *Cmt1* locus

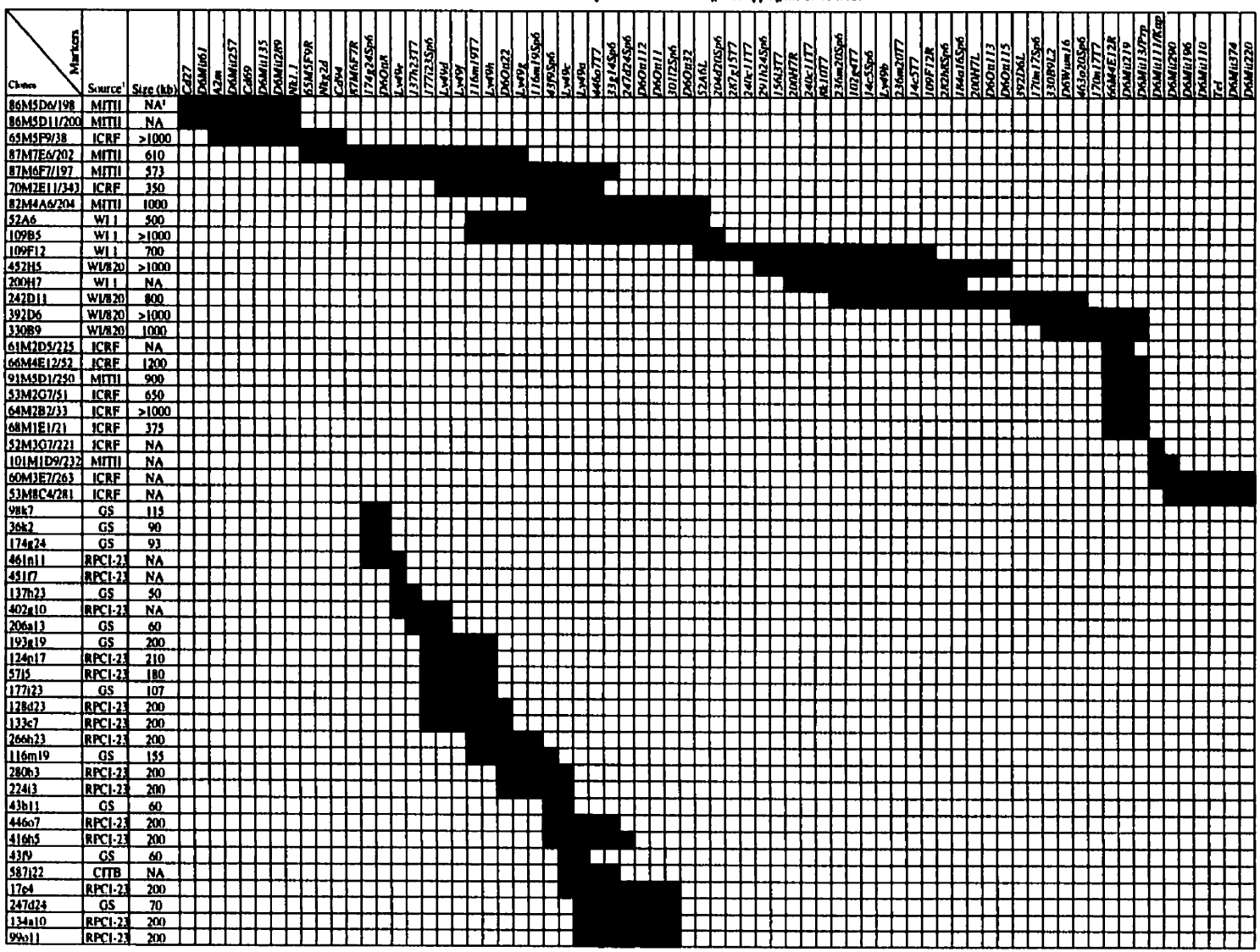

Continued

Clones \ Markers	Source[1]	Size (kb)[2]	Cd27	D6Mit61	A2m	D6Mit257	Cd69	D6Mit135	D6Mit289	Nkl.1	65M5F9R	Nkg2d	Cd94	N7M6F7R	174g24Sp6	D6OnR*	Ly49e*	137h23T7	177i23Sp6	Ly49d	Ly49f	116m19T7	Ly49h	D6On22	Ly49g	116m19Sp6	43f0Sp6	Ly49c	Ly49a	446o7T7	33g14Sp6	247d24Sp6	D6On112	D6On11	30112Sp6	D6On32	52A6L	204d20Sp6	287g15T7	240c11T7	291h24Sp6	156l3T7	200H7R	240c11T7	Rt10T7	236m20Sp6	102g4T7	14c5Sp6	Ly49b	236m20T7	14c5T7	109F12R	282h8Sp6	184a16Sp6	200H7L	D6On113*	D6On115*	392D6L	170n17Sp6	330B9L2	D6Wum16	463o20Sp6	170n17T7	66M4E12R	D6Mit219	D6Mit13/Prp	D6Mit111/Kap	D6Mit290	D6Mit196	D6Mit110	Tel	D6Mit374	D6Mit220
162h22	GS	80																														■	■																																							
204d20	GS	170																													■	■	■	■	■	■	■																																			
117f3	RPCI-23	200																													■	■	■	■	■	■	■																																			
142p5	RPCI-23	200																																■	■	■	■	■																																		
30112	RPCI-23	170																																■	■	■	■	■																																		
287g15	RPCI-23	150																																	■	■	■	■																																		
289i19	RPCI-23	200																																	■	■	■	■																																		
437h15	RPCI-23	200																																		■	■	■	■																																	
109n22	RPCI-23	200																																		■	■	■	■																																	
38e2	RPCI-23	200																																				■	■																																	
291h24	RPCI-23	190																																				■	■	■																																
139n15	RPCI-23	200																																				■	■	■	■	■																														
66a2	RPCI-23	200																																				■	■	■	■	■																														
156l3	GS	80																																						■	■																															
240c11	RPCI-23	140																																					■	■	■	■	■																													
204o14	RPCI-23	200																																					■	■	■	■	■																													
111e4	RPCI-23	170																																						■	■	■	■																													
222e14	RPCI-23	170																																								■	■	■																												
102p18	RPCI-23	200																																								■	■	■																												
2115	RPCI-23	200																																								■	■	■																												
182c5	GS	85																																								■	■	■																												
140e2	GS	65																																								■	■	■																												
8k10	GS	85																																										■	■	■	■																									
102g4	GS	60																																											■	■	■																									
126p15	GS	100																																											■	■	■	■	■																							
236m20	GS	60																																											■	■	■	■	■																							
73o22	RPCI-23	170																																												■	■	■	■	■																						
14c5	GS	90																																													■	■	■	■																						
183m22	GS	NA																																														■	■	■																						
293m2	RPCI-23	250																																														■	■	■																						
348i10	RPCI-23	200																																														■	■	■																						
285g10	RPCI-23	165																																																■	■	■																				
184a16	RPCI-23	115																																																	■	■	■																			
76n21	RPCI-23	200																																																	■	■	■																			
284b15	RPCI-23	160																																																			■	■	■	■																
282h8	RPCI-23	190																																																			■	■	■	■																
13i11	RPCI-23	200																																																			■	■	■	■																
443i6	RPCI-23	190																																																						■	■															
128c2	RPCI-23	200																																																							■															
463o20	RPCI-23	190																																																							■	■	■	■	■											
463n19	RPCI-23	190																																																							■	■	■	■	■											
85i11	RPCI-23	NA																																																							■	■	■	■	■											
92c22	RPCI-23	NA																																																							■	■	■	■	■											
193k3	RPCI-23	NA																																																							■	■	■	■	■											
167o15	GS	NA																																																							■	■	■	■	■											
170n17	GS	105																																																								■	■	■	■	■										
188i14	GS	NA																																																										■	■	■										
604o19	CITB	NA																																																													■									
139n7	CITB	NA																																																													■									

[1] WI/1 = Whitehead I Mouse YAC Library
WI/820 = Whitehead MIT 820 Mouse YAC Library
GS = Genome Systems
[2] NA = not available

Table 4

Primers used in Transcript Mapping

Locus Name	Primer Sequence 5' to 3'	Location
Ly49c	CAGGGTTGCAGAAACAAGTA	Exon 2
Ly49d-5'	GTCATCTCGGGAGTATGTAG	5' UTR
Ly49d-3'	AATAATTACTGTGATCAATC	3' UTR
Ly49f	CCTCAAGGTTGCAGAAACTT	Exon 2
Ly49h	CTATCACAATGAGCTGCCAA	Exon 4
Ly49i	McQueen et al., 1998	Exon 4
Ly49j	ATAGTATTGGTTTCACTATT	Exon 4
Ly49k	CTGTTCTCTGTTGAGGGATC	Exon 4
Ly49l	AATGATTTATCACATTTATC	Exon 4
Ly49m	TGCCAAGATAAGTGCAGCAC	Exon 7
Ly49n	CTTTAAGTCTATAGGATGTT	Exon 4
MagohlikeR	CTTAGATATGCCAACAACAG	6-22[1]
Y-box-likeR	CAGTTTCTCCATCCCCCACA	336-354[2]

[1]Corresponding sequence in Genbank #L35549

[2]Corresponding sequence in Genbank #AF035939

CHAPTER 4

ASSESSMENT OF *Cmv1* CANDIDATES BY GENETIC MAPPING AND IN VIVO ANTIBODY DEPLETION OF NK CELL SUBSETS

The work described in this chapter had the purpose of testing candidates that were located within the *Cmv1* interval. *Ly49a, Ly49c, Ly49g*, three members of the *Ly49* gene family encoding receptors expressed on subsets of NK cells, were genetically mapped in the high-resolution linkage map described in chapter 2. Cosegregation of theses genes to *Cmv1* prompted studies assessing their contribution to resistance to MCMV by following cell surface expression of the encoded receptors and performing selective *in vivo* antibody depletions of NK cell subsets expressing Ly49A, Ly49C, Ly49G2.

The manuscript that follows is published and is reproduced with the permission from the editor. Depatie C., Chalifour A,, Paré, C., Vidal S.M., and Lemieux S. Assessment of *Cmv1* candidates by genetic mapping and *in vivo* antibody depletion of NK cell subsets. International Immunology, 9: p1541-1551 (1999).

Footnote: CD and AC equally contributed to this study

Abstract

The mouse chromosome 6 locus *Cmv1* controls resistance to infection with murine Cytomegalovirus (MCMV). We have previously shown that *Cmv1* is tightly linked to members of the Natural Killer gene complex (NKC) including the *Ly49* gene family. To assess the candidacy of individual NKC members for *Cmv1*, first we followed the cosegregation of *Cd94*, *Nkg2d* and the well-characterized *Ly49a*, *Ly49c* and *Ly49g2* genes with respect to *Cmv1* in preexisting panels of intraspecific backcross mice. Gene order and intergene distances (in cM) were: centromere- *Cd94/Nkg2d*-(0.05)- *Ly49a/Ly49c/Ly49g/Cmv1*-(0.3)- *Prp/Kap/D6Mit13/111/219*. This result excludes *Cd94* and *Nkg2d* as *Cmv1* candidates whereas it localizes the *Ly49* genes within the minimal genetic interval for *Cmv1*. Second, we monitored the cell surface expression of individual Ly49 receptors in MCMV-infected mice over two weeks. The proportion of Ly49C+ and Ly49C/I+ cells decreased, the proportion of Ly49A+ and Ly49G2+ remained constant and the cell surface density of Ly49G2 increased during infection, suggesting that NK cell subsets might have different roles in the regulation of MCMV infection. Third, we performed *in vivo* antibody depletion of specific NK cell subsets. Depletion with single antibodies did not affect the resistant phenotype suggesting that Ly49A$^+$, Ly49C$^+$, Ly49G2$^+$ and/or Ly49C/I$^+$ populations are not substantial players in MCMV resistance and arguing for exclusion of the respective genes as candidates for *Cmv1*. In contrast, depletions with combined antibodies showed an intermediate phenotype. Whether residual NK cells post-depletion belong to a particular subset expressing another Ly49 receptor, or a molecule encoded by a yet to identify gene of the NKC, is discussed.

Introduction

In the mouse, natural resistance to murine cytomegalovirus (MCMV) infection is controlled by a dominant gene on chromosome 6 named *Cmv1* (Scalzo et al., 1990). Common inbred strains present two allelic forms for *Cmv1*: a dominant resistant allele, *Cmv1*^{r}, expressed in mice of the C57BL background and a recessive susceptible allele, *Cmv1*^{s}, expressed in BALB/c, A/J and DBA/2 strains. Phenotypically, resistant mice display splenic viral titers 10^3 to 10^4 times lower than those found in susceptible mice from day 2 post-infection when inoculated with a sublethal dose of virus. Studies in radiation chimeras following bone marrow transplantation together with *in vivo* depletion experiments using the mAb PK136 indicated that the effect of *Cmv1* is mediated by NK cells (Welsh et al., 1990; Scalzo et al., 1992). PK136 binds to NK1.1, a receptor encoded by the *Nk1* gene that is expressed on the surface of almost all NK cells and a small population of T cells in C57BL mice and a few strains (Koo and Peppard, 1984; MacDonald, 1995)). The NK cell population is an important player in the innate response towards a variety of viral infections through lysis of infected target cells and production of an array of cytokines (reviewed in Biron, 1997).

We and others (Scalzo et al., 1995; Depatie et al., 1997; Forbes et al., 1997)) positioned *Cmv1* to the NK gene complex (NKC), a chromosomal segment bearing numerous NK cell receptor genes, including *Nk1*, that stand as potential candidates for *Cmv1* (Yokoyama et al., 1991; Brown et al., 1997). By segregation analysis of two informative backcrosses totaling over 1967 meioses, we identified a 0.7 cM interval for *Cmv1* (Depatie et al., 1997) excluding the *Nk1* gene. Segregation of *Nk1* from *Cmv1* was confirmed by Forbes *et al*, shortly after. However, many other candidates remain, such

as members of the *Ly49* multigene family (Takei et al., 1997; McQueen et al., 1998) and the *Cd94* (Vance et al., 1997) and *Nkg2* (Ho et al., 1998; Vance et al., 1998) genes. Murine *Ly49* genes encode NK cell receptors that form disulfide-linked dimeric type II integral membrane proteins and belong to the C-type lectin superfamily. The *Ly49* family is composed of at least 14 members, most of which still await characterization (Takei et al., 1997; McQueen et al., 1998). Allelic polymorphisms were established for some *Ly49* genes expressed in BALB/c (*Cmv1*^{s}) and C57BL/6 (*Cmv1*^{r}) mice (Held et al., 1995, Mason et al., 1995; Brennan et al., 1996). Genes encoding several homologous Ly49 molecules were found in rats and localized on chromosome 4 (Dissen et al., 1996). However, only one Ly49 family member (Ly49L) has been detected in human thus far. As expected, the Ly49L locus was localized in the NKC on syntenic chromosome 12p12-p13 (Westgaard et al., 1998). To date, no Ly49 receptor has been shown to have a ubiquitous NK cell surface expression. Rather, Ly49 receptors are expressed on overlapping cell subsets of variable size (Mason et al., 1995; Brennan et al., 1996a; Brennan et al., 1994; Held et al., 1996; Mason et al., 1996). These receptors are involved in activation or inhibition of NK cell functions upon cross-linking with specific mAbs or by interacting with MHC class I ligands (Mason et al., 1995; Brennan et al., 1994; Mason et al., 1996; Karlhofer et al., 1992; Yu et al., 1996; Brennan et al., 1996b; Nakamura et al., 1999). Ly49 molecules with inhibitory properties, such us Ly49A, have immunoreceptor tyrosine-based inhibitory motifs (ITIM) in their cytoplasmic tail capable of recruiting cytoplasmic phosphatases (Nakamura et al., 1997). Ly49 receptors lacking cytoplasmic ITIM motifs transduce activating signals leading to target cell lysis and cytokine secretion (Smith et al., 1998).

Human and mouse CD94/NKG2 receptors are type II heterodimeric proteins that also belong to the C-type lectin superfamily and are expressed on NK cells. Unlike Ly49 receptors, they interact with non-classical MHC class I molecules bound to peptide (Vance et al., 1998; Braud et al., 1998). Signal transduction after engagement of human activating or inhibitory CD94/NKG2 receptors proceeds as for Ly49 molecules (LeDrean et al., 1998; Lanier et al., 1998). Whether this will also be the case for CD94/NKG2 murine receptors has yet to be elucidated.

Numerous allelic variations in NKC genes complicate the task of assessing candidate mutations potentially underlying the *Cmv1* phenotype (Vance et al., 1997, 1998; Ho et al., 1998; Held et al., 1995; Mason et al., 1995; Brennan et al., 1996a). Therefore, to address the candidacy of individual NKC members, [1] we studied the segregation of *Cd94*, *Nkg2d*, and the well characterized *Ly49a*, *Ly49c* and *Ly49g* genes with respect to *Cmv1* in two informative backcrosses. These *Ly49* genes were chosen based on the availability of receptor-specific mAbs for *in vivo* analysis as a means to assess functionally their candidacy for *Cmv1*. Using mAbs, [2] we monitored the cell surface expression of Ly49A, Ly49C and Ly49G2 in splenic *Cmv1*^{r} NK cell populations during the course of infection. Finally, [3] we analyzed the role of specific NK-cell subsets in MCMV resistance by assaying MCMV spleen and liver titers after *in vivo* cell depletion with individual or combined anti-Ly49 mAbs.

Materials and Methods

Mice

Inbred mouse strains A/J, BALB/cJ, C57BL/6J and B10.D2/nSnJ (6- to 10-weeks old) were purchased from the Jackson Laboratory (Bar Harbour, ME). We have previously described the breeding and maintenance of (A/J x C57BL/6)F1 x A/J and (BALB/c x C57BL/6)F1 x BALB/c segregating backcross mice (Depatie et al., 1997).

Virus, infection and virus titration

The Smith strain of MCMV, obtained from the American Type Culture Collection (ATCC, Rockville, MD) was propagated by salivary gland passages in 3-week-old BALB/c mice as previously described (Depatie et al., 1997). Otherwise, mice were infected intraperitoneally (i.p.) with 2 x 10^3 PFU of MCMV. Spleens harvested at indicated days were used for NK cell enrichment, and flow cytometry analysis and for virus titration by plaque assay on monolayers of mouse embryo fibroblasts, as described (Depatie et al., 1997). To ensure that every mouse was properly infected, liver viral load, which is not controlled by *Cmv1*, was also determined. Viral titers are expressed as Log_{10} of MCMV PFU per organ.

Detection of polymorphisms and linkage analysis

Oligonucleotide sequences are presented in Table 1. *Ly49c* was mapped by ASO (allele specific oligonucleotide) hybridization of a 144 bp PCR product within *Ly49c* exon 4, amplified with Ly49c-L/R oligos . The PCR reaction was performed using 20 ng of genomic DNA in a 20 µl volume reaction for 30 cycles of 94°C for 30 sec, 55°C for 30 sec and 72°C for 30 sec. A 5 µl aliquot of the PCR reaction was fractionated by electrophoresis on a 1.5% agarose gel containing ethidium bromide to verify successful

amplification. The remaining PCR products were denatured in a solution of 0.4 N NaOH and 10 mM EDTA and boiled for 5 min prior to transfer to nylon membrane (Hybond-N, Amersham) with a DOT-Blot apparatus (BioRAD, CA). The filter was then hybridized with [γ-^{32}P]ATP labeled Ly49c-3 oligonucleotide specific for the C57BL/6 allele. Washing conditions were 56°C with 0.5x SSC (1x SSC is 0.15 M sodium chloride, 0.015 M sodium citrate) and 0.1% SDS for 40 min. Hybridization signals were detected only from PCR products of the C57BL/6 allele. The mapping of *Ly49a* and *Ly49g* was accomplished by SSLP (single sequence length polymorphism) using sequence specific primers flanking novel (CA)n repeats closely linked to each of the genes. For this, total genomic DNA from YAC 109B6 (Research Genetics) containing the *Ly49a* and *Ly49g* genes (data not shown) was used to create a cosmid library of mouse specific clones as previously described (Vidal et al., 1993). A total of 120 clones were screened by oligonucleotide hybridization using oligonucleotide Ly49a-3, corresponding to the promoter region of *Ly49a* (Kubo et al., 1993), and oligonucleotide Ly49g-3, corresponding to unique exon 3 sequences of *Ly49g* (Smith et al., 1994). The same oligonucleotides were used to confirm the presence of the respective genes by cosmid DNA sequencing. To create small insert libraries, cosmid DNA was digested with *Mbo* I and subcloned into the *BamH* I site of plasmid pBluescript II KS$^+$ (Stratagene, CA). Inserts containing (CA)n repeated sequences were identified as previously described (Malo et al., 1993) and used to derive *Ly49a/D6Ott11* and *Ly49g/D6Ott22* primer pairs. SSLPs were identified by PCR amplification using 20 ng of genomic DNA as described (Depatie et al., 1997). *Cd94* was mapped by following the segregation of two transversions (T666C and C670T), which distinguish BALB/c and A/J from C57BL/6

strains (Vance et al., 1997), by direct DNA sequencing of a 244bp PCR product corresponding to the 3' UTR. The PCR product, obtained from genomic DNA with oligonucleotides Cd94-L/R, was gel purified and sequenced using dye terminator chemistry (Amersham). *Nkg2d* was mapped by following the segregation of an *Xba* I restriction fragment length polymorphism (RFLP) identified within a 700 bp PCR product corresponding to intron 11 and amplified with oligonucleotides Nkg2d-L/R. For genetic mapping we followed the segregation of these polymorphisms on a panel of 981 (A/J x C57BL/6)F1 x A/J and 920 (BALB/c x C57BL/6)F1 x BALB/c segregating backcross mice described previously (Depatie et al., 1997). Genetic linkage was determined by segregation analysis. Gene order was deduced by minimizing the number of crossovers between different loci within the linkage group (Green, 1981).

Antibodies

Hybridomas producing anti-HSA (rat IgG2b, clone M1/69), anti-CD8 (rat IgG2a, clone 53-6.72), anti-FcγRII/FcγRIII (rat IgG2b, clone 2.4G2), and anti-NK1.1 (mouse IgG2a, clone PK136) mAbs were purchased from ATCC (Rockville, MD). Hybridomas producing anti-CD4 [rat IgG2b, clone MT4] and anti-Ly49A [mouse IgG2a, clone A1] mAbs were kindly provided by Dr E.F. Potworowski (INRS-Institut Armand-Frappier, Laval) and Dr. J. P. Allison (UCA, Berkeley, CA), respectively. 4LO3311 and 4LO439 mouse IgG3 mAbs have been described (Lemieux et al., 1991). To derive 5GA5, a novel mAb recognizing Ly49C and Ly49I, Armenian hamsters (obtained from Dr. G. Yerganian, Cytogen Research & Development Inc., West Roxbury, MA) were immunized 4 times at 3-week intervals with BALB/c splenic LAK cells. Cell fusion and cloning of hybridomas were as described (Lemieux et al., 1991). Screening of hybridoma

supernatants was done by dot blot on Ly49C antigen purified from BALB/c LAK cells by affinity chromatography over 4LO3311 mAb-coated Sepharose 4B beads (Pharmacia). The 5GA5 mAb detects an epitope, common to Ly49C and Ly49I receptors, localized within the carbohydrate recognition domain (data not shown). Two-color FCM analysis of C57BL/6 NK-enriched spleen cells with 5GA5 and 4LO3311 mAbs showed that both antibodies recognized the same $Ly49C^+$ population, and that the $Ly49C^+$ and $Ly49I^+$ populations are of comparable size (data not shown). Similar studies in BALB/c cells showed that 5GA5 and 4LO3311 mAbs detect the same percentage of cells indicating that 5GA5 does not detect a $Ly49I^+$ population in this strain. This finding, consistent with data obtained with another anti-Ly49C/I mAb, SW5E6 (Brennan et al., 1996b), suggests that Ly49I is not expressed in BALB/c mice or, alternatively, that the antibody detects a polymorphic determinant that affects binding. Cold competition assays in BALB/c NK-enriched spleen cells showed that 5GA5 and 4LO3311 do not compete for binding (data not shown). Characteristics and reactivity of all antibodies used in this study are summarized in Table 2. With the exception of mAbs PK136 and 4LO439, which were purified from ascitic fluid, all other mAbs were purified from hybridoma supernatants using protein G Sepharose 4 Fast Flow (Pharmacia). The mAbs were conjugated to fluorescein isothiocyanate (FITC) or biotin (both from Sigma) using standard procedures. Isotype control mAbs were purchased from Pharmingen (San Diego, CA).

Depletion of NK cell subsets

Forty-eight hours before infection with MCMV, C57BL/6 or B10.D2 mice were inoculated i.p. with 1 mg of purified anti-Ly49 mAb of a given specificity, a mixture of 3 or 4 mAbs (1 mg of each) or 200 µl of a 1:4 dilution of ascitic fluid containing the anti-

NK1.1 mAb PK136. At day 2 post-infection, the extent of depletion was assessed by FCM analysis using the corresponding biotin-conjugated antibody.

Enrichment of splenic NK cells

Splenic NK cells were prepared by a negative selection procedure. Briefly, nylon wool non-adherent cells were incubated for 45 min on ice with a mixture of rat anti-HSA, anti-CD4 and anti-CD8 mAbs and then reactive cells were eliminated with sheep anti-rat IgG-coated magnetic beads (Dynal, Great Neck, NY). When applied to C57BL/6 spleen cells, this procedure yields a population containing 70-85% NK1.1$^+$ cells.

FCM analysis

Splenic NK cells (2-3 x 10^5/sample) suspended in PBS containing 1% BSA and 0.02% sodium azide were first incubated for 20 min at room temperature with mAb 2.4G2 to block FcRs. Cells were then incubated for 30 min on ice with optimal concentrations (30ng-2µg/sample) of FITC- or biotin-conjugated mAbs or both, added in sequence. Phycoerythrin (PE)-labeled streptavidin (SA-PE) and RED670-labeled streptavidin (SA-RED670™) conjugates (Canadian Life Sciences, Burlington, Ontario) were used for the detection of the red fluorescence in one and two-color analyses, respectively. After washing, stained cells were analyzed on a Epics XL-MCL flow cytometer (Coulter, Hialeah, FL) calibrated with FLOWCHECK™ Fluorospheres. Results are expressed as the percentage of lymphocytes gated with forward and side scatters that reacted with mAbs. The mean fluorescence intensity (MFI) was established on a logarithmic scale. Data analysis using XL software, version 1.5, was based on the collection of 5,000-10,000 events per sample.

Statistical analysis

Significance of the differences observed in reference to control groups was assessed using the two-tailed Student's *t*-test. Only p values < 0.01 (*) and < 0.001 (**) are indicated.

Results

Linkage analysis

We previously reported the generation of a genetic linkage map, comprised of 45 DNA markers corresponding to either cloned genes or microsatellites, which has improved the resolution of the genetic localization of the murine host resistance locus *Cmv1* on mouse chromosome 6 (Depatie et al., 1997). Segregation analysis of the above markers with respect to *Cmv1* in 1967 backcross animals defined a minimal genetic interval for *Cmv1* of 0.7 cM with the following gene order and intergene distances: centromere -*Nk1/D6Mit61/135/257/289/338*-0.4-*Ly49a/ D6Mit370/Cm* -0.3-*Tel/D6Mit374/290 /220/196/195/110. Ly49a* (Smith et al., 1994) was the only gene to cosegregate with *Cmv1* in 1967 meioses. This locus was mapped using a diagnostic RFLP detected by an *Ly49a* cDNA probe. As such, it was not possible to determine if this RFLP corresponded uniquely to *Ly49a* or to another member of the *Ly49* gene family as multiple bands were seen on Southern blots of digested genomic DNA hybridized with the cDNA probe.

The testing for possible candidates for *Cmv1*, initially required improving the resolution of our genetic linkage map to precisely localize individual *Ly49* family members in addition to the newly identified NKC members, *Nkg2d* and *Cd94*. To this end, we developed novel polymorphic markers in the vicinity of *Cmv1* and used them for linkage analysis in our reported intraspecific panels of 981 (A/J x C57BL/6)F1 x A/J mice and 920 (BALB/c x C57BL/6)F1 x BALB/c mice (Depatie et al., 1997). *Ly49c* was mapped by exploiting the existence of two proximal nucleotide transversions between BALB/c, A/J and C57BL/6 strains. Using ASO hybridization, we followed the

segregation of these transversions (T442G and A444C: A/J, BALB/c->C57BL/6) using a C57BL/6-specific primer (Brennan et al., 1996a). Allelic variants have also been reported for *Ly49a* and *Ly49g* in the above strains (Held et al., 1995; Mason et al., 1995). At present, however, it is difficult to determine if these variants correspond to homolog or paralog genes. To ascertain the genetic localization, simple sequence repeats (SSRs) in the vicinity of the *Ly49a* and *Ly49g* genes were cloned and mapped by SSLP. The nomenclature and characteristics of the two SSRs, *D6Ott11* and *D6Ott22*, together with the polymorphisms used to map *Cd94* and *Nkg2d*, are listed in Table 1. The SSR markers were isolated from YAC-derived cosmid clones containing either *Ly49a* or *Ly49g*. *D6Ott11*, which lies within 35 kb of the *Ly49a* promoter region (Kubo et al., 1993), generated polymorphic fragments for the strains analyzed, whereas *D6Ott22*, which lies within 45 kb of *Ly49g* exon 3, amplified a C57BL/6 specific fragment.

The segregation of the SSRs, as well as the other novel markers in this study, was followed on a subset of animals from our backcross panels (Depatie et al., 1997). Thirty seven animals that presented a recombination event between the anchor loci *D6Mit216* and *D6Mit25* were typed. As these panels have been phenotyped for *Cmv1*, this approach provided direct information regarding *Cmv1* linkage. To determine gene order, the individual haplotypes of the 37 informative meioses were established, and the location of the new markers and genes was integrated with the established 45 markers (Fig. 1). Assuming that there were no double crossover events, a single crossover was detected between *Cd94/Nkg2d* and *Cmv1*, and no recombination was observed between *Cd94* and *Nkg2d*. This result positions *Cd94/Nkg2d* proximal to *Cmv1* at an estimated recombinational distance of 0.05 cM, and decreased our genetic interval from 0.7 cM to

Figure 1. Segregation analysis and linkage map in the vicinity of the *Cmv1* host resistance locus. (A) Each column represents a chromosomal haplotype identified in the backcross progeny (BALB/cxC57BL/6) F1 x BALB/c. Solid boxes: C57BL/6 alleles. Open boxes: BALB/c alleles. The number of the progeny with each haplotype is shown at the bottom of each column. Haplotype analysis of the (A/J xC57BL/6) F1 x A/J is not shown. (B) Schematic representation of the composite map position of *Cmv1* on mouse chromosome 6. The gene order and the mapped loci were determined by pedigree analysis, and the intergene distances are given as estimates of recombination frequencies within backcross animals. The centromere of the chromosome is shown as a black circle. Recombination frequencies are shown to the right of the chromosome.

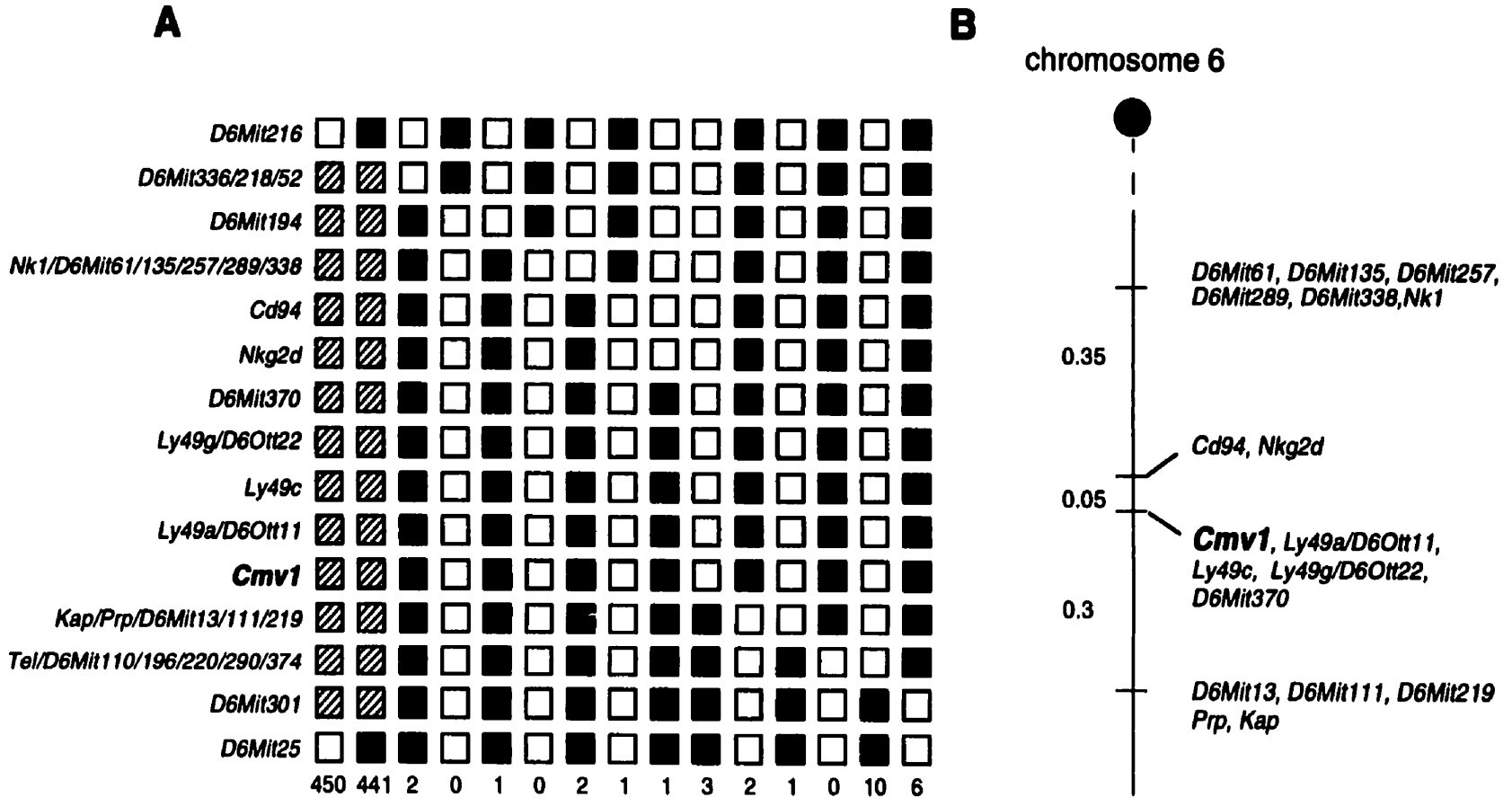
A
D6Mit216
D6Mit336/218/52
D6Mit194
Nk1/D6Mit61/135/257/289/338
Cd94
Nkg2d
D6Mit370
Ly49g/D6Ott22
Ly49c
Ly49a/D6Ott11
Cmv1
Kap/Prp/D6Mit13/111/219
Tel/D6Mit110/196/220/290/374
D6Mit301
D6Mit25
450 441 2 0 1 0 2 1 1 3 2 1 0 10 6
B
chromosome 6
D6Mit61, D6Mit135, D6Mit257,
D6Mit289, D6Mit338,Nk1
0.35
Cd94, Nkg2d
0.05
Cmv1, Ly49a/D6Ott11,
Ly49c, Ly49g/D6Ott22,
D6Mit370
0.3
D6Mit13, D6Mit111, D6Mit219
Prp, Kap

0.35 cM. However, no crossovers were detected between *Cmv1* and *Ly49a/D6Ott11*, *Ly49c* and *Ly49g/D6Ott22*, identifying these loci as attractive candidates for the host resistance locus. Combined pedigree analysis for the 7.9 cM segment encompassing *Cmv1* produced the following locus order and interlocus distance (cM): *D6Mit216*-(5.1)-*D6Mit52*-(0.5)-*D6Mit94*-(0.2)-N*k1/D6Mit61/135/257/289/338*-(0.35)-*Nkg2d/Cd94*-(0.05)-*Cmv1/Ly49a(D6Ott11)/Ly49c/Ly49g(D6Ott22)/D6Mit370*-(0.3) *Prp/Kap/D6Mit13/ 11/219*-(0.3)-*Tel/ D6Mit374 /290/220/196/195/110*. These results delineate a minimal genetic interval for *Cmv1* of 0.35 cM that is defined by 12 tightly linked markers.

Cell surface expression of Ly49A, Ly49C and Ly49G2 receptors during early MCMV infection

The anti-Ly49 mAbs used in this study for FCM analysis and *in vivo* depletion were either allele specific [A1: anti-Ly49A (Nagasawa et al., 1987); 4LO439: anti-Ly49G2 (Lemieux et al., 1991 and unpublished observations)]; or receptor specific [4LO3311: anti-Ly49C (Brennan et al., 1996a; Lemieux et al., 1991, Gosselin et al., 1997)] (Table 2). 5GA5 recognizes both Ly49C and Ly49I, and is the only mAb that has dual specificity in this study (see Materials and Methods for a description of 5GA5). However, it is possible that some of the mAbs used react with the *Ly49j-n* gene products for which no cDNA has been cloned so far (McQueen et al., 1998). The relative proportion of NK cells which express a given Ly49 molecule in normal C57BL/6 mice is as follows: Ly49G2$^+$>Ly49C$^+$=Ly49I$^+$>Ly49A$^+$. Two-color FCM analysis of C57BL/6 NK-enriched spleen cells revealed that, collectively, the subsets of NK cells stained by A1, 4LO3311, 4LO439 and 5GA5 constitute 85% of the NK1.1$^+$ cell population (Fig. 2).

Figure 2. FCM analysis of Ly49$^+$ NK cell subsets. Co-expression of NK1.1 and Ly49 receptors was assessed by incubating NK-enriched spleen cells from C57BL/6 mice with FITC-conjugated anti-NK1.1 mAb PK136 and a mixture of the biotinylated mAbs A1 (anti-Ly49A), 4LO3311 (anti-Ly49C), 5GA5 (anti-Ly49C/I and 4LO439 (anti-Ly49G2)) The red fluorescence was detected with SA-RED670™ conjugate. Numbers indicate the percentage of cells in each quadrant.

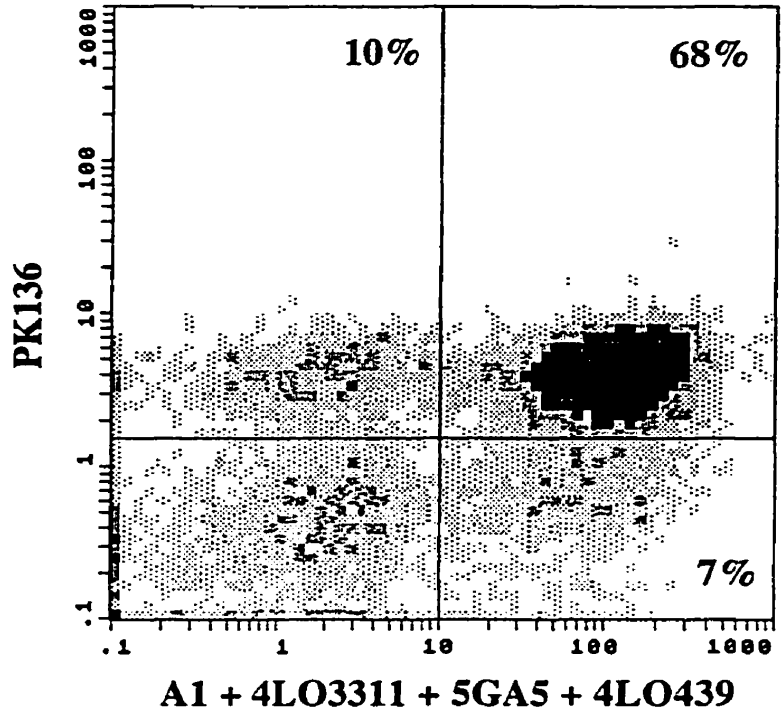
10%
68%
7%
PK136
1000
100
10
1
.1
.1
1
10
100
1000
A1 + 4LO3311 + 5GA5 + 4LO439

The cell surface expression of Ly49 receptors was monitored by FCM analysis of NK-enriched spleen cells over a two-week period after *Cmv1*^{r} C57BL/6 mice were infected with a sublethal dose of MCMV. At no time point, was there significant variation in the mean number of spleen cells harvested from infected mice. However, whereas in normal mice, the yield of splenic NK cells recovered after the enrichment procedure was 1.52% ± 0.38 (0.7-1.5 x 10^6 cells per spleen), this value dropped significantly in infected mice, reaching a maximal 2.3-fold reduction at day 3 post-infection. To control for variability within the entire NK cell population during the course of infection, NK1.1 cell surface expression was followed using the PK136 mAb (4). From 2 to 14 days post-infection, the percentage of NK1.1$^+$ cells was reduced (Fig. 3). Maximal effect was seen at 3 days post-infection when NK1.1$^+$ represent 60% of control values ($p < 0.01$). The cell surface expression of the Ly49$^+$ cell subsets display different variation patterns during the course of infection. The proportion of Ly49C$^+$ and Ly49C/I$^+$ cells decreased to 60% and 46% of the control values, respectively, 3 days post-infection ($p < 0.001$); the proportion of cells expressing either Ly49A or Ly49G2 at their cell surface remained relatively constant over the infection period. Interestingly, the cell surface density of Ly49G2 increased two-fold 3 and 4 days post-infection ($p < 0.001$). Except for a minor variation in the level of surface expression of the NK1.1 receptor 2 days after infection, the levels of all other receptors remained unchanged.

Splenic MCMV replication in mice depleted of selected NK cell subsets

In vivo depletion of NK cells with PK136 prior to MCMV infection converted resistant C57BL/6 and C57BL/6→BALB.B bone marrow chimeric mice to the susceptible phenotype (Welsh et al., 1990; Scalzo et al., 1992). We therefore investigated

Figure 3. Modulation of cell surface expression of NK cell receptors in C57BL/6 (*Cmv1*^{r}) mice infected with MCMV. Surface expression of NK1.1, Ly49A, Ly49C, Ly49C/I and Ly49G2 receptors in MCMV-infected mice was followed during 2 weeks post-infection by FCM analysis of NK-enriched spleen cells stained with biotinylated mAbs and SA-PE conjugate. The relative size of each cell subset and the density of expression (MFI) of the corresponding receptor are illustrated. Except for the control group which included 10 mice individually tested, each bar corresponds to the mean ± SD of 3 to 7 determinations. Due to the decrease in spleen cell recovery in infected mice, NK-enriched cells were prepared occasionnally from pooled spleen cells of 2 to 3 infected mice. Statistically significant differences in comparison with uninfected mice at p values < 0.01 (*) and < 0.001 (**) are indicated.

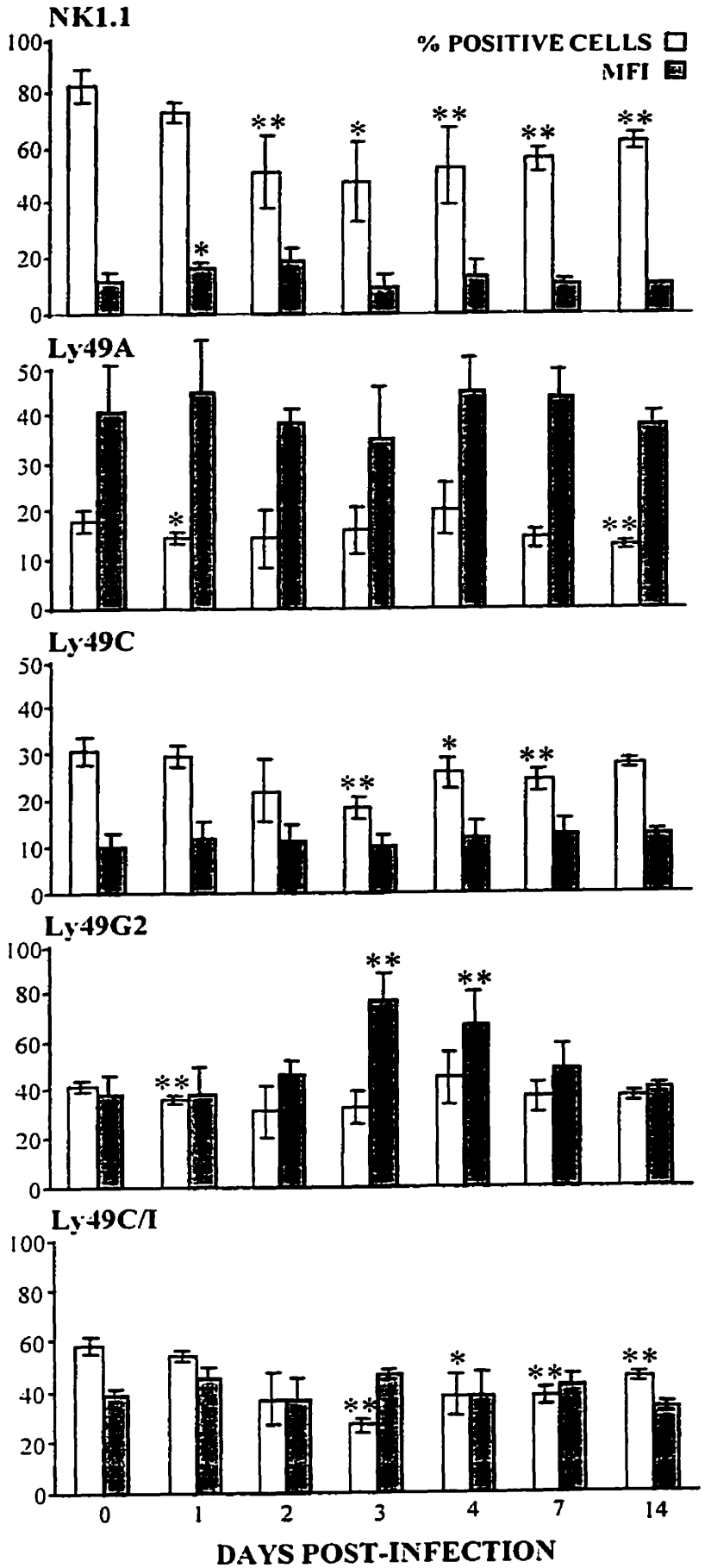
NK1.1
% POSITIVE CELLS
MFI
Ly49A
Ly49C
Ly49G2
Ly49C/I
DAYS POST-INFECTION

the phenotypic effect of selectively depleting cell populations which express specific Ly49 receptors in MCMV-infected resistant mice. Two days prior to infection, C57BL/6 mice were inoculated with anti-Ly49 mAbs or PK136. The extent of depletion was assessed by staining NK-enriched spleen cells with biotinylated mAbs and SA-PE conjugate at 2 days post-infection. Due to the high quantum yield of PE it was possible to detect residual cells expressing low levels of targeted receptors which are missed when using FITC-conjugated mAbs (data not shown). To rule out the possibility that Ly49$^+$ receptors are masked by the respective antibodies, NK-enriched spleen cells from treated mice were assayed for surface IgG and showed no positive staining. Furthermore, as expected, the recoveries of NK-enriched spleen cells from treated mice and their content of NK1.1$^+$ were reduced according to depletion efficiencies of the targeted cell populations (data not shown).

A 79-89% reduction in the proportion of NK cells expressing Ly49A or Ly49G2 was obtained after depletion with either anti-Ly49A or anti-Ly49G2 allele-specific mAbs but all mice remained resistant (Fig.4A, upper panel). Depletion of the Ly49C$^+$ cell population of greater than 50%, using either the receptor-specific mAb 4LO3311 or the Ly49C/I cross-specific mAb 5GA5, could not be achieved, even with higher doses of antibody (data not shown). As Ly49C cell surface expression is markedly down-regulated in the presence of the H-2K^b ligand (Gosselin et al., 1997; Salcedo et al., 1998), we envisaged the possibility that the efficiency of depletion was adversely affected by the low receptor density in the C57BL/6 strain. Therefore, we attempted to deplete Ly49C$^+$ cells in the B10.D2 (*Cmv1*^{r}, non-H-2K^b) strain which displays a higher cell surface expression level of Ly49C than C57BL/6 mice (Gosselin et al., 1997). The proportion of

Figure 4: Effect of Ly49 cell subset depletion on splenic MCMV replication. (A) C57BL/6 (upper panel) or B10.D2 (lower panel) (*Cmv1*^{r}) mice were depleted of selected Ly49 cell subsets as described in Materials and Methods and then infected with MCMV. At day 2 post-infection, spleen and liver were harvested and used for virus load determination and depletion control. * < 2.39 Log_{10} PFU. Left panels display mean viral loads ± S.D. as Log_{10} PFU/organ from 2 to 7 mice individually tested. BALB/c (*Cmv1*^{s}), C57BL/6 and B10.D2 (*Cmv1*^{r}) infected mice, either not depleted or depleted of total NK cells with the anti-NK1.1 mAb PK136, were used as controls. Profiles of residual spleen cells reacting with a given FITC- or biotin-conjugated mAb (solid line) are shown in right panels as overlays on those obtained from non-depleted infected mice of the same strain (dotted line). (B) B10.D2 mice inoculated with 3- (A1, 4LO3311 and 4LO439) or 4-mAb (A1, 4LO3311, 5GA5 and 4LO439) mixtures were infected and tested 2 days-later as described above. Histograms in the right panel illustrate the extent of depletion achieved with the 3- (upper panel) and 4-mAb (lower panel) mixtures on the NK1.1$^+$ cell population (stained with PK136) and on the Ly49+ populations (stained with mixed biotinylated mAbs). Data illustrated are representative of 2 to 4 identical experiments. Numbers indicated correspond to the mean percentage of depletion in reference to cell subset size in non-depleted infected mice.

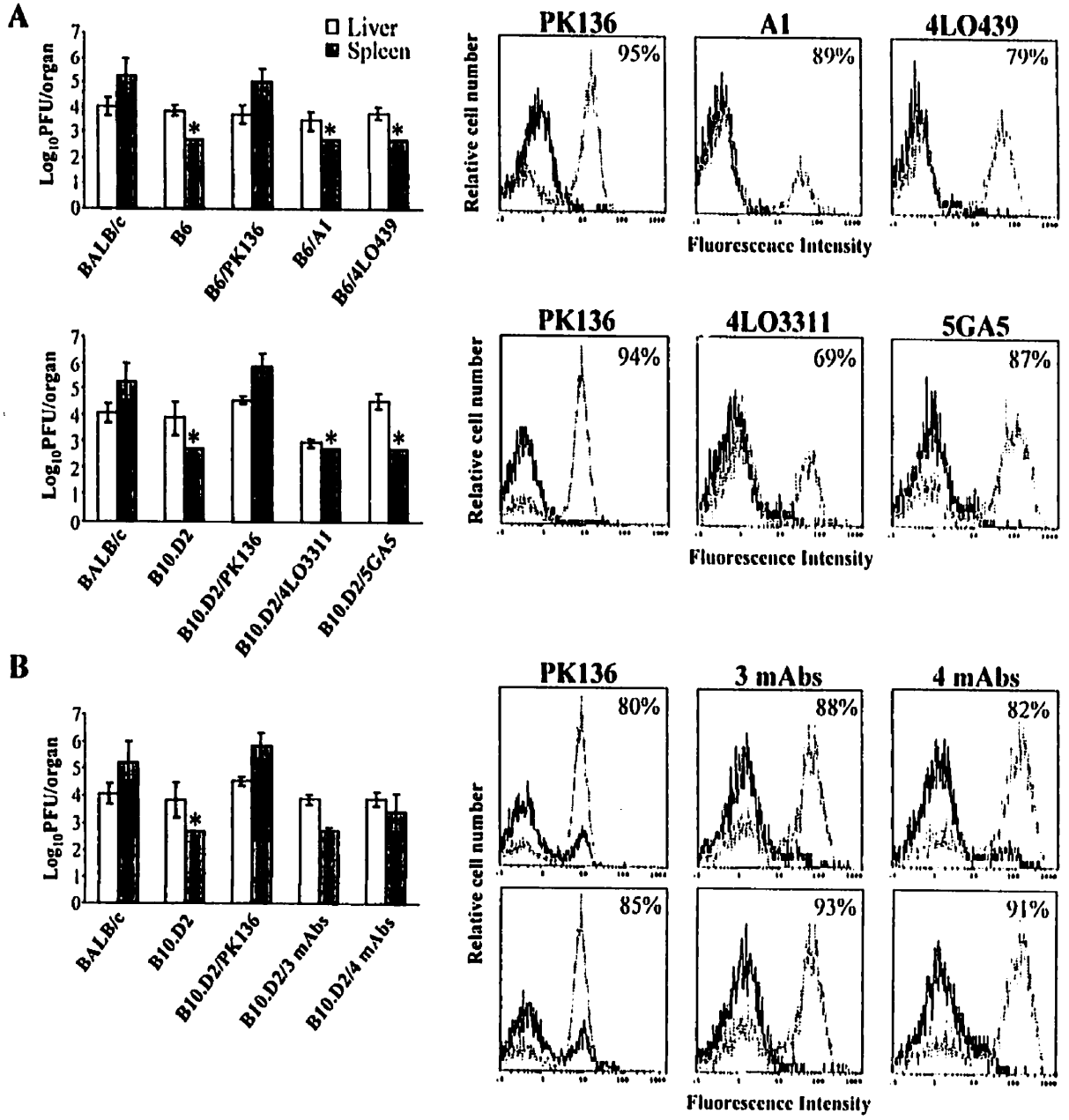
A
Liver
Spleen
Log10PFU/organ
BALB/c
B6
B6/PK136
B6/A1
B6/4LO439
PK136
A1
4LO439
95%
89%
79%
Relative cell number
Fluorescence Intensity
BALB/c
B10.D2
B10.D2/PK136
B10.D2/4LO3311
B10.D2/5GA5
PK136
4LO3311
5GA5
94%
69%
87%
B
BALB/c
B10.D2
B10.D2/PK136
B10.D2/3 mAbs
B10.D2/4 mAbs
PK136
3 mAbs
4 mAbs
80%
88%
82%
85%
93%
91%

Ly49C$^+$ and Ly49C/I$^+$ cells decreased by 69% and 87% in B10.D2 mice inoculated with 4LO3311 and 5GA5, respectively (Fig.4A, lower panel). If Ly49C$^+$ cells are a major component in mediating resistance to MCMV, the level of depletion should arguably be sufficient to detect variations in splenic viral load. However, depletion of Ly49C$^+$ cells and all other Ly49$^+$ cell subsets did not alter the resistance phenotype of C57BL/6 and B10.D2 MCMV-infected mice. No positive cells were detected when NK-enriched spleen cells from mAb-depleted mice were stained with biotinylated anti-mouse IgG antibodies and SA-PE conjugate showing that Ly49$^+$ cell subsets were really depleted and not Ly49 receptors only masked by their respective antibodies.

Next we assessed the resistance/susceptibility phenotype of B10.D2 MCMV-infected mice inoculated with a combination of three (A1, 4LO3311 and 4LO439; '3-mAb') or four (A1, 4LO3311, 4LO439 and 5GA5; '4-mAb') anti-Ly49 mAbs (Fig. 4B). The efficiency of these depletions was determined by staining with PK136 or 3-mAb or 4-mAb to detect residual cells. Injection of 3-mAb successfully depleted 88% of the targeted cells and 80% of NK1.1$^+$ cells but, as expected, the residual population still reacted with 4-mAb, which detects Ly49I$^+$ cells (Fig.4B, upper right panel). After inoculation with 4-mAb, less than 10% of cells stained with 3-mAb or 4-mAb, corresponding to a depletion of 85% of the NK1.1$^+$ cells (Fig.4B, lower right panel). As expected, expression of Ly49A and Ly49G2 receptors was reduced in B10.D2 mice that express H-2D^d, a ligand for these two receptors (Karlhoher et al., 1992; Mason et al., 1996). However, despite the low expression levels of Ly49A and, to a lower extent, of Ly49G2 in B10.D2 mice, 82% of Ly49A$^+$ cells and 89% of Ly49G2$^+$ cells were depleted in mice inoculated with 3 mAb and 4-mAb mixtures (data not shown). On the basis of the

splenic viral load, the resistance phenotype of mice depleted with 3-mAb was unchanged. However, some mice depleted with 4-mAb exhibited up to a 50-fold increase in splenic titers, suggestive of a progression towards susceptibility (Fig.4B: left panel).

Discussion

The host resistance locus *Cmv1* is expressed in the splenic NK cell population and sits in a region containing numerous NK cell-related genes with a high degree of polymorphism within families, such as the *Ly49*. Therefore, for our positional cloning approach, relying solely on sequence comparison is not sufficient to identify candidate genes. Thus, using methods complementary to genetic localization, which serves to eliminate potential genes and helps decrease the encompassing interval, has become imperative to assess candidacy. Previously published results segregated *Ly49a* and *Ly49g* from the *Cmv1* locus (Forbes et al., 1997). However, these genes could not be excluded as possible candidates as the mice that exhibited crossovers directly proximal to *Cmv1* displayed intermediate phenotypes. Experimental error affecting phenotype assignment or alternatively, contribution of other closely linked genes to control of viral replication could explain these observations. The results presented here show that *Cd94* and *Nkg2d* are positioned 0.05 cM proximal to the *Cmv1* locus, thereby excluding these two genes from the list of candidate genes. In contrast, we show that *Ly49a*, *Ly49c* and *Ly49g* do not segregate from *Cmv1* in 1901 meiosis analyzed and stand as *Cmv1* candidates.

Modulation of Ly49 receptor expression with respect to that of MHC class I ligands has been reported but not in the context of viral infection (Karlhofer et al., 1994; Held et al., 1996; Gosselin et al., 1997; Salcedo et al., 1997,1998; ; Olsson-Alheim et al., 1997). Considering that MCMV causes a downregulation of MHC class I molecules (Campbell et al., 1994; Slater et al., 1997), it was of interest to monitor the cell surface expression of Ly49 receptors during the course of infection. The receptor calibration model postulates that the level of receptor expression decreases in the presence of its

cognate MHC class I ligand (Sentman et al., 1995). This allows NK cells to increase their sensitivity in distinguishing between cells bearing normal amounts of MHC class I molecules and those expressing aberrant levels. Therefore, down-regulation of MHC class I surface expression, as in the case of MCMV-infected cells, should lead to NK cell-mediated lysis of these cells. The only Ly49 receptor known to have specificity for an MHC class I molecule of the H-2^b haplotype expressed in C57BL/6 (*Cmv1*^{r}) mice is Ly49C (Yu et al., 1996; Brennan et al., 1996b). In agreement with the receptor calibration model, the lowest density of Ly49C receptors is found in H-2^b mice (Gosselin et al., 1997). In H-2 congenic mice on C57BL and BALB backgrounds, the expression level of Ly49C is 3-4 times lower in H-2^b than in H-2^d mice. Furthermore, in C57BL/6 TAP1/ß2m-/- mutant mice, deficient in MHC class I expression, the level of Ly49C detected by the receptor-specific 4LO3311 is 8 times higher than in C57BL/6 mice (Salcedo et al., 1998). Since H-$2K^b$, which binds to Ly49C with high affinity, is down-regulated during MCMV infection (Campbell et al., 1994), we would have predicted a selective increase in the cell surface expression of Ly49C in MCMV-infected C57BL/6 mice. However, no changes in Ly49C surface expression were observed. Two recent reports using MHC class I mosaic mouse models, demonstrate that Ly49 expression is regulated by the NK cell's own MHC class I expression (Kase et al., 1998; Andersson et al., 1998). This observation might explain the absence of any increase in Ly49C expression in MCMV-infected mice.

The only significant change concerning level of expression of Ly49 receptors during the course of infection was an up-regulation in cell surface density of Ly49G2 at days 3 and 4. Ly49G2, a splice variant of Ly49G, has been characterized as an inhibitory

receptor which only binds to an H-2^d MHC class I ligand (Mason et al., 1995). Despite the absence of an established ligand in H-2^b mice, a moderate increase in the level of Ly49G2 cell surface expression was reported in ß2m-/- mice and a 25% increase in TAP1/ß2m-/- mice, both of which have C57BL background (Brennan et al., 1996b; Salcedo et al., 1997). The 2-fold increase of Ly49G2 detected in this study with the allele-specific anti-Ly49G2 4LO439 is significant and might point to a yet unidentified role for this receptor during MCMV infection. However, this role would be different from resistance to MCMV as it is observed only 3-4 days after infection whereas control of splenic viral replication is seen earlier. Moreover, antibody depletion of the NK cell subset expressing the Ly49G2 receptor in *Cmv1*^{r} mice did not abolish resistance.

Concerning the variation in size of NK cell sub-populations, we observed a decrease in the proportion of the Ly49C$^+$ cells starting at day 3 and no change in the Ly49A$^+$ and Ly49G2$^+$ populations. As we mentioned above, the Ly49C$^+$ population is the only one expressing a receptor for which a known ligand is present in the resistant C57BL/6 strain. Therefore, it is possible to speculate that down-regulation of the ligand in response to MCMV infection results in activation of the cognate NK cell by cytokines in the microenvironment or other mechanism resulting in the regulation of the population by apoptosis. In contrast to our observations, Tay *et al.* reported an increase in the number of Ly49A and Ly49G2 expressing cells at day 3 post-infection only (Tay et al., 1999). These discrepancies can be explained in part by the use of a different mAb for Ly49G2 detection. Our data were obtained using the allele specific mAb 4LO439 which recognizes specifically *Ly49g2* cDNA-transfected COS cells whereas the 4D11 mAb used in the Tay study cross-reacts with cells transfected with *Ly49g2* and *Ly49a* cDNAs

(Takei et al., 1997; Salcedo et al., 1997). In addition, rather than using total spleen cell suspensions our results are based on FCM analysis of NK enriched splenic cells to reduce non-specific binding of antibodies thereby increasing the sensitivity of our assay.

Previous reports have demonstrated the successful conversion of resistant mice towards susceptibility using antibodies to selectively deplete NK cells (Welsh et al., 1990; Scalzo et al., 1992; Bukowski et al., 1984). To test the candidacy of *Ly49* genes, we selectively depleted subpopulations of NK cells in *Cmv1*^{r} mice expressing a specific receptor at their cell surface prior to infection and looked for susceptibility. Conversion would not provide absolute validation of candidacy as the depleted NK cell population expresses other molecules at its surface that might be responsible for resistance. However, non-conversion permits exclusion of possible candidates. Depletion of single Ly49 cell subsets did not alter the resistant phenotype, indicating that the targeted subsets do not play a significant role in resistance to MCMV. Although depletion levels ranged from 69% to 89%, we believe that depletions were sufficient to justify the experiments as removal of NK1.1$^+$ cells with PK136 was also not 100% but conversion to susceptibility was still seen. Using a different set of monoclonal antibodies for depleting NK cell subsets in C57BL/6 mice, Tay *et al.* recently reached similar conclusions (Tay et al., 1999).

The data pertaining to targeted depletion of multiple subsets might suggest a threshold amount of NK cells needed to restrict viral growth. With a depletion of 80% of NK1.1$^+$ cells achieved with 3-mAb, a resistant phenotype persisted whereas mice inoculated with 4-mAb, had 15% NK1.1$^+$ cells left and the majority of these mice exhibited a significant increase in viral load. The Ly49I$^+$ population depleted with 4

mAbs (but not with 3 mAbs) is unlikely to be responsible for the resistance as no change in phenotype was seen in B10.D2 mice inoculated with the anti-Ly49C/I mAb 5GA5 alone. This suggests that the threshold value for maintaining resistance is likely between 15-20% of NK1.1$^+$ cells. This would indicate that the *Cmv1* locus encodes a protein ubiquitously expressed on NK cells. Alternatively, *Cmv1* may be expressed in a small subset which does not express Ly49A, Ly49C and Ly49G2, and therefore remains undepleted. NK1.1$^+$ T cells expressing either αβ or γδ T cell receptors are unlikely to be involved as these cells are not eliminated in mice inoculated with anti-asialo GM1 antiserum, a treatment that abrogates MCMV resistance (Bukowski et al., 1984; Tsukahara et al., 1998).

The *Ly49* family includes, so far, 14 identified members, the majority of which have unknown cell subset distribution and functions. To better evaluate candidates, experiments are in progress to use transgenic technology to create animals expressing different allelic forms of *Ly49* genes. The generation of a panel of transgenic animals with an overlapping set of genomic clones spanning the *Cmv1* domain will also facilitate dissection of other NKC loci. This includes the *Chok* locus responsible for preferential target cell lysis of CHO cells by splenic cells of C57BL/6 mice (Idris et al., 1998), and the *Rmp1* locus responsible for innate resistance to lethal ectromelia infection (Delano and Brownstein, 1995).

Acknowledgements

The authors are grateful to Jack Brennan and Fumio Takei for their contribution in the determination of the 4LO439 and 5GA5 mAb specificity. We also acknowledge Yvette Lusignan and Marcel Desrosiers for their expert assistance in FCM analyses, to Line Laroche and Pierre Bérubé for technical support. We also thank the Medical Research Council of Canada for their grant support. A.C and C.P. were supported by scholarships from NSERC and S.M.V. is recipient of an MRC scholarship.

TABLE I

SUMMARY OF PCR PRIMERS USED FOR GENETIC MAPPING

LOCUS	PRIMER	PRIMER SEQUENCE (5'-3)	PCR PRODUCT SIZE	POLYMORPHISM (size in bp)
Ly49a	Ly49a-3	GATTTCCCATCACCGTGAC		
	D6Ott11-L	GAAGTCATACTGCTTCAGTC	374bp	C57BL/6>BALB/c=A/J
	D6Ott11-R	ACTCTCTGCTTGCCACTTTG		
Ly49c	Ly49c-L	CTCTAAACCACCACCATAAC	144bp	
	Ly49c-R	GTCCCATCTGTCCTGTTCTC		
	Ly49c-3	CATGCAAAGGGCTTTCAAC		C57BL/6 detected by ASO
Ly49g	Ly49g-3	GGAGATGGGTCTTTCGTGAA		
	D6Ott22-L	GAAATATTTGTTTTCTGGGATTTATC	242bp	C57BL/6 detected
	D6Ott22-R	TGGAATTGTGATTGTGTCTATCTC		
Cd94	Cd94-L	TACAGTCCAAGCAAAAGCG	244bp	T666C and C670T[1]
	Cd94-R	GAAGCCATCAAGTATAAATTAC		
Nkg2d	Nkg2d-L	CCAAGCTTCCTGTTTGTCTCA	700bp	C57BL/6 (300,300,100)[2]
	Nkg2d-R	TCCCATCCAGTGATAGGACTT		A/J, BALB/c (600,100)

[1]Detected by sequencing

[2]Detected after *Xba* I digest of PCR product

TABLE 2

REACTIVITY OF ANTI-NK ANTIBODIES USED FOR FLOW CYTOMETRY ANALYSES AND NK CELL DEPLETIONS

MAB	ISOTYPE	SPECIFICITY	REACTIVITY IN			
			C57BL/6		BALB/c	
			% positive cells	MFI	% positive cells	MFI
PK136[1]	mIgG2a	NK1.1	78.56 ± 7.36[2]	12.02 ± 2.69	-	-
A1[1]	mIgG2a	Ly49A	17.95 ± 2.05	39.31 ± 9.28	-	-
4LO3311	mIgG3	Ly49C	30.15 ± 2.40	10.08 ± 2.84	54.58 ± 6.21	85.90 ± 17.80
4LO439[1]	mIgG3	Ly49G2[3]	40.80 ± 2.56	37.36 ± 8.16	-	-
5GA5	hIgG	Ly49C/I[3]	56.66 ± 3.45	39.35 ± 4.10	55.01 ± 5.50	101.10± 15.30

[1]Monoclonal antibodies specific for allotypic determinants not expressed in BALB/c mice

[2]Mean ± S.D. from 6 to 14 mice individually tested by staining NK-enriched spleen cells with optimal concentrations of biotinylated mAbs and SA-PE conjugate

[3]Specificity of these mAbs was established on the basis of reactivity with COS cells transfected with Ly49 cDNAs as described for the 4LO3311 mAb (Brennan et al., 1996)

Chapter 5: General Discussion

DISCUSSION

1. Immunogenetics of infection

The traditional approach to treating human infectious diseases has been to focus on the study of important pathogens. However limited advances have been made to uncover host response mechanisms that are critical to a robust host defense. Understanding and manipulating these responses could provide an alternate form of therapy. This becomes important in situations where pathogens encode proteins able to manipulate the immune system to its own advantage such as the case for HCMV.

The study of host genetics in human has identified several host genes mediating resistance to viral infections. MHC class I genes have prevailed as important determinants of susceptibility to a variety of viral infections including HIV, hepatitis B and C viruses (Hill, 1998). Other genes including mannose-binding protein, vitamin D receptor and several cytokines genes have also been reported to contribute to resistance or susceptibility to both HIV and hepatitis B virus (Mead et al., 1997; Summerfield et al., 1997; Bellamy et al., 1998; Ali et al., 1998). Perhaps the best example of the benefits of studying host resistance is the discovery that individuals homozygous for a 32-bp deletion in the CC chemokine receptor gene gene-5 (CCR-5) are very resistant to HIV infection (Samson et al., 1996; Liu et al., 1996). CCR-5 is a co-receptor for the entry of macrophage-tropic strains of HIV into cells (Deng et al., 1996). The identification of key components of the immune response to viral infection provides a means to design novel therapeutic agents to treat and cure these diseases.

Considering the model organisms available to study genetic analysis, the mouse has prevailed as the best system to study host resistance as it is physiologically relevant and extensively developed with the advent of the mouse genome project (Bedell et al., 1997).

There are several examples of cloned host resistance loci associated with viral infections. The *Mx1* locus was described as a single autosomal dominant locus that confers resistance to influenza virus in A2G mice (Lindenmann, 1964). *Mx1* encodes an IFN-stimulated nuclear protein that is only expressed in resistant mice where it inhibits transcription of the virus (Staeheli et al., 1986; Pavlovic et al., 1992). Mice homozygous for the *beige* mutation (described in Chapter 1) are more susceptible to MCMV infection than heterozygous litter mates (Shellam et al., 1980, 1985). The cloning of the *beige* locus was able to identify a gene encoding a protein involved in regulation of lysosomal fission (Perou et al., 1996, 1997). Mice homozygous for the mutation are unable to mount a proper NK cell response as they are impaired in their cytolytic activity against MCMV-infected cells. In addition to these cloned loci, other host resistance loci have yet to be identified, including *Cmv1*. Resistance to ectromelia virus (mouse pox) has been linked to several loci including *Rmp1* which maps to the NKC (Brownstein et al., 1991, 1992, 1995; Delano and Brownstein, 1995). Host resistance to flavivirus has also identified a locus, *Flvr*, mapping to chromosome 5 and acting in an autosomal dominant fashion (Sangster et al., 1993).

Successful identification of several host resistance loci by positional cloning has been reported, including the cloning of the *beige* mutation described above, and loci associated with host resistance to *Mycobacterium* spp. infection (*bcg*: Vidal et al., 1993) and *S. typhimurium* (*xid*: Thomas et al., 1993; Rawlings et al., 1993). The mouse model for Human Cytomegalovirus (HCMV), Murine Cytomegalovirus (MCMV) has been well characterized for host susceptibility to infection. Major contributors to outcome of infection are genes of the MHC and the *Cmv1* host resistance locus. We have chosen a positional cloning approach to clone *Cmv1* as no *in vitro* model has yet been established that could faithfully replicate the

in vivo model. In addition, this method of cloning will allows us to extrapolate our findings to human via comparison mapping to the homologous region in human. It is therefore possible to test for susceptibility to CMV infection in the human population.

Given the importance of NK cells as first line of defense against viral infections, the cloning and characterization of *Cmv1* will help define its role in the process of infection will be valuable in determining mechanisms dictating NK cell function. This thesis outlines the step taken to clone *Cmv1* using a positional cloning approach and reports (1) the generation of linkage map surrounding the *Cmv1* locus (Chapter 2), (2) the assembly of a detailed physical map of the critical interval and (3) the generation of a transcription map (Chapter 3), and finally functional analysis of 3 *Ly49* genes during MCMV infection (Chapter 4).

2. Results

2.1. Genetic map of the *Cmv1* region

Low-resolution genetic mapping of the *Cmv1* locus defined a 1 cM interval (Scalzo et al., 1995). The high-resolution genetic map described in this thesis was able to reduce this interval to 0.35 cM (Chapter 2). In addition, precise mapping of NKC genes excluded several *Cmv1* candidates, including *Nk1.1*, *Nkg2d* and *Cd94*. However, *Cmv1* cosegregated with members of the *Ly49* family also part of the NKC. Moreover, genetic localization of over 70 polymorphic markers to the region provides a detailed map of the region that can be used to precisely map other genes or loci in the region.

Comparison data between our genetic and physical map has demonstrated that the *Cmv1* genetic interval of 0.35 cM represents 1.82 Mb of genomic DNA. In addition, markers that cosegregate with *Cmv1* span 1.6 Mb while the 5 crossovers defining our distal boundary

are all located within a 200 kb region. A similar high-resolution linkage map described by Forbes et al., positioned *Cmv1* to a 390 kb region that segregates distally to the *Ly49* gene family and the rest of the NKC (Forbes et al., 1997). Although the number of crossover sites defining the *Cmv1* interval were similar in both linkage maps, the distribution of these sites was very different. However, both mapping efforts report a clustering of recombination events within the distal region of *Cmv1* suggestive of non-random distribution of recombination within the region. Several factors have been shown to deviate the distribution of crossovers from randomness. In general, telomeric portions of all chromosomes are associated with increase frequency of recombination in both mouse and human (de Boer and Groen, 1974; Laurie and Hulton, 1985). Given that Cmv1 is located well upstream from the telomere, this factor seems to be an unlikely contributor. Both strain-specific and gender-specific differences, will influence rates of recombination (Davisson et al., 1989; Seldin et al., 1989; Reeves et al., 1991). Therefore, the setup of the backcrosses that generated the recombinant progenies could affect the distribution of the crossover sites within the *Cmv1* region and explain the differences between results in this thesis and those by Forbes et al. (1997).

2.2. Physical map of *Cmv1* region

Cloning of the region was accomplished by screening genomic insert libraries (YACs and BACs). This process enabled the assembly of an overlapping array of both YAC and BAC clones that covers the entire candidate region (Chapter 3). Physical distances within the region were assigned by combining data from restriction analysis and FISH analysis. A similar study by Brown et al. (1999), reports comparable physical distances for the region

and therefore supports data extrapolated from analysis of genomic clones. Most importantly, a contiguous BAC contig spanning the critical interval was assembled with at least 3-fold coverage, thus providing an array of clones ready for sequencing analysis.

There are many characteristic features in this region that would profit from complete sequence analysis of the region. The organization of the NKC-encoded family of genes, *Nkrp1*, *Nkg2* and *Ly49*, in clusters is a common feature. Genes families have already been described, such as the β-globin (Karlsson and Nienhuis, 1985). The known mechanisms of gene duplication leading to the formation of clustered gene families include unequal crossing over and gene conversion. As yet, sequence analysis of large genomic regions in the syntenic region of human chromosome 12p, has suggested that gene expansion of the NKG2 family could have arisen by unequal homologous crossing over between related L1 long interspersed repetitive elements (Plougastel and Trowsdale, 1998). However, it might be that these homologous repeats were carried along during the duplication event. Sequencing of the BAC insert ends identified repetitive sequences in half the ends sequenced. The homology between cloned repeats remains to be assessed.

There is evidence for existence of other *Ly49*-related genes within this segment (S.H. Lee et al., unpublished). Cloning of one *Ly49* homologs in human has not demonstrated the multiplicity of *Ly49* genes found in mouse (Westgaard et al., 1998). This would suggest that the mouse has somehow selected *Ly49* genes as receptors for MHC class I interaction whereas human have relied on different gene families to support the role of Ly49 genes. Indeed, human chromosome 19 harbors a cluster of NK cell receptor structurally related to the Ig superfamily that bind to MHC class I molecules (Long et al., 1997). Therefore, the probability that *Ly49* genes may play a role in host resistance to HCMV is unlikely.

In addition to providing evolutionary information, sequencing analysis will provide information pertaining to regulatory sequences affecting transcription and especially cell-specific expression to NK cell. Both the β-globin and the granzyme clusters of genes seem to exhibit some semblance of coordinated regulation as targeted disruption of promotor regions affects transcription of other family members situated as far as 100 kb away (Pham et al., 1996). Whether this coordinated regulation can be applied to the *Ly49* gene family as well as other NKC clusters, remains to be determined from analysis of regulatory regions. Considering that NKC members are all expressed in the same cell type, namely NK cells, identifying regulatory sequences responsible for their cell-specific expression will be very informative. Deletion mapping studies of the promoter region of the human FcγRIIIA gene encoding the FcγRIII (CD16) receptor expressed on NK cells, identified a 93 bp sequence able to confer NK-cell specific expression (Gessner et al., 1996).

3. Candidates for *Cmv1*

The mapping of *Cmv1* within a chromosomal region rich in genes encoding NK cell receptors, would predict a receptor function for *Cmv1*. Genetic mapping studies have excluded all but one known receptor family as possible candidates, the *Ly49* family (Chapter 3 and 4). However, functional analysis of Ly49A, Ly49C, Ly49G2 and Ly49I has discouraged the candidacy of these inhibitory receptors (Chapter 4). In contrast, *Ly49d*, encoding an NK cell activating receptor not tested in our study, has been identified as the gene product of the phenotypically defined locus, *Chok* also mapping to the NKC (Idris et al., 1999). The *Chok* locus regulates NK cell cytolytic activity against Chinese hamster ovary (CHO) cells (Idris et al., 1998). Whether *Chok* and *Cmv1* are

allelic, remains to be determined. Nonetheless, this study would suggest that *Cmv1* might encode an activation receptor rather than an inhibitory receptor such as Ly49A, Ly49C, Ly49G2 and Ly49I. However, we can propose that *Cmv1* encodes an Ly49 molecule with activating properties similar to Ly49D, or a structurally related receptor also involved in MHC class I recognition.

Mutation analysis studies of *Ly49* genes have identified regions of the molecule that could present block downstream signaling if mutated. Inability to bind ligand via the CRD domain and stalk region in the extracellular domain of Ly49 molecules has been demonstrated (Brennan et al. 1996). Mutation analysis of a tyrosine residue in the ITIM motif of Ly49A abrogates receptor downstream signaling (Nakamura et al., 1996). Ly49D, an activating receptor lacking an ITIM, requires association with DAP12 via a charged residue in its transmembrane domain to initiate activation (Lanier et al., 1998). Finally, cell surface expression studies of Ly49D, Ly49I and Nk1.1, a receptor expressed on most NK cells, molecules have shown that these receptors are only detected in $Cmv1^r$ strains (Idris et al., 1999; Depatie et al., 1999). Differential expression of NK cell receptors between $Cmv1^r$ and $Cmv1^s$ strains could underlie the phenotypic difference. Indeed, cell surface expression is modulated my MHC class I expression where Ly49 molecules reactive with the host's MHC class I are downregulated to avoid lysis of self cells (Sentman et al., 1995). Therefore, resistance/susceptibility could be the result of a lack or presence of crucial receptor.

Signaling pathways involved in NK cell activation share common mechanism including association with either SH2 containing protein tyrosine kinases, such as ZAP-70 and $p72^{syk}$) or protein tyrosine phosphatases, such as SHP-1 and SHP-2, generation of

inositol intermediates and a subsequent rise in intracellular Ca^{++} (Renard et al., 1997; Lanier et al., 1998). *Cmv1* might encode a molecule crucial to the downstream signaling that ultimately affects NK cell activation. Studies of Ly49 receptor signaling in NK cell from "motheaten" mice, decifient in SHP-1, show failure to transmit inhibitory signals leading to NK cell activation rather than inhibition (Burshtyn et al., 1996. 1997). As yet, the study of MCMV infection in *Cmv1*^{r} mice that are *shp-/-* has not been performed but could be useful to identify triggered pathways.

Finally, chapter 3 of this thesis describes the identification of potential transcripts, besides *Ly49* genes, that could suggest roles for *Cmv1*. The cloning of a segment containing well-conserved zinc-finger motifs would suggest the presence of a transcription factor as these motif are often associated with this class of proteins (Pieler et Bellefroid, 1994). Alternatively, the NKLAM gene, containing a potential zinc finger motif, encodes a protein found in the cytolytic granules of NK cells with an expression pattern that parallels NK cell cytolytic function (Kozlowski et al., 1999). As well, sequence homologies to Y-box proteins, also suggests the presence of a DNA binding protein. Y-box protein binding sites include MHC class II genes, histone H2B and the cystic fibrosis CFTR gene (Wolffe et al., 1992).

In addition to exons exhibiting homologies to known sequences, 11 exons representing unique sequences were also identified. Characterization and candidacy of these transcripts will rely on several parameters: identification of a mutation between *Cmv1*^{s} and *Cmv1*^{r} strains likely to underlie a phenotypic difference, expression in the proper cell-type, namely NK cells, and sequence conservation among other organisms. Assessing the level of conservation will indicate if a mutation might cause a similar

phenotype in other organism. Subsequent analysis of the gene product and protein function will offer an important clue to the mechanism underlying resistance. Finally, performing *in vivo* complementation with insertion of a gene from the *Cmv1*^{r} genome into a *Cmv1*^{s} background will provide the ultimate functional proof that a particular gene is *Cmv1*.

4. *Cmv1* and MCMV resistance

An advantage of using a positional cloning approach is that candidate genes are selected on a non-functional basis, thereby giving way to the possibility that *Cmv1* could encode any type of protein. However, given several considerations, it is possible to speculate on the true nature of *Cmv1* and its role in MCMV infection. Firstly, several studies have identified the cytolytic properties of NK cells as the effector mechanism for mediating resistance in the spleen of *Cmv1*^{r} strains (Scalzo et al., 1992; Lathbury et al., 1996). Secondly, NK cells from *Cmv1*^{s} strains are able to lyse YAC-1 cells, indicating that an effective cytolytic response can be mounted in susceptible strains (Idris et al., 1998). Thirdly, the genomes of both MCMV and HCMV have genes encoding proteins that function to downregulate MHC class I expression in infected cells (Wiertz et al., 1996; Thale et al., 1995). Moreover, they both encode homologs of MHC class I (Browne et al., 1990; Rawlinson et al., 1996).

Taking these facts into account, the most likely stage at which *Cmv1*^{r} NK cells differ from *Cmv1*^{s} cells is the receptor ligand interaction that leads to downstream signaling. If the products of the *Cmv1* locus is an inhibitory NK cell receptor then it might be envisaged that it could interact with viral MHC class I homolog or modified

cellular MHC class I molecules. Mouse strain-dependent allelism of the *Cmv1* product would then dictate the outcome of this interaction. Hence, the susceptible mouse strains may encode an allelic form of the receptor that is inhibitory due to its ability to bind these MHC class molecules, whereas NK cells from resistant mice may lack this receptor. Alternatively, since activation receptors are encoded in the NKC, the resistance may be mediated by an activating receptor that is absent in susceptible mice as proposed previously for *Ly49d*, or that is incapable of recognition of MCMV-infected cells. Thus, identification of the *Cmv1*-encoded product will be important in understanding NK cell-mediated host control of virus infection. The cloning of *Cmv1* will determine which of these scenarios are correct or if a totally different mechanism underlies the differences in resistance.

References

Alford CA, Britt WJ. 1990. In "Virology" (B. N. Fields, D. M. Knipe et al., eds.), 2nd ed., pp. 1981-2010.

Allan JE, Shellam GR. 1985. Characterization of interferon induction in mice of resistant and susceptible strains during murine cytomegalovirus infection. J Gen Virol. 66:1105.

Allan JE, Shellam GR. 1984. Genetic control of murine cytomegalovirus infection: virus titres in resistant and susceptible strains of mice. Arch Virol. 81:139.

Altschul SF, Madden TL, Schaffer AA, Zhang J, Zhang Z, Miller W, Lipman DJ. 1997. Gapped BLAST and PSI-BLAST: a new generation of protein database search programs. Nucleic Acids Res. 25:3389.

Andersson M, Freland S, Johansson MH, Wallin R, Sandberg JK, Chambers BJ, Christensson B, Lendahl U, Lemieux S, Salcedo M, Ljunggren HG. 1998. MHC class I mosaic mice reveal insights into control of Ly49C inhibitory receptor expression in NK cells. J Immunol. 161:6475.

Arase H, Arase N, Saito T. 1996. Interferon gamma production by natural killer (NK) cells and NK1.1+ T cells upon NKR-P1 cross-linking. J Exp Med. 183:2391.

Azen EA, Davisson MT, Cherry M, Taylor BA. 1989. *Prp* (proline-rich protein) genes linked to markers *Es-12* (esterase-12), *Ea-10* (erythrocyte alloantigen), and loci on distal mouse chromosome 6. Genomics 5:415.

Ballas ZK, Turner JM, Turner DA, Goetzman EA, Kemp JD. 1990. A patient with simultaneous absence of "classical" natural killer cells (CD3-, CD16+, and NKH1+) and expansion of CD3+, CD4-, CD8-, NKH1+ subset. J Allergy Clin Immunol.85:453.

Bancroft GJ, Shellam GR, Chalmer JE. 1981. Genetic influences on the augmentation of natural killer (NK) cells during murine Cytomegalovirus infection: correlation with patterns of resistance. J Immunol. 126: 988.

Bedell MA, Jenkins NA, Copeland NG. 1997. Mouse models of human disease. Part I: techniques and resources for genetic analysis in mice. Genes Dev. 11:1.

Bellamy R, Ruwende C, McAdam KP, Thursz M, Sumiya M, Summerfield J, Gilbert SC, Corrah T, Kwiatkowski D, Whittle HC, Hill AV. 1998. Mannose binding protein deficiency is not associated with malaria, hepatitis B carriage nor tuberculosis in Africans. QJM. 91:13.

Beutler B, Greenwald D, Hulmes JD, Chang M, Pan YC, Mathison J, Ulevitch R, Cerami A. 1985. Identity of tumour necrosis factor and the macrophage-secreted factor cachectin. Nature. 316:552.

Bezouska K, Nepovim A, Horvath O, Pospisil M, Hamann J, Feizi T. 1995. CD69 antigen of human lymphocytes is a calcium-dependent carbohydrate-binding protein. Biochem Biophys Res Commun. 208:68.

Bezouska K, Yuen CT, O'Brien J, Childs RA, Chai W, Lawson AM, Drbal K, Fiserova A, Pospisil M, Feizi T. 1994. Oligosaccharide ligands for NKR-P1 protein activate NK cells and cytotoxicity. Nature. 372:150.

Biassoni R, Pessino A, Bottino C, Pende D, Moretta L, Moretta A. 1999. The murine homologue of the human NKp46, a triggering receptor involved in the induction of natural cytotoxicity. Eur J Immunol. 29:1014.

Bird AP. 1986. CpG-rich islands and the function of DNA methylation. Nature. 321:209.

Biron CA. 1997. Activation and function of natural killer cell responses during viral infections. Curr Opin Immunol. 9:24.

Biron CA, Byron KS, Sullivan JL. 1988. Susceptibility to viral infections in an individual with a complete lack of natural killer cells. Nat Immun Cell Growth Regul. 7:47.

Bluestone JA, Cron RQ, Barrett TA, Houlden B, Sperling AI, Dent A, Hedrick S, Rellahan B, Matis LA. 1991. Repertoire development and ligand specificity of murine TCR gamma delta cells. Immunol Rev. 120:5.

Bonavida B, Katz J, Gottlieb M. 1986. Mechanism of defective NK cell activity in patients with acquired immunodeficiency syndrome (AIDS) and AIDS-related complex. I. Defective trigger on NK cells for NKCF production by target cells, and partial restoration by IL 2. J Immunol. 137:1157.

Borrego F, Ulbrecht M, Weiss EH, Coligan JE, Brooks AG. 1998. Recognition of human histocompatibility leukocyte antigen (HLA)-E complexed with HLA class I signal sequence-derived peptides by CD94/NKG2 confers protection from natural killer cell-mediated lysis. J Exp Med. 187:813.

Borysiewicz LK, Rodgers B, Morris S, Graham S, Sissons JG. 1985. Lysis of human cytomegalovirus infected fibroblasts by natural killer cells: demonstration of an interferon-independent component requiring expression of early viral proteins and characterization of effector cells. J Immunol. 134: 2695.

Bowden, RA. 1995. Hematology/oncology Clinics of North America. 9:155.

Braud VM, Allan DS, O'Callaghan CA, Soderstrom K, D'Andrea A, Ogg GS, Lazetic S, Young NT, Bell JI, Phillips JH, Lanier LL, McMichael AJ. 1998. HLA-E binds to natural killer cell receptors CD94/NKG2A, B and C. Nature. 391:795.

Brautigam AR, Dutko FJ, Olding LB, Oldstone MB. 1979. Pathogenesis of murine cytomegalovirus infection: the macrophage as a permissive cell for cytomegalovirus infection, replication and latency. J Gen Virol. 44:349.

Brennan J, Lemieux S, Freeman JD, Mager DL, Takei F. 1996. Heterogeneity among Ly-49C natural killer (NK) cells: characterization of highly related receptors with differing functions and expression patterns. J Exp Med. 184:2085.

Brennan J, Mager D, Jefferies W, Takei F. 1994. Expression of different members of the *Ly49* gene family defines distinct natural killer cell subsets and cell adhesion properties. J Exp Med. 6:2287.

Brennan J, Mahon G, Mager DL, Jefferies WA, Takei F. 1996. Recognition of class I major histocompatibility complex molecules by Ly-49: specificities and domain interactions. J Exp Med. 183:1553.

Brooks AG, Posch PE, Scorzelli CJ, Borrego F, Coligan JE. 1997. NKG2A complexed with CD94 defines a novel inhibitory natural killer cell receptor. J Exp Med. 185:795.

Brown MG, Fulmek S, Matsumoto K, Cho R, Lyons PA, Levy ER., Scalzo AA, Yokoyama WM. 1997. A 2-Mb YAC contig and physical map of the natural killer gene complex on mouse chromosome 6. Genomics. 42:16.

Brown MG, Scalzo AA, Matsumoto K, Yokoyama WM. 1997. The natural killer gene complex: a genetic basis for understanding natural killer cell function and innate immunity. Immunol Rev.155:53.

Brown MG, Zhang J, Du Y, Stoll J, Yokoyama WM, Scalzo AA. 1999. Localization on a physical map of the NKC-linked *Cmv1* locus between *Ly49b* and the *Prp* gene cluster on mouse chromosome 6. J Immunol. 163:1991.

Browne H, Smith G, Beck S, Minson T. 1990. A complex between the MHC class I homologue encoded by human cytomegalovirus and beta-2-microglobulin. Nature. 347:770.

Brownstein D, Bhatt PN, Jacoby RO. 1989. Mousepox in inbred mice innately resistant or susceptible to lethal infection with ectromelia virus. Genetics of resistance to the. Moscow strain. Arch Virol. 107(1-2):35.

Brownstein DG, Bhatt PN, Gras L, Jacoby RO. 1991. Chromosomal locations and gonadal dependence of genes that mediate resistance to ectromelia (mousepox) virus-induced mortality. J Virol. 65:1946.

Brownstein DG, Gras L. 1995. Chromosome mapping of *Rmp-4*, a gonad-dependent gene encoding host resistance to mousepox. J Virol. 69:6958.

Brownstein DG, Gras L. 1997. Differential pathogenesis of lethal mousepox in congenic DBA/2 mice implicates natural killer cell receptor NKR-P1 in necrotizing hepatitis and the fifth component of complement in recruitment of circulating leukocytes to spleen. Am J Pathol. 150:1407.

Buckler AJ, Chang DD, Graw SL, Brook JD, Haber DA, Sharp PA, Housman DE. 1991. Exon amplification: a strategy to isolate mammalian genes based on RNA splicing. Proc Natl Acad Sci USA. 88:4005.

Bukowski JF, Woda BA, Welsh RM. 1984. Pathogenesis of murine cytomegalovirus infection in natural killer cell-depleted mice. J Virol. 52:119.

Burshtyn DN, Scharenberg AM, Wagtmann N, Rajagopalan S, Berrada K, Yi T, Kinet JP, Long EO. 1996. Recruitment of tyrosine phosphatase HCP by the killer cell inhibitor receptor. Immunity. 4:77.

Campbell AE, Slater JS, Cavanaugh VJ, Stenberg RM. 1992. An early event in murine cytomegalovirus replication inhibits presentation of cellular antigens to cytotoxic T lymphocytes. J Virol. 66:3011.

Campbell AE, Slater JS. 1994. Down-regulation of major histocompatibility complex class I synthesis by murine cytomegalovirus early gene expression. J Virol. 68:1805.

Carretero M, Cantoni C, Bellon T, Bottino C, Biassoni R, Rodriguez A, Perez-Villar JJ, Moretta L, Moretta A, Lopez-Botet M. 1997. The CD94 and NKG2-A C-type lectins covalently assemble to form a natural killer cell inhibitory receptor for HLA class I molecules. Eur J Immunol. 27:563.

Cebrian M, Yague E, Rincon M, Lopez-Botet M, de Landazuri MO, Sanchez-Madrid F. 1998. Triggering of T cell proliferation through AIM, an activation inducer molecule expressed on activated human lymphocytes. J Exp Med. 168:1621.

Chambers WH, Vujanovic NL, DeLeo AB, Olszowy MW, Herberman RB, Hiserodt JC. 1989. Monoclonal antibody to a triggering structure expressed on rat natural killer cells and adherent lymphokine-activated killer cells. J Exp Med. 169:1373.

Chan PY, Takei F. 1989. Molecular cloning and characterization of a novel murine T cell surface antigen, YE1/48. J Immunol. 142:1727.

Chartier FL, Keer JT, Sutcliffe MJ, Henriques DA, Mileham P, Brown SD. 1992. Construction of a mouse yeast artificial chromosome library in a recombination-deficient strain of yeast. Nat Genetics. 1:132.

Cheng J, Mielnicki LM, Pruitt SC, Maquat LE. 1990. Nucleotide sequence of murine triosphosphate isomerase cDNA. Nucleic Acids Res. 18:4261.

Ching C, Lopez C. 1979. Natural killing of herpes simplex virus type 1-infected target cells: normal human responses and influence of antiviral antibody. Infect Immun. 26:49.

Cifone MG, Alesse E, Di Marzio L, Ruggeri B, Zazzeroni F, Moretti S, Famularo G, Steinberg SM, Vullo E, De Simone C. 1997. Effect of L-carnitine treatment *in vivo* on apoptosis and ceramide generation in peripheral blood lymphocytes from AIDS patients. Proc Assoc Am Physicians. 109:146.

Cole R, Knuttner AG. 1926. A filtratable virus present in the submaxilliary glands of guinea pigs. J Exp Med 44:855.

Colonna M, and Samaridis J. 1995. Cloning of immunoglobulin-superfamily members associated with HLA-C and HLA-B recognition by human natural killer cells. Science. 268:405.

Cosman D, Fanger N, Borges L, Kubin M, Chin W, Peterson L, Hsu ML. 1997. A novel immunoglobulin superfamily receptor for cellular and viral MHC class I molecules. Immunity. 7:273.

Cox DR, Burmeister M, Price ER, Kim S, Myers RM. 1990. Radiation hybrid mapping: a somatic cell genetic method for constructing high-resolution maps of mammalian chromosomes. Science. 250:245.

Cunliffe V, Koopman P, McLaren A, Trowsdale J. 1990a. A mouse zinc finger gene which is transiently expressed during spermatogenesis. EMBO J. 9:197.

Cunliffe V, Williams S, Trowsdale J. 1990b. Genomic analysis of a mouse zinc finger gene, *Zfp-35*, that is up-regulated during spermatogenesis. Genomics. 8:331.

Dahle AJ, McCollister FP, Stagno S, Reynolds DW, Hoffman HE. 1979. Progressive hearing impairment in children with congenital cytomegalovirus infection. J Speech Hear Disord. 44:220.

D'Andrea A, Chang C, Franz-Bacon K, McClanahan T, Phillips JH, Lanier LL. 1995. Molecular cloning of NKB1. A natural killer cell receptor for HLA-B allotypes. J Immunol. 155:2306.

Daniels BF, Karlhofer FM, Seaman WE, Yokoyama WM. 1994. A natural killer cell receptor specific for a major histocompatibility complex class I molecule. J Exp Med. 180: 687.

Davis-Poynter NJ, Lynch DM, Vally H, Shellam GR, Rawlinson WD, Barrell BG, Farrell HE. 1997. Identification and characterization of a G protein-coupled receptor homolog encoded by murine cytomegalovirus. J Virol. 71:1521.

de Boer P, Groen A. 1974. Fertility and meiotic behavior of male T70H tertiary trisomics of the mouse (Mus musculus). A case of preferential telomeric meiotic pairing in a mammal. Cytogenet Cell Genet. 13:489.

Dechanet J, Merville P, Berge F, Bone-Mane G, Taupin JL, Michel P, Joly P, Bonneville M, Potaux L, Moreau JF. 1999. Major expansion of gamma/delta T lymphocytes following cytomegalovirus infection in kidney allograft recipients. J Infect Dis. 179:1.

del Val M, Hengel H, Hacker H, Hartlaub U, Ruppert T, Lucin P, Koszinowski UH. 1992. Cytomegalovirus prevents antigen presentation by blocking the transport of peptide-loaded major histocompatibility complex class I molecules into the medial-Golgi compartment. J Exp Med. 176:729.

Delano M., Brownstein DG. 1995. Innate resistance to lethal mousepox is genetically linked to the NK gene complex on chromosome 6 and correlates with early restriction of virus replication by cells with an NK phenotype. J Virol. 69:5875.

Demmler GJ. 1991. Infectious Diseases Society of America and Centers for Disease Control. Summary of a workshop on surveillance for congenital cytomegalovirus disease. Rev Infect Dis. 13:315.

Deng H, Liu R, Ellmeier W, Choe S, Unutmaz D, Burkhart M, Di Marzio P, Marmon S, Sutton RE, Hill CM, Davis CB, Peiper SC, Schall TJ, Littman DR, Landau NR. 1996. Identification of a major co-receptor for primary isolates of HIV-1. Nature. 381:661.

Depatie C, Chalifour A, Pare C, Lee SH, Vidal SM, Lemieux S. 1999. Assessment of *Cmv1* candidates by genetic mapping and *in vivo* antibody depletion of NK cell subsets. Internatl Immunol. 9: 1541.

Depatie C, Muise E, Lepage P, Gros P, Vidal SM. 1997. High-resolution linkage map in the proximity of the host resistance locus *Cmv1*. Genomics. 39:154.

Devriendt K, Zhang J, van Leuven F, van den Berghe H, Cassiman JJ, Marynen P. 1989. A cluster of alpha 2-macroglobulin-related genes (alpha 2M) on human chromosome 12p: cloning of the pregnancy-zone protein gene and an alpha 2M pseudogene. Gene 81:325.

Dietrich W, Katz H, Lincoln SE, Shin HS, Friedman J, Dracopoli NC, Lander ES. 1992. A genetic map of the mouse suitable for typing intraspecific crosses. Genetics. 131:423.

Dietrich WF, Miller JC, Steen RG, Merchant M, Damron D, Nahf R, Gross A, Joyce DC, Wessel M, Dredge RD, and *et al.* 1994. A genetic map of the mouse with 4,006 simple sequence length polymorphisms. Nat. Genetics 7: 220.

Diez E, Beckers MC, Ernst E, DiDonato CJ, Simard LR, Morissette C, Gervais F, Yoshida SI, and Gros P. 1997. Genetic and physical mapping of the mouse host resistance locus *Lgn1*. Mamm. Genome. 8:682.

Dissen E, Ryan JC, Seaman WE, Fossum S. 1996. An autosomal dominant locus, *Nka*, mapping to the *Ly-49* region of a rat natural killer (NK) gene complex, controls NK cell lysis of allogeneic lymphocytes. J Exp Med. 183:2197.

Duh JL, Zhu H, Shertzer HG, Nebert DW, Puga A. 1995. The Y-box motif mediates redox-dependent transcriptional activation in mouse cells. J Biol Chem. 270:30499.

Elliott RW, Moore KJ. 1994. Mouse chromosome 6. Mamm Genome. 5: S79.

Erice A.1999. Resistance of human cytomegalovirus to antiviral drugs. Clin Microbiol Rev. 12:286.

Farrell HE, Vally H, Lynch DM, Fleming P, Shellam GR, Scalzo AA, Davis-Poynter NJ. 1997. Inhibition of natural killer cells by a cytomegalovirus MHC class I homologue in vivo. Nature. 386:510.

Feinberg AP, Vogelstein B. 1984. A technique for radiolabeling DNA restriction endonuclease fragments to high specific activity. Addendum Anal. Biochem. 137:266.

Fish KN, Stenglein SG, Ibanez C, Nelson JA. 1995. Cytomegalovirus persistence in macrophages and endothelial cells. Scand J Infect Dis Suppl. 99:34.

Fleming P, Davis-Poynter N, Degli-Esposti M, Densley E, Papadimitriou J, Shellam G, Farrell H. 1999. The murine cytomegalovirus chemokine homolog, m131/129, is a determinant of viral pathogenicity. J Virol. 73:6800.

Fletcher CV, Collier AC, Rhame FS, Bennett D, Para MF, Beatty CC, Jones CE, Balfour HH Jr. 1994. Foscarnet for suppression of human immunodeficiency virus replication. Antimicrob Agents Chemother. 38:604.

Forbes CA, Brown MG, Cho R, Shellam GR, Yokoyama WM, Scalzo AA. 1997. The *Cmv1* host resistance locus is closely linked to the *Ly49* multigene family within the natural killer cell gene complex on mouse chromosome 6. Genomics. 41:406.

Fossum S, Ager A, Rolstad B. 1987. Specific inhibition of natural killer (NK) activity against different alloantigens. Immunogenetics. 26:329.

Gallant JE, Moore RD, Richman DD, Keruly J, Chaisson RE. 1992. Incidence and natural history of cytomegalovirus disease in patients with advanced human immunodeficiency virus disease treated with zidovudine. The Zidovudine Epidemiology Study Group. J Infect Dis. 166:1223.

Gavioli R, Risso A, Smilovich D, Baldissarro I, Capra MC, Bargellesi A, Cosulich ME. 1992. CD69 molecule in human neutrophils: its expression and role in signal-transducing mechanisms. Cell Immunol. 142:186.

Gessner JE, Grussenmeyer T, Dumbsky M, Schmidt RE. 1996. Separate promoters from proximal and medial control regions contribute to the natural killer cell-specific transcription of the human FcgammaRIII-A (CD16-A) receptor gene. J Biol Chem. 271:30755.

Ghosh S, Palmer SM, Rodrigues NR, Cordell HJ, Hearne CM, Cornall RJ, Prins J-B, McShane P, Lathrop GM, Peterson LB, Wiker LS, Todd JA. 1993. Polygenic control of autoimmune diabetes in nonobese diabetic mice. Nature Genet. 4: 404.

Gibbons AE, Shellam GR, Price P. 1997. Correlation between natural killer cell activation in the bone marrow and haemopoietic dysfunction following cytomegalovirus infection of mice. Immunology. 91:227.

Giorda R, and Trucco M. 1991. Mouse NKR-P1. A family of genes selectively coexpressed in adherent lymphokine-activated killer cells. J Immunol. 147:1701.

Golub TR, Barker, G.F., Lovett, M., and Gilliland, D.G. 1994. Fusion of PDGF receptor beta to a novel ets-like gene, tel, in chronic myelomonocytic leukemia with t(5;12)

Goodpasture EW, Talbot FB. 1921. Concerning the nature of " proteozoan-like cells in certains lesions of infancy. Am J Dis Child 21:415.

Gosselin P, Lusignan Y, Brennan J, Takei F, Lemieux S. 1997. The NK2.1 receptor is encoded by *Ly-49C* and its expression is regulated by MHC class I alleles. Intl Immunol. 9:533.

Green EL. 1981. Breeding systems. In "The Mouse in Biomedical Research" (H.L. Foster, JD. Small, and JG Fox, Eds.), Academic Press, New York. p.91.

Grundy JE, Melief CJ. 1982. Effect of *Nu/Nu* gene on genetically determined resistance to murine cytomegalovirus. J Gen Virol. 61:133.

Grundy JE, Mackenzie JS, Stanley NF. 1981. Influence of H-2 and non-H-2 genes on resistance to murine Cytomegalovirus infection. Infect Immunol. 32:277.

Haldi ML, Strickland C, Lim P, VanBerkel V, Chen X, Noya D, Korenberg JR, Husain Z, Miller J, Lander, ES. 1996. A comprehensive large-insert yeast artificial chromosome library for physical mapping of the mouse genome. Mamm Genome. 7:767.

Hanshaw JB. 1995. Cytomegalovirus infections. Pediatr Rev. 16: 43.

Hanson LK, Slater JS, Karabekian Z, Virgin HW 4th, Biron CA, Ruzek MC, van Rooijen N, Ciavarra RP, Stenberg RM, Campbell AE.1999. Replication of murine cytomegalovirus in differentiated macrophages as a determinant of viral pathogenesis. J Virol. 73:5970.

Hara T, Jung LK, Bjorndahl JM, Fu SM. 1986. Human T cell activation. III. Rapid induction of a phosphorylated 28 kD/32 kD disulfide-linked early activation antigen (EA 1) by 12-o-tetradecanoyl phorbol-13-acetate, mitogens, and antigens. J Exp Med. 164:1988.

Hayashi K, Saze K, Uchida Y. 1985. Studies of latent cytomegalovirus infection: the macrophage as a virus-harboring cell. Microbiol Immunol. 29:625.

He X, Yoshida H, Minamishima Y, Nomoto K. 1995. Analysis of the role of CD4+ T-cells during murine cytomegalovirus infection in different strains of mice. Virus Res. 36:233.

Heise MT, Pollock JL, O'Guin A, Barkon ML, Bormley S, Virgin HW. 1998. Murine cytomegalovirus infection inhibits IFN gamma-induced MHC class II expression on macrophages: the role of type I interferon. Virology. 241:331.

Held W, Dorfman JR, Wu MF, Raulet DH. 1996. Major histocompatibility complex class I-dependent skewing of the natural killer cell Ly49 receptor repertoire. Eur J Immunol. 26:2286.

Held W, Roland J, Raulet DH. 1995. Allelic exclusion of *Ly49*-family genes encoding class I MHC-specific receptors on NK cells. Nature. 376:355.

Hengel H, Burke K, Kyburz D, Zinkernagel RM, Koszinowski UH. 1995. Peptides control the gain and loss of allele specificity by mutated MHC class I molecules. J Immunol. 154:4557.

Hermanson GG, Hoekstra MF, McElligott DL, Evans GA. 1991. Rescue of end fragments of yeast artificial chromosomes by homologous recombination in yeast. Nucleic Acids Res. 19:4943.

Hibberd PL, Tolkoff-Rubin NE, Conti D, Stuart F, Thistlethwaite JR, Neylan JF, Snydman DR, Freeman R, Lorber MI, Rubin RH. 1995. Preemptive ganciclovir therapy to prevent cytomegalovirus disease in cytomegalovirus antibody-positive renal transplant recipients. A randomized controlled trial. Ann Intern Med. 123:18.

Hill AV. 1998. Host genetics of infectious diseases: old and new approaches converge. Emerg Infect Dis. 4:695.

Hiromatsu K, Yoshikai Y, Matsuzaki G, Ohga S, Muramori K, Matsumoto K, Bluestone JA, Nomoto K A. 1992. Protective role of gamma/delta T cells in primary infection with Listeria monocytogenes in mice. J Exp Med. 175:49.

Ho EL, Heusel JW, Brown MG, Matsumoto K, Scalzo AA, Yokoyama WM. 1998. Murine *Nkg2d* and *Cd94* are clustered within the natural killer complex and are expressed independently in natural killer cells. Proc Natl Acad Sci USA. 95:6320.

Ho M. 1994. Advances in understanding cytomegalovirus infection after transplantation. Transplant Proc. 26 (Suppl.1):7.

Horwitz CA, Henle W, Henle G. 1979. Diagnostic aspects of the cytomegalovirus mononucleosis syndrome in previously healthypersons. Postgrad Med. 66:153.

Hudson JB, Walker DG, Altamirano M. 1988. Analysis *in vitro* of two biologically distinct strains of murine cytomegalovirus. Arch Virol. 102: 289.

Idris AH, Iizuka K, Smith HRC, Scalzo AA, Yokoyama WM. 1998. Genetic control of natural killing and in vivo tumor elimination by the *Chok* locus. J Exp Med. 188:2243.

Idris AH, Smith HR, Mason LH, Ortaldo JR, Scalzo AA, Yokoyama WM. 1999. The natural killer gene complex genetic locus *Chok* encodes Ly-49D, a target recognition receptor that activates natural killing. Proc Natl Acad USA. 96:6330.

Ishikawa R, Biron CA. 1993. IFN induction and associated changes in splenic leukocyte distribution. J Immunol. 150:3713.

Iwamoto T, Taniguchi M, Asai N, Ohkusu K, Nakashima I, Takahashi M. 1993. cDNA cloning of mouse ret proto-oncogene and its sequence similarity to the cadherin superfamily. Oncogene. 8:1087.

Jacoby RO, Bhatt PN, Brownstein DG. 1989. Evidence that NK cells and interferon are required for genetic resistance to lethal infection with ectromelia virus. Arch Virol. 108: 49.

Joncas J, Monczak Y, Ghibu F, Alfieri C, Bonin A, Ahronheim G, Rivard G. 1989. Brief report: killer cell defect and persistent immunological abnormalities in two patients with chronic active Epstein-Barr virus infection. J Med Virol. 28:110.

Jonjic S, Mutter W, Weiland F, Reddehase MJ, Koszinowski UH. 1989. Site-restricted persistent cytomegalovirus infection after selective long-term depletion of $CD4^+$T lymphocytes. J Exp Med. 169:1199.

Jonjic S, Pavic I, Lucin P, Rukavina D, Koszinowski UH. 1990. Efficacious control of cytomegalovirus infection after long-term depletion of $CD8^+$ T lymphocytes. J Virol. 64:5457.

Kagi D, Seiler P, Pavlovic J, Ledermann B, Burki K, Zinkernagel RM, Hengartner H. 1995. The roles of perforin- and Fas-dependent cytotoxicity in protection against cytopathic and noncytopathic viruses. Eur J Immunol. 25:3256.

Karlhofer FM, Ribaudo RK, Yokoyama WM. 1992. MHC class I alloantigen specificity of Ly-49^+ IL-2-activated natural killer cells. Nature. 358:66.

Karlhofer FM, Hunziker R, Reichlin A, Margulies DH, Yokoyama WM. 1994. Host MHC class I molecules modulate *in vivo* expression of a NK cell receptor. J Immunol. 153:2407.

Karlsson S, Nienhuis AW. 1985. Developmental regulation of human globin genes. Annu Rev Biochem. 54:1071.

Karre K, Ljunggren HG, Piontek G, Kiessling R. 1986. Selective rejection of H-2-deficient lymphoma variants suggests alternative immune defence strategy. Nature. 319:675.

Kase A, Johansson MH, Olsson-Alheim MY, Karre K, Hoglund P. 1998. External and internal calibration of the MHC class I-specific receptor Ly49A on murine natural killer cells. J Immunol. 161:6133.

Kiessling R, Klein E, Pross H, Wigzell H.1975. "Natural" killer cells in the mouse. II. Cytotoxic cells with specificity for mouse Moloney leukemia cells. Characteristics of the killer cell. Eur J Immunol. 5:117.

Kleijnen MF, Huppa JB, Lucin P, Mukherjee S, Farrell H, Campbell AE, Koszinowski UH, Hill AB, Ploegh HL. 1997. A mouse cytomegalovirus glycoprotein, gp34, forms a complex with folded class I MHC molecules in the ER which is not retained but is transported to the cell surface. EMBO J. 16:685.

Koo GC, Peppard JR. 1984. Establishment of monoclonal anti-NK-1.1 antibody. Hybridoma 3:301.

Kozlowski M, Mlinaric-Rascan I, Feng GS, Shen R, Pawson T, Siminovitch KA. 1993. Expression and catalytic activity of the tyrosine phosphatase PTP1C is severely impaired in motheaten and viable motheaten mice. J Exp Med. 178:2157.

Kozlowski M, Schorey J, Portis T, Grigoriev V, Kornbluth J. 1999. NK lytic-associated molecule: a novel gene selectively expressed in cells with cytolytic function. J Immunol. 163:1775.

Krauter K, Montgomery K, Yoon SJ, LeBlanc-Straceski J, Renault B, Marondel I, Herdman V, Cupelli L, Banks A, Lieman J, *et al.* 1995. A second-generation YAC contig map of human chromosome 12. Nature. 377 (6547 Suppl): 321.

Kubo S, Itoh Y, Ishikawa N, Nagasawa R, Mitarai T, Maruyama N. 1993. The gene encoding mouse lymphocyte antigen Ly-49: structural analysis and the 5'-flanking sequence. Gene. 136:329.

Kubota A, Kubota S, Farrell HE, Davis-Poynter N, Takei F. 1999. Inhibition of NK cells by murine CMV-encoded class I MHC homologue *m144*. Cell Immunol. 191:145.

Kuribayashi K, Gillis S, Kern DE, Henney CS. 1981. Murine NK cell cultures: effects of interleukin-2 and interferon on cell growth and cytotoxic reactivity. J Immunol. 126:2321.

Kusumi K, Smith JS, Segre JA, Koos DS, Lander ES. 1993. Construction of a large-insert yeast artificial chromosome library of the mouse genome. Mamm Genome. 4:391.

Lang DJ, *et al.* 1975. Cytomegalovirus in semen: observations in selected populations. J Infect Dis. 132:472.

Lanier LL, Buck DW, Rhodes L, Ding A, Evans E, Barney C, Phillips JH. 1988. Interleukin 2 activation of natural killer cells rapidly induces the expression and phosphorylation of the Leu-23 activation antigen. J Exp Med. 167:1572.

Lanier LL, Chang C, Phillips JH. 1994. Human NKR-P1A. A disulfide-linked homodimer of the C-type lectin superfamily expressed by a subset of NK and T lymphocytes. J Immunol. 153:2417.

Lanier LL. 1998. NK cell receptors. Annual Rev Immunol. 16:359.

Lanier LL, Corliss B, Wu J, Phillips JH. 1998. Association of DAP12 with activating CD94/NKG2C NK cell receptors. Immunity. 8:693.

Larin Z, Monaco AP, Lehrach H. 1991. Yeast artificial chromosome libraries containing large inserts from mouse and human DNA. Proc Natl Acad USA. 88:4123.

Lathbury LJ, Allan JE, Shellam GR, Scalzo AA. 1996. Effect of host genotype in determining the relative roles of natural killer cells and T cells inmediating protection against murine cytomegalovirus infection. J Gen Virol. 77:2605.

Laurie DA, Hulten MA. 1985. Further studies on chiasma distribution and interference in the human male. Ann Hum Genet. 49:203.

Lawrence JB, Singer RH, McNeil JA. 1990. Interphase and metaphase resolution of different distances within the human dystrophin gene. Science. 249:928.

Lawrence JB, Villnave CA, Singer RH. 1988. Sensitive, high-resolution chromatin and chromosome mapping in situ: presence and orientation of two closely integrated copies of EBV in a lymphoma line. Cell. 52:51.

Lazetic S, Chang C, Houchins JP, Lanier LL, Phillips JH. 1996. Human natural killer cell receptors involved in MHC class I recognition are disulfide-linked heterodimers of CD94 and NKG2 subunits. J Immunol. 157:4741.

Le Drean E, Vely F, Olcese L, Cambiaggi A, Guia S, Krystal G, Gervois N, Moretta A, Jotereau F, Vivier E. 1998. Inhibition of antigen-induced T cell response and antibody-induced NK cell cytotoxicity by NKG2A: association of NKG2A with SHP-1 and SHP-2 protein-tyrosine phosphatases. Eur J Immunol. 28:264.

Lemieux S, Ouellet-Talbot F, Lusignan Y, Morelli L, Labrèche N, Gosselin P, Lecomte J. 1991. Identification of murine natural killer cell subsets with monoclonal antibodies derived from 129 anti-C57BL/6 immune spleen cells. Cell Immunol. 134:191.

Levine MA, Smallwood PM, Moen PT, Helman LJ, Ahn TG. 1990. Molecular cloning of ß3 subunit, a third form of the G protein ß-subunit polypeptide. Proc Natl Acad Sci USA. 87:2329.

Levy JA. 1997. HIV neuropathogenesis. J Neurovirol. 3 (Suppl 1):S14.

Lewin B. 1997. "Genes VI" Oxford University Press and Cell Press, Oxford. pp.548.

Lichter P, Ledbetter SA, Ledbetter DH, Ward DC. 1990. Fluorescence *in situ* hybridization with Alu and L1 polymerase chain reaction probes for rapid characterization of human chromosomesin hybrid cell lines. Proc Natl Acad Sci USA. 87:6634.

Liu R, Paxton WA, Choe S, Ceradini D, Martin SR, Horuk R, MacDonald ME, Stuhlmann H, Koup RA, Landau NR. 1996. Homozygous defect in HIV-1 coreceptor accounts for resistance of some multiply-exposed individuals to HIV-1 infection. Cell. 86:367.

Ljunggren HG, Karre K. 1985. Host resistance directed selectively against H-2-deficient lymphoma variants. Analysis of the mechanism. J Exp Med. 162:1745.

Lohwasser S, Hande P, Mager DL, Takei F. 1999. Cloning of murine NKG2A, B and C: second family of C-type lectin receptors on murine NK cells. Eur J Immunol. 29:755.

Long EO, Wagtmann N. 1997. Natural killer cell receptors. Curr Opin Immunol. 9:344.

Lucin P, Pavic I, Polic B, Jonjic S, Koszinowski UH. 1992. Gamma interferon-dependent clearance of cytomegalovirus infection in salivary glands. J Virol. 66:1977.

MacDonald MR, Li XY, Virgin HW 4th. 1997. Late expression of a beta chemokine homolog by murine cytomegalovirus. J Virol. 71:1671.

MacDonald HR. 1995. NK1.1$^+$ T cell receptor alpha-beta positive cells: new clues to their origin, specificity, and function. J Exp Med. 182: 633.

Malkinson AM, Nesbitt MN, Skamene E. 1985. Susceptibility to urethan-induced pulmonary adenomas between A/J and C57BL/6J mice: use of AXB and BXA recombinant inbred lines indicating a three-locus genetic model. J Natl Cancer Inst. 75: 971.

Malo D, Vidal SM, Hu J, Skamene E, Gros P. 1993. High-resolution linkage map in the vicinity of the host resistance locus *Bcg*. Genomics. 16:655.

Manly KF. 1993. A Macintosh program for storage and analysis of experimental genetic mapping data. Mamm Genome. 4:303.

Marchuk D, Drumm M, Saulino A, Collins FS. 1991. Construction of T-vectors, a rapid and general system for direct cloning of unmodified PCR products. Nucleic Acids Res. 19:1154.

Mason LH, Anderson SK, Yokoyama WM, Smith HR, Winkler-Pickett R, Ortaldo JR. 1996. The Ly-49D receptor activates murine natural killer cells. J Exp Med. 184:2119.

Mason LH, Ortaldo JR, Young HA, Kumar V, Bennett M, Anderson SK. 1995. Cloning and functional characteristics of murine large granular lymphocyte-1: a member of the *Ly-49* gene family (*Ly-49G2*). J Exp Med. 182:293.

McQueen KL, Freeman JD, Takei F, Mager DL. 1998. Localization of five new *Ly49* genes, including three closely related to *Ly49c*. Immunogenetics. 48:174.

Mead R, Jack D, Pembrey M, Tyfield L, Turner M. 1997. Mannose-binding lectin alleles in a prospectively recruited UK population. The ALSPAC Study Team. Avon Longitudinal Study of Pregnancy and Childhood. Lancet. 349:1669.

Medearis, DN. 1982. CMV immunity:imperfect but protective. N Engl J Med. 306:985.

Melanitou E, Simon-Chazottes D, Guenet JL, Rougeon F. 1991. The gene coding for the kidney androgen-regulated protein (*Kap*), maps between the *Gapd* and *Kras-2* genes on mouse chromosome 6. Mamm Genome. 1:191.

Misra J, Hudson JB. 1980. Minor base sequence differences between the genomes of two strains of murine cytomegalovirus differing in virulence. Arch Virol. 64: 1.

Monbaerts P, Arnoldi J, Russ F, Tonegawa S, Kaufmann SH. 1993. Different roles of ß and T cells in immunity against intracellular bacterial pathogen. Nature. 365:53.

Muller U, Steinhoff U, Reis LF, Hemmi S, Pavlovic J, Zinkernagel RM, Aguet M. 1994. Functional role of type I and type II interferons in antiviral defense. Science. 1994 264:1918.

Nagasawa R, Gross J, Kanagawa O, Townsend K, Lanier LL, Chiller J, Allison JP. 1987. Identification of a novel T cell surface disulfide-bonded dimer distinct from the α/β antigen receptor. J Immunol. 138:815.

Nakamura MC, Niemi EC, Fisher MJ, Shultz LD, Seaman WE, Ryan JC. 1997. Mouse Ly-49A interrupts early signaling events in natural killer cell cytotoxicity and functionally associates with the SHP-1 tyrosine phosphatase. J Exp Med. 185: 673.

Nakamura MC, Linnemeyer PA, Niemi EC, Mason LH, Ortaldo JR, Ryan JC, Seaman WE. 1999. Mouse Ly-49D recognizes H-2D^{d} and activates natural killer cells cytotoxicity. J Exp Med. 189:493.

Nathan C. 1992. Nitric oxide as a secretory product of mammalian cells. FASEB J. 6:3051.

Natuk RJ, Welsh RM. 1987. Accumulation and chemotaxis of natural killer/large granular lymphocytes at sites of virusreplication. J Immunol. 138:877.

Newmark PA, Boswell RE. 1994. The *mago nashi* locus encodes an essential product required for germ plasm assembly in Drosophila. Development. 120:1303.

Oberg B. 1989. Antiviral effects of phosphonoformate (PFA, foscarnet sodium). Pharmacol Ther. 40:213.

Olcese L, Lang P, Vely F, Cambiaggi A, Marguet D, Blery M, Hippen KL, Biassoni R, Moretta A, Moretta L, Cambier JC, Vivier E. 1996. Human and mouse killer-cell inhibitory receptors recruit PTP1C and PTP1D protein tyrosine phosphatases. J Immunol. 156:4531.

Olsson-Alheim MY, Salcedo M, Ljunggren HG, Karre K, Sentman CL. 1997. NK cell receptor calibration: effects of MHC class I induction on killing by Ly49A^{high} and Ly49A^{low} NK cells. J Immunol. 159:3189.

Orange JS, Biron CA. 1996. Characterization of early IL-12, IFN-alpha/beta, and TNF effects on antiviral state and NK cell responses during murine cytomegalovirus infection. J Immunol. 156:4746.

Orange JS, Wang B, Terhorst C, Biron CA. 1995. Requirement for natural killer cell-produced interferon gamma in defense against murine cytomegalovirus infection and enhancement of this defense pathway by interleukin 12 administration. J Exp Med. 182:1045-56.

Pavlovic J, Haller O, Staeheli P. 1992. Human and mouse Mx proteins inhibit different steps of the influenza virus multiplication cycle. J Virol. 66:2564.

Penha-Goncalves C, Leijon K, Persson L, Homberg D. 1995. Type I diabetes and the control of dexamethazone-induced apoptosis in mice maps to the same region on chromosome 6. Genomics. 28: 398.

Perou CM, Leslie JD, Green W, Li L, Ward DM, Kaplan J. 1997. The Beige/Chediak-Higashi syndrome gene encodes a widely expressed cytosolic protein. J Biol Chem. 272:29790.

Perou CM, Moore KJ, Nagle DL, Misumi DJ, Woolf EA, McGrail SH, Holmgren L, Brody TH, Dussault BJ Jr,Monroe CA, Duyk GM, Pryor RJ, Li L, Justice MJ, Kaplan J. 1996. Identification of the murine *beige* gene by YAC complementation and positional cloning. Nat Genet. 13:303.

Pessino A, Sivori S, Bottino C, Malaspina A, Morelli L, Moretta L, Biassoni R, Moretta A. 1998. Molecular cloning of *NKp46*: a novel member of the immunoglobulin superfamily involved in triggering of natural cytotoxicity. J Exp Med. 188:953.

Pham CT, MacIvor DM, Hug BA, Heusel JW, Ley TJ. 1996. Long-range disruption of gene expression by a selectable marker cassette. Proc Natl Acad Sci USA. 93:13090.

Philippsen P, Stotz A, Scherf C. 1991. DNA of Saccharomyces cerevisiae. Methods Enzymol. 194:169.

Pieler T, Bellefroid E. 1994. Perspectives on zinc finger protein function and evolution--an update. Mol Biol Rep. 20:1.

Pleskoff O, Treboute C, Brelot A, Heveker N, Seman M, Alizon M. 1997. Identification of a chemokine receptor encoded by human cytomegalovirus as a cofactor for HIV-1 entry. Science. 276:1874.

Plosker GL, Noble S. 1999. Cidofovir: a review of its use in cytomegalovirus retinitis in patients with AIDS. Drugs. 58:325.

Plougastel B, Trowsdale J. 1998. Sequence analysis of a 62-kb region overlapping the human KLRC cluster of genes. Genomics. 49:193.

Polic B, Jonjic S, Pavic I, Crnkovic I, Zorica I, Hengel H, Lucin P, Koszinowski UH. 1996. Lack of MHC class I complex expression has no effect on spread and control of cytomegalovirus infection *in vivo*. J Gen Virol. 77:217.

Price P, Allcock RJ, Coombe DR, Shellam GR, McCluskey J. 1995. MHC proteins and heparan sulphate proteoglycans regulate murine cytomegalovirus infection. Immunol Cell Biol. 73:308.

Price P, Gibbons AE, Shellam GR. 1990. H-2 class I loci determine sensitivity to MCMV in macrophages and fibroblasts. Immunogenetics. 32: 20.

Price P, Olver SD, Gibbons AE, Teo HK, Shellam GR. 1993. Characterization of thymic involution induced by murine cytomegalovirus infection. Immunol Cell Biol. 71:155.

Quinnan GV Jr, Manischewitz JF, Kirmani N. 1982. Involvement of natural killer cells in the pathogenesis of murine cytomegalovirus interstitial pneumonitis and the immune response to infection. J Gen Virol. 58:173.

Quinnan GV, Manischewitz, JF. 1987. Genetically determined resistance to lethal murine cytomegalovirus infe4ction is mediated by interferon-dependant and -independant restriction of virus replication. J Virol. 61:1875.

Rawlings DJ, Saffran DC, Tsukada S, Largaespada DA, Grimaldi JC, Cohen L, Mohr RN, Bazan JF, Howard M, Copeland NG, *et al.* 1993. Mutation of unique region of Bruton's tyrosine kinase in immunodeficient XID mice. Science. 261:358.

Reddehase MJ, Weiland F, Munch K, Jonjic S, Luske A, Koszinowski UH. 1985. Interstitial murine cytomegalovirus pneumonia after irradiation: characterization of cells that limit viral replication during established infection of the lungs. J Virol. 55:264.

Reddehase MJ, Mutter W, Munch K, Buhring JJ, Koszinowski UH. 1987. CD8-positive lymphocytes specific for murine Cytomegalovirus immediate-early antigens mediate protective immunity. J Virol. 61: 3102.

Reddy MM, Grieco MH, McKinley GF, Causey DM, van der Horst CM, Parenti DM, Hooton TM, Davis RB, Jacobson MA. 1992. Effect of foscarnet therapy on human immunodeficiency virus p24 antigen levels in AIDS patients with cytomegalovirus retinitis. J Infect Dis. 166:607.

Redpath S, Angulo A, Gascoigne NR, Ghazal P. 1999. Murine cytomegalovirus infection down-regulates MHC class II expression on macrophages by induction of IL-10. J Immunol. 162:6701.

Reeves RH, Crowley MR, Moseley WS, Seldin MF. 1991. Comparison of interspecific to intersubspecific backcrosses demonstrates species and sex differences in recombination frequency on mouse chromosome 16. Mamm Genome. 1:158.

Renard V, Cambiaggi A, Vely F, Blery M, Olcese L, Olivero S, Bouchet M,Vivier E. 1997. Transduction of cytotoxic signals in natural killer cells: a general model of fine tuning between activatory and inhibitory pathways in lymphocytes. Immunol Rev. 155:205.

Reyburn HT, Mandelboim O, Vales-Gomez M, Davis DM, Pazmany L, Strominger JL. 1997. The class I MHC homologue of human cytomegalovirus inhibits attack by natural killer cells. Nature. 386:514.

Reynolds DW, Stagno S, Hosty TS, Tiller M, Alford CA Jr. 1973. Maternal cytomegalovirus excretion and perinatal infection. N Engl J Med. 289:1.

Riley J, Butler R, Ogilvie D, Finniear R, Jenner D, Powell S, Anand R, Smith JC, Markham AF. 1990. A novel, rapid method for the isolation of terminal sequences from yeast artificial chromosome (YAC) clones. Nucleic Acids Res. 18:2887.

Rolstad B, Fossum S. 1987. Allogeneic lymphocyte cytotoxicity (ALC) in rats: establishment of an in vitro assay, and direct evidence that cells with natural killer (NK) activity are involved in ALC. Immunology. 60:151.

Rowe WP, Hartley JW, Waterman S, Turner HC, Huebner RJ. 1956. Cytophatogenic agents resembling human salivary gland virus recovered from tissue cultures of human adenoids. Proc Soc Exp Biol Med. 92:418.

Ryan JC, Niemi EC, Goldfien RD, Hiserodt JC, Seaman WE. 1991. NKR-P1, an activating molecule on rat natural killer cells, stimulates phosphoinositide turnover and a rise in intracellular calcium. J Immunol. 147:3244.

Ryan JC, Turck J, Niemi EC, Yokoyama WM, Seaman WE. 1992. Molecular cloning of the NK1.1 antigen, a member of the NKR-P1 family of natural killer cell activation molecules. J Immunol. 149:1631.

Salazar-Mather TP, Ishikawa R, Biron CA. 1996. NK cell trafficking and cytokine expression in splenic compartments after IFN induction and viral infection. J Immunol. 157:3054.

Salcedo M, Andersson M, Lemieux S, Van Kaer L, Chambers BJ, Ljunggren HG. 1998. Fine tuning of natural killer cell specificity and maintenance of self tolerance in MHC class I-deficient mice. Eur J Immunol. 28:1315.

Salcedo M, Diehl AD, Olsson-Alheim MY, Sundback J, Van Kaer L, Karre K, Ljunggren, HG. 1997. Altered expression of Ly49 inhibitory receptors on natural killer cells from MHC class I-deficient mice. J Immunol. 158:3174.

Sambrook J, Fritsch EF, Maniatis T. 1989. "Molecular Cloning: A Laboratory Manual" 2nd ed. Cold Spring Harbor Laboratory, Cold Spring Harbor, NY.

Samson M, Libert F, Doranz BJ, Rucker J, Liesnard C, Farber CM, Saragosti S, *et al.* 1996. Resistance to HIV-1 infection in caucasian individuals bearing mutant alleles of the CCR-5 chemokine receptor gene. Nature. 382:722.

Sangster MY, Heliams DB, MacKenzie JS, Shellam GR. 1993. Genetic studies of flavivirus resistance in inbred strains derived from wild mice: evidence for a new resistance allele at the flavivirus resistance locus (Flv). J Virol. 67:340.

Scalzo AA, Brown MG, Chu DT, Heusel JW, Yokoyama WM, Forbes CA. 1999. Development of intra-natural killer complex (NKC) recombinant and congenic mouse strains for mapping and functional analysis of NK cell regulatory loci. Immunogenetics. 49:238.

Scalzo AA, Fitzgerald NA, Simmons A, La Vista AB, Shellam GR. 1990. *Cmv1*, a genetic locus that controls murine cytomegalovirus replication in the spleen. J Exp Med. 171:1469.

Scalzo AA, Fitzgerald NA, Wallace CR, Gibbons AE, Smart YC, Burton RC, Shellam GR. 1992. The effect of the *Cmv1* resistance gene, which is linked to the natural killer cell gene complex, is mediated by natural killer cells. J Immunol. 149: 581.

Scalzo AA, Lyons PA, Fitzgerald NA, Forbes CA, Yokoyama WM, Shellam GR. 1995. Genetic mapping of *Cmv1* in the region of mouse chromosome 6 encoding the NK gene complex-associated loci *Ly49* and *musNKR-P1*. Genomics. 27: 435.

Scharf JM, Damron D, Frisella A, Bruno S, Beggs AH, Kunkel LM, Dietrich WF. 1996. The mouse region syntenic for human spinal muscular atrophy lies within the *Lgn1* critical interval and contains multiple copies of *Naip* exon 5. Genomics. 38:405.

Schild H, Mavaddat N, Litzenberger C, Ehrich EW, Davis MM, Bluestone JA, Matis L, Draper RK, Chien Y. 1994. The nature of major histocompatibility complex recognition by gamma delta T cells. Cell. 76:29.

Schurr E, Skamene E, Morgan K, Chu ML, Gros P. 1990. Mapping of *Col3a1* and *Col6a3* to proximal murine chromosome 1 identifies conserved linkage of structural protein genes between murine chromosome 1 and human chromosome 2q. Genomics. 8: 477.

Schwartz DC, Cantor CR. 1984. Separation of yeast chromosome-sized DNAs by pulsed field gradient gel electrophoresis. Cell. 37:67.

Sciammas R, Kodukula P, Tang Q, Hendricks RL, Bluestone JA. 1997. T cell receptor-gamma/delta cells protect mice from herpes simplex virus type 1-induced lethal encephalitis. J Exp Med. 185:1969.

Scott P, Trinchieri G. 1995. The role of natural killer cells in host-parasite interactions. Curr Opin Immunol. 7:34.

Seldin MF, Howard TA, D'Eustachio P. 1989. Comparison of linkage maps of mouse chromosome 12 derived from laboratory strain intraspecific and Mus spretus interspecific backcrosses. Genomics. 5:24.

Sentman CL, Olsson MY, Karre K. 1995. Missing self recognition by natural killer cells in MHC class I transgenic mice. A 'receptor calibration' model for how effector cells adapt to self. Sem Immunol. 7:109.

Shanley JD, Pesanti EL. 1983. Murine peritoneal macrophages support murine cytomegalovirus replication. Infect Immun. 41:1352.

Shanley JD. 1990. *In vivo* administration of monoclonal antibody to the NK 1.1 antigen of natural killer cells: effect on acute murine cytomegalovirus infection. J Med Virol. 30:58.

Shellam GR, Flexman JP, Farrell HE, Papadimitriou JM. 1985. The genetic background modulates the effect of the *beige* gene on susceptibility to cytomegalovirus infection in mice. Scand J Immunol. 22:147.

Shellam GR, Winterbourn V, Dawkins HJ. 1980. Augmentation of cell-mediated cytotoxicity to a rat lymphoma. III. *In vitro* stimulation of natural killer cells by a soluble factor. Int J Cancer. 25:331.

Shellam GR, Allan JE, Papadimitriou JM, Bancroft GJ. 1981. Increased susceptibility to cytomegalovirus infection in beige mutant mice. Proc Natl Acad Sci USA. 78:5104.

Shizuya H, Birren B, Kim UJ, Mancino V, Slepak T, Tachiiri Y, Simon M. 1992. Cloning and stable maintenance of 300-kilobase-pair fragments of human DNA in Escherichia coli using an F-factor-based vector. Proc Natl Acad Sci USA. 89:8794.

Shultz LD, Schweitzer PA, Rajan TV, Yi T, Ihle JN, Matthews RJ, Thomas ML, Beier DR. 1993. Mutations at the murine *motheaten* locus are within the hematopoietic cell protein-tyrosine phosphatase (*Hcph*) gene. Cell. 73:1445.

Silver LM. 1995. "Mouse Genetics: Concepts and Applications", Oxford University Press, Oxford.

Sinzger C, Jahn G. 1996. Human cytomegalovirus cell tropism and pathogenesis. Intervirology. 39:302.

Slater JS, Campbell AE. 1997. Down-regulation of MHC class I synthesis by murine cytomegalovirus occurs in immortalized but not primary fibroblasts. Virology. 229:221.

Smith KM, Wu J, Bakker AB, Phillips JH, Lanier LL. 1998. Ly-49D and Ly-49H associate with mouse DAP12 and form activating receptors. J Immunol. 161:7.

Smith MG. 1956. Propagation in tissue cultures of a cytopathogenic virus from human salivary gland virus disease. Proc Soc Exp Biol Med. 92:424.

Smith HRC, Karlhofer FM, Yokoyama WM. 1994. *Ly-49* Multigene Family Expressed by IL-2-Activated NK Cells. J Immunol. 153:1068.

Spritz RA. 1998. Genetic defects in Chediak-Higashi syndrome and the *beige* mouse. J Clin Immunol. 18:97.

Staczek J. 1990. Animal Cytomegaloviruses. Microbiol Rev. 54: 247.

Staeheli P, Haller O, Boll W, Lindenmann J, Weissmann C. 1986. Mx protein: constitutive expression in 3T3 cells transformed with cloned Mx cDNA confers selective resistance to influenza virus. Cell. 44:147.

Stagno S, Reynolds DW, Pass RF, Alford CA. 1980. Breast milk and the risk of cytomegalovirus infection. N Engl J Med. 302:1073.

Stinski MF. 1990. Fields Virology, Rappincott-Raven, PA.p. 2493.

Sudweeks JD, Todd JA, Blankenhorn EP, Wardell BB, Woodward SR, Meeker ND, Estes SS, Teuscher C. 1993. Locus controlling Bordetella pertussis-induced histamine sensitization (*Bphs*), an autoimmune disease-susceptibility gene, maps distal to T-cell receptor beta-chain gene on mouse chromosome 6. Proc Natl Acad Sci USA. 90: 3700.

Summerfield JA, Sumiya M, Levin M, Turner MW. 1997. Association of mutations in mannose binding protein gene with childhood infection in consecutive hospital series. BMJ. 314:1229.

Sundback, J, Karre K, Sentman CL. 1996. Cloning of minimally divergent allelic forms of the natural killer (NK) receptor Ly-49C, differentially controlled by host genes in the MHC and NK gene complexes. J Immunol. 157:3936.

Suto Y, Yabe T, Maenaka K, Tokunaga K, Tadokoro K, Juji T. 1997. The human natural killer gene complex (NKC) is located on chromosome 12p13.1-p13.2. Immunogenetics. 46:159.

Takei F, Brennan J, Mager DL. 1997. The *Ly-49* family: genes, proteins and recognition of class I MHC. Immunol Rev. 155:67.

Tay CH, Welsh RM, Brutkiewicz RR. 1995. NK cell response to viral infections in beta 2-microglobulin-deficient mice. J Immunol. 154:780.

Tay CH, Welsh RM. 1997. Distinct organ-dependent mechanisms for the control of murine cytomegalovirus infection by natural killer cells. J Virol. 71:267.

Tay CH, Yu LY, Kumar V, Mason L, Ortaldo JR, Welsh RM. 1999. The role of Ly49 NK cell subsets in the regulation of murine cytomegalovirus infections. J Immunol. 162:718.

Tempel BL, Jan YN, Jan LY. 1988. Cloning of a probable potassium channel gene from mouse brain. Nature. 332:837.

Testi R, D'Ambrosio D, De Maria R, Santoni A. 1994. The CD69 receptor: a multipurpose cell-surface trigger for hematopoietic cells. Immunol Today. 15:479.

Testi R, Phillips JH, Lanier LL. 1989. T cell activation via Leu-23 (CD69). J Immunol. 143:1123.

Thomas JD, Sideras P, Smith CI, Vorechovsky I, Chapman V, Paul WE. 1993. Colocalization of X-linked agammaglobulinemia and X-linked immunodeficiency genes. Science. 261:355.

Thomas ML. 1995. Positive and negative regulation of leukocyte activation by protein tyrosine phosphatases. Semin Immunol. 7:279.

Trask B, Pinkel D. 1990. Fluorescence *in situ* hybridization with DNA probes. Methods Cell Biol. 33:383.

Trask B, Pinkel D, van den Engh G. 1989. The proximity of DNA sequences in interphase cell nuclei is correlated to genomic distance and permits ordering of cosmids spanning 250 kilobase pairs. Genomics. 5:710.

Tsui HW, Siminovitch KA, de Souza L, Tsui FW. 1993. *Motheaten* and viable *motheaten* mice have mutations in the haematopoietic cell phosphatase gene. Nat Genet. 4:124.

Tsukahara A, Kawamura H, Iiai T, Moroda T, Suzuki S, Tada T, Minagawa M, Musha N, Hatakeyama K, Abo T. 1998. Participation of NK1.1$^+$ T cells in the rejection of *lpr* $\alpha\beta$ T

cells when bone marrow cells of *lpr* mice are transplanted into B6 mice. Microbio Immunol. 42:447.

Turner JM, Brodsky MH, Irving BA, Levin SD, Perlmutter RM, Littman DR. 1990. Interaction of the unique N-terminal region of tyrosine kinase p56lck with cytoplasmic domains of CD4 and CD8 is mediated by cysteine motifs. Cell. 60:755.

Vaage JT, Naper C, Lovik G, Lambracht D, Rehm A, Hedrich HJ, Wonigeit K, Rolstad B. 1994. Control of rat natural killer cell-mediated allorecognition by a major histocompatibility complex region encoding nonclassical class I antigens. J Exp Med. 180:641.

van der Meer JT, Drew WL, Bowden RA, Galasso GJ, Griffiths PD, Jabs DA, Katlama C, Spector SA, Whitley RJ. 1996. Summary of the International Consensus Symposium on Advances in the Diagnosis, Treatment and Prophylaxis and Cytomegalovirus Infection. Antiviral Res. 32:119.

Vance RE, Tanamachi DM, Hanke T, Raulet DH. 1997. Cloning of a mouse homolog of *CD94* extends the family of C-type lectins on murine natural killer cells. Eur J Immunol. 27:3236.

Vance RE, Kraft JR, Altman JD, Jensen PE, Raulet DH. 1998. Mouse CD94/NKG2A is a natural killer cell receptor for the nonclassical major histocompatibility complex (MHC) class I molecule Qa-1. J Exp Med. 188:1841.

Venema H, van den Berg AP, van Santen C, van Son WJ, van der Giessen M The TH. 1994. Natural killer cell responses in renal transplant patients with cytomegalovirus infection. J Med Virol. 42:188.

Vidal SM, Malo D, Vogan K, Skamene E, Gros P. 1993. Natural resistance to infection with intracellular parasites: isolation of a candidate for *Bcg*. Cell. 73:469.

Vidal SM, Epstein DJ, Malo D, Weith A, Vekemans M, Gros P. 1992. Identification and mapping of six microdissected genomic DNA probes to the proximal region of mouse chromosome 1. J Immunol. 14: 32.

Vitale M, Bottino C, Sivori S, Sanseverino L, Castriconi R, Marcenaro E, Augugliaro R, Moretta L, Moretta A. 1998. NKp44, a novel triggering surface molecule specifically expressed by activated natural killer cells, is involved in non-major histocompatibility complex-restricted tumor cell lysis. J Exp Med. 187:2065.

Wagtmann N, Rajagopalan S, Winter CC, Peruzzi M, Long EO. 1995. Killer cell inhibitory receptors specific for HLA-C and HLA-B identified by direct binding and by functional transfer. Immunity. 3:801.

Walmsley S, Tseng A. 1999. Comparative tolerability of therapies for cytomegalovirus retinitis. Drug Saf. 21:203.

Weber JL. 1990. Informativeness of human (dC-dA)n.(dG-dT)n polymorphisms. Genomics. 7:524.

Weller TH, Macauley JC, Craig JM, Wirth, P. 1957. Isolation of intranuclear inclusion producing agents from infants with illnesses resembling cytomegalic inclusion disease. Proc Soc Exp Biol Med. 94:4.

Weller TH. 1971. The cytomegaloviruses: ubiquitous agents with protean clinical manifestations. N Engl J Med. 285:203.

Welsh RM, Brubaker JO, Vargas-Cortes M, O'Donnell CL. 1991. Natural killer (NK) cell response to virus infections in mice with severe combined immunodeficiency. The stimulation of NK cells and the NK cell-dependent control of virus infections occur independently of T and B cell function. J Exp Med. 173:1053.

Welsh RM, O'Donnell CL, Shultz LD. 1994. Antiviral activity of NK 1.1+ natural killer cells in C57BL/6 *scid* mice infected with murine cytomegalovirus. Nat Immun. 13:239.

Welsh RM. 1978. Mouse natural killer cells: induction specificity, and function. J Immunol. 121:1631.

Welsh RM, Dundon PL, Eynon EE, Brubaker JO, Koo GC, O'Donnell CL. 1990. Demonstration of the antiviral role of natural killer cells in vivo with a natural killer cell-specific monoclonal antibody (NK 1.1). Nat Immunity Cell Growth Regul.9:112.

Westgaard IH, Berg SF, Orstavik S, Fossum S, Dissen E. 1998. Identification of a human member of the *Ly-49* multigene family. Eur J Immunol. 28:1839.

Whiteside TL, Herberman RB. 1995. The role of natural killer cells in immune surveillance of cancer. Curr Opin Immunol. 7:704.

Wiertz EJ, Jones TR, Sun L, Bogyo M, Geuze HJ, Ploegh HL. 1996. The human cytomegalovirus *US11* gene product dislocates MHC class I heavy chains from the endoplasmic reticulum to the cytosol. Cell. 84:769.

Wiltrout RH, Pilaro AM, Gruys ME, Talmadge JE, Longo DL, Ortaldo JR, Reynolds CW. 1989. Augmentation of mouse liver-associated natural killer activity by biologic response modifiers occurs largely via rapid recruitment of large granular lymphocytes from the bone marrow. J Immunol. 143:372.

Wolffe AP, Tafuri S, Ranjan M, Familari M. 1992. The Y-box factors: a family of nucleic acid binding proteins conserved from Escherichia coli to man. New Biologist. 4:290.

Wykes MN, Shellam GR, McCluskey J, Kast WM, Dallas PB, Price P. 1993. Murine cytomegalovirus interacts with major histocompatibility complex class I molecules toestablish cellular infection. J Virol. 67:4182.

Yabe T, McSherry C, Bach FH, Fisch P, Schall RP, Sondel PM, Houchins JP. 1993. A multigene family on human chromosome 12 encodes natural killer-cell lectins. Immunogenetics. 37:455.

Yokoyama WM. 1995. Natural Killer cell receptors specific for major histocompatibility complex class I molecules. Proc Natl Acad Sci USA. 92: 3081.

Yokoyama WM, Ryan JC, Hunter JJ, Smith HR, Stark M, Seaman WE. 1991. cDNA cloning of mouse *NKR-P1* and genetic linkage with *Ly49*. Identification of a natural killer cell gene complex on mouse chromosome 6. J Immunol. 147:3229.

Yokoyama WM, Kehn PJ, Cohen DI, Shevach EM. 1990. Chromosomal location of the *Ly-49* (a1, YE1/48) multigene family. Genetic association with the NK1.1 antigen. J Immunol. 145:2353.

Young HA, Ortaldo JR. 1987. One-signal requirement for interferon-gamma production by human large granular lymphocytes. J Immunol. 139:724.

Yu YY, George T, Dorfman JR, Roland J, Kumar V, Bennett M. 1996. The role of Ly49A and 5E6(Ly49C) molecules in hybrid resistance mediated by murine natural killer cells against normal T cell blasts. Immunity. 4:67.

Zhao XF, Colaizzo-Anas T, Nowak NJ, Shows TB, Elliott RW, Aplan PD. 1998. The mammalian homologue of *mago nashi* encodes a serum-inducible protein. Genomics 47:319.

Ziegler H, Thale R, Lucin P, Muranyi W, Flohr T, Hengel H, Farrell H, Rawlinson W, Koszinowski UH. 1997. A mouse cytomegalovirus glycoprotein retains MHC class I complexes in the ERGIC/cis-Golgi compartments. Immunity. 6:57.

Ziegler SF, Ramsdell F, Hjerrild KA, Armitage RJ, Grabstein KH, Hennen KB, Farrah T, Fanslow WC, Shevach EM, Alderson MR. 1993. Molecular characterization of the early activation antigen CD69: a type II membrane glycoprotein related to a family of natural killer cell activation antigens. Eur J Immunol. 23:1643.

Ziegler SF, Levin SD, Johnson L, Copeland NG, Gilbert DJ, Jenkins NA, Baker E, Sutherland GR, Feldhaus AL, Ramsdell F. 1994. The mouse *CD69* gene. Structure, expression, and mapping to the NK gene complex. J Immunol. 152:1228.